NUREG-0744
Vol. 1
For Comment

Resolution of the Reactor Vessel Materials Toughness Safety Issue

Task Action Plan A-11

Main Report and Appendices A and B

Manuscript Completed: April 1981
Date Published: September 1981

R. Johnson

Division of Safety Technology
Office of Nuclear Reactor Regulation
U.S. Nuclear Regulatory Commission
Washington, D.C. 20555

ABSTRACT

The central problem in the unresolved safety issue A-11, "Reactor Vessel Materials Toughness," was to provide guidance in performing analyses required by 10 CFR Part 50, Appendix G, Section V.C. for reactor pressure vessels (RPVs) which fail to meet the toughness requirement during service life as a result of neutron radiation embrittlement. Although the methods of linear-elastic fracture mechanics (LEFM) were adequate for low-temperature RPV problems, they were inapplicable under operating conditions because vessel steels, even those which exhibit less than 50 ft-lb of C_v energy, were relatively tough at temperatures where the impact energy reached its upper shelf values. A technical team of recognized experts was organized to assist the NRC staff in addressing the problem. Using the foundation of the tearing modulus concept, which had been developed under earlier NRC sponsorship, relationships were obtained which provided approximate solutions to the problem of RPV fracture with assumed beltline region flaws. The first paper of this report is a summary of the problem, the solutions, and the results of verification analyses. The details are provided in a series of appendices in Volumes I and II.

Blank Page

Contents

Volume I

Blank Page

ACKNOWLEDGMENTS

The following individuals participated in the work of the technical team organized to resolve the safety issue in the A-11 Task, "Reactor Vessel Material Toughness," and contributed to this evaluation report:

Richard E. Johnson, USNRC, Division of Safety Technology (A-11 Task Manager)
R. G. Berggren, Oak Ridge National Laboratory
D. A. Canonico, formerly with Oak Ridge National Laboratory
W. E. Cooper, Teledyne Engineering Services
H. T. Corten, University of Illinois
R. M. Gamble, formerly with USNRC, Division of Engineering
J. R. Hawthorne, U.S. Naval Research Laboratory
W. S. Hazelton, USNRC, Division of Engineering
C. S. Hinson, USNRC, Division of Systems Integration
G. R. Irwin, University of Maryland
F. J. Loss, U.S. Naval Research Laboratory
J. G. Merkle, Oak Ridge National Laboratory
P. C. Paris, Washington University, St. Louis
P. N. Randall, USNRC, Office of Nuclear Regulatory Research
P. C. Riccardella, NUTECH
W. G. Reuter, EG&G Idaho, Inc.
G. M. Slaughter, Oak Ridge National Laboratory (ORNL Task Manager)
J. Strosnider, USNRC, Office of Nuclear Regulatory Research
C. Z. Serpan, USNRC, Office of Nuclear Regulatory Research

The following individuals also participated and contributed to the TAP A-11 team effort on a voluntary basis:

J. P. Gudas, Naval Ship Research and Development Center
M. F. Kanninen, Battelle-Columbus Laboratories
T. U. Marston, Electric Power Research Institute

Resolution of the Reactor Vessel Materials Toughness Safety Issue

R. E. Johnson and others

CONTENTS

List of Figures

CONTENTS (Continued)

List of Tables

FOREWORD

NUREG-0744 is being issued for public comment to describe the method which has been developed by the NRC staff and contractors and has been found acceptable as a means of complying with 10 CFR 50, Appendix G, Section V.C. The analyses described in NUREG-0744 provide a rational basis for meeting the regulations and do not constitute a substitute for, nor do they countermand, any regulations. Other means of demonstrating that adequate margins against fracture exist in nuclear reactor pressure vessels which fail to meet the toughness requirements of 10 CFR 50 will be accepted if the substitute approach can be shown to have a well-defined theoretical and experimental basis.

1 SUMMARY

Task Action Plan (TAP) A-11, "Reactor Vessel Materials Toughness" (Appendix A to this Report), addresses one of the unresolved safety issues identified by the Nuclear Regulatory Commission (NRC). The fundamental goals of Task A-11 were to provide an improved engineering method to assess the safety margin in nuclear reactor pressure vessels (RPVs), and to develop appropriate new licensing safety criteria for use in the evaluation of normal, transient, or postulated accident conditions. This method then could be used to provide an assessment of older reactor pressure vessels that will eventually have marginal toughness, Relatively large amounts of prefracture plastic deformation can be expected at high temperatures, even in pressure vessel steels of low toughness. The new evaluation method will employ advanced elastic-plastic fracture mechanics concepts. The basis for this improved methodology was published in NUREG-0311, "A Treatment of the Subject of Tearing Instability."[1] Safety margins will be evaluated by comparing fracture resistance to a structural parameter where both are based on elastic-plastic fracture mechanics concepts. To ensure an adequate margin of safety, the structural parameter will have to remain sufficiently below the measure of fracture resistance. However, the quantitative relationship may depend on the reactor plant conditions. For example, a much larger margin would be required for normal/upset conditions than for low-probability accident events. The engineering method developed will account for radiation-induced material degradation.

The need for such an engineering method is dictated by the fact that some materials (primarily weld metals) used in RPVs will have Charpy V-notch (C_V) impact test upper shelf energy (USE) levels of less than 50 ft-lb before the end of their design life.* When RPV steel exhibits a C_V USE level of less than 50 ft-lb, the requirements of Title 10 of the Code of Federal Regulations (10 CFR 50)[2] are not being met**, and a safety analysis must be performed to

*Design life is generally considered to be 40 calendar years or 32 years of effective full power operation(EFPY).

**See footnote on page 3-2 of this report.

ensure continued safe operation of the reactor. Linear-elastic fracture mechanices (LEFM) would be inapplicable because of the large, prefracture crack tip plastic zone size observed in steels with 50 ft-lb or more of C_V energy at upper shelf temperatures. As a result, Task A-11 was designed to provide an acceptable elastic-plastic engineering method. The task focused on the RPV beltline because of the radiation-induced loss of USE in that region. The problem, the proposed solution, and related regulatory requirements are presented in the material that follows.

2 MATERIAL ASPECTS

Steels commonly used in the construction of RPVs exhibit a fracture toughness which varies greatly with temperature. Fracture tests of steel samples as a function of temperature will show relatively high toughness at high temperatures but low toughness at low temperatures. The temperature or temperature range over which the fracture changes from high-toughness (ductile) to low-toughness (brittle) behavior occurs is commonly referred to as the ductile-brittle transition temperature. Thus the temperature dependent fracture toughness has three more or less distinct zones: a lower shelf with low toughness, an intermediate transition region, and an upper shelf with high toughness.

"Size effect" further complicates the problem of assessing fracture toughness. As specimen sizes increase from 0.5 in. to ~12 in., there is an upward shift in the ductile-brittle transition temperature. Although reasons for this effect are complex, it is essentially caused by an increased constraint to local plastic flow in thick sections, or by an increased tendency of the thick sections to maintain plane strain conditions with increasing stress.

Charpy impact test data in the form of specimen fracture energy as a function of temperature reflect the ductile-brittle transition and follow a sigmoidal function. The transition temperature has been defined in several ways, the simplest of which is the temperature at an arbitrary C_v energy level (for example, 35 or 50 ft-lb). The USE is the energy level of the upper asymptote of the $E_{C-V} = f(T)$ curve.

Neutron radiation from an operating reactor core will embrittle the RPV steel. The embrittlement is shown in two important ways. In one, the transition temperature is increased; in the second, the USE is decreased. For the most part, the emphasis in the material that follows will be on the latter because it is more important to TAP A-11.

The embrittling effect of neutron radiation may so change the mechanical properties that the steel in an RPV will fail to meet the toughness requirements of 10 CFR 50.[2] The nature of the embrittlement could be either too large a temperature increase in the reference transition temperature (RT_{NDT}), or too large an energy decrease in the C_v USE, or both.

The magnitude of the irradiation-induced changes will depend, among other things, on the chemical and metallurgical details of the steel. For brevity, the effect of copper content can be singled out because it plays a major role in the USE behavior. Copper was introduced by the practice (later abandoned) of copper-coating the consumable electrode weld wire to protect it from rusting and to increase its electrical conductivity. Radiation experiments have shown that both the transition temperature and the C_v USE changes increase with copper content, and the most sensitive steels are weld metals with relatively high copper content (in the range of 0.2 to 0.5 w/o). Because the high copper welds exhibited relatively low initial USE levels, the decrease in that parameter was found to be more significant than the transition temperature increase.

Other important radiation-related comments about RPV steel include the following: Some of the variability in radiation-induced notch ductility changes has been traced to residual element compositional differences, especially the copper and phosphorus contents.[3,4] Special limits on copper and phosphorus contents are included in specifications for nuclear steels from the American Society of Testing Materials (ASTM) and the American Welding Society (AWS). In older steels, welds with high copper and nickel combinations had the highest radiation sensitivity. The experimental evidence suggested that for nickel contents up to about 1 percent, nickel reinforced the detrimental copper effects. Among samples from plates, forgings, and welds, the lowest radiation sensitivities were in forgings.

Regulatory Guide 1.99 (Rev. 1)[5] was prepared to provide conservative measures of the changes in transition temperature and C_v upper shelf with fluence; copper and phosphorus contents were included parametrically. The guide is updated as

significant additional data from surveillance or test reactor programs become available. Conservatism was included by constructing the curves as upper bounds of property changes rather than averages. A different viewpoint will be provided by a document in preparation by the Metal Properties Council (MPC) to present the average transition temperature increase with fluence, including 1σ and 2σ confidence bounds* on the data rather than upper limits. A companion study on upper shelf trends by the MPC is in the very early planning stage.

When the USE decrease dictated by the upper limit curves of the guide is applied to the many steels (plates, forgings, and weld metals) found in domestic operating reactors, it appears that about 20 RPVs will have unacceptable values before the end of their design life. The standard against which the calculated USE decrease is compared is presented in the following section.

*Where σ is one statistical standard deviation.

3 REGULATORY ASPECTS

Pressure vessels built to the requirements of the Boiler and Pressure Vessel Code of the American Society of Mechanical Engineers (ASME Code Section III)[6] are expected to withstand pressures more than twice their nominal design pressure under normal conditions. That this has been achieved was shown with particular clarity by the series of vessel failure tests run at Oak Ridge National Laboratory (ORNL) over the past 10 years as part of the NRC Heavy Section Steel Technology (HSST) program.[7] In the experiments, intermediate size (39-in. diameter) vessels built to ASME Code requirements failed at pressures ranging from about 2.5 to 3 times the design pressures, even though very large flaws were intentionally introduced before testing.

Fracture toughness requirements for RPV steels are given in 10 CFR 50.[2] Most of the details of the requirements can be found in Appendix G to Part 50; the rules for monitoring radiation-induced changes through surveillance programs are given in Appendix H.

The fracture toughness criteria originally adopted were developed by a special Task Group of the Pressure Vessel Research Committee and were recommended for inclusion in the ASME Boiler and Pressure Vessel Code in 1971.[8] The criteria were published as a nonmandatory Appendix to Section III of the Code in the Winter 1972 Addendum. After a thorough review by the Atomic Energy Commission (AEC), the criteria were incorporated into the 1973 version of Appendix G to 10 CFR 50, along with additional necessary items.

Although the new ASME criteria used LEFM principles exclusively, the difficulty in performing tests to determine valid LEFM fracture toughness led to an approach which employed the two traditional tests: drop weight$_{NDT}$ and Charpy. The goal was to provide a specific safety margin (a factor of 2 on pressure) in the presence of an assumed large flaw (1/4 of the wall thickness) for all conditions of normal operation, including cold startup and shutdown. A smaller margin (a factor of 1.5) was specified for test conditions.

To perform the necessary calculations, the LEFM fracture toughness (K_{Ic}) as a function of temperature was needed, and it was recognized that data were not available for each and every material in every RPV. This problem was overcome by correlating all available K_{Ic}, K_D, and K_{Ia} test results to the specific nil-ductility transition (NDT) of the tested material. The lower limit of the data scatter band was used to establish what was called the "reference" K_I curve (symbolized as K_{IR}). Charpy tests also were specified to provide additional assurance that the specific material being evaluated had a normal transition temperature behavior; that is, that the rate of toughness increases with temperature was as expected and that a reasonably high upper shelf was achieved. The somewhat redundant additional tests also provided protection against possible errors in determining the NDT.

The Charpy criterion selected was the 50 ft-lb temperature; the requirement was that the material must develop 50 ft-lb of Charpy energy at a temperature no higher than 60F° above the NDT. Thus, the reference temperature used to index to the K_{IR} curve was basically the drop weight NDT, with additional assurance provided by the 50 ft-lb Charpy check.

The specific transition temperature used is the reference temperature for the nil-ductility transition, symbolized as RT_{NDT}; it is defined in the ASME Code. The C_v 50 ft-lb level is used to measure ΔRT_{NDT}; thus, if the USE level drops to less than 50 ft-lb, ΔRT_{NDT} is infinite, which constitutes a failure to meet the 10 CFR 50 requirements.*

All operating reactor licenses require that a surveillance program be maintained in accordance with Appendix H of 10 CFR 50 to monitor irradiation-induced fracture toughness changes. In surveillance programs, specimens are

*In Appendix G, Revised (now available for public comment), ΔRT_{NDT} is measured at the 30 ft-lb level, but the 50 ft-lb USE requirement is established as a specific attribute.

irradiated in operating RPVs, removed according to an established schedule, and tested to provide fracture toughness data. The data are used to determine the conditions under which the vessel can be operated with adequate margins of safety against fracture throughout its service life.

The RPV material and design requirements of 10 CFR 50 were established to provide ample safety margins for normal and upset conditions during the operation. The technical basis for those requirements can be found in Reference 8. The ASME Code recognizes four conditions: normal (Level A), upset (Level B, anticipated transients), emergency (Level C), and faulted (Level D). The plant conditions covered by Levels A and B are clear, but Level C and D conditions deserve explanation. Quoting from the consequence statements of Section III of the Code (NCA-2421.2):

(a) For Level C (Emergency): "These sets of limits permit large deformations in areas of structural discontinuity. The occurrence of stress to Level C limits may necessitate the removal of the component from service for inspection or repair of damage to the component or support."

(b) For Level D (Faulted): "These sets of limits permit gross general deformations with some consequent loss of dimensional stability and damage requiring repair, which may require removal of the component from service."

Both conditions require shutdown; neither condition implies loss of coolant retention. An emergency condition may require removal from service for repair, but a faulted condition may require removal from service. Operation after an emergency condition is expected, but it must be assumed that operation after a faulted condition is not possible.

The lesser need for the "normal" and "upset" conditions may be illustrated by considering the result of a typical RPV evaluation. A flaw* is assumed to be

*Appendix G stipulates: a semi-elliptical flaw, normal to the hoop stress, with a depth $a = T/4$ and a total surface length $l = 3T/2$, T being the wall (shell) thickness.

present, and the pressure-induced stress intensity factor, K_{IP}, is calculated according to

$$K_{IP} = C\ (P/2500),\ \text{Ksi}\ (\text{in.})^{\frac{1}{2}}$$

where the factor C depends on wall thickness and P is the internal pressure. Illustrative values are

Wall Thickness, in.	Flaw Depth, in.	K_I at P=2250 psi, ksi $(\text{in.})^{\frac{1}{2}}$
4	1.0	45
6	1.5	54
8	2.0	63
10	2.5	76

It is required that

$$K_I \leq K_{IR}/\sqrt{10} \simeq K_{IR}/(3.2)$$

Therefore, for a vessel of 8-in. wall thickness (typical of PWRs), K_{IR} should be about 200 ksi $(\text{in.})^{\frac{1}{2}}$, or more, at the operating pressure. That will be so for temperatures of RT_{NDT} + 200°F, or more; that is, for temperatures comfortably below and up to the operating temperature of about 550°F. Therefore, it is believed that the present LEFM procedures are completely adequate and conservative for the evaluation of inservice indications subject to normal and upset conditions.

If the C_v upper shelf remains at or above the 10 CFR 50 requirement of 50 ft-lb, there is no concern about the evaluation of emergency and faulted conditions, because (1) these conditions are not treated in Appendix G and (2) Section XI imposes a relatively low safety factor on these conditions. Therefore, priority must be given to rules applicable to emergency and faulted conditions. Once they are developed, modifications to the rules for normal and upset conditions, if any, should be evident.

When it is determined that the materials toughness requirements of 10 CFR 50 are no longer met, the licensee must complete three tasks; the continued

operation of the plant depends on satisfactory completion of all three. First, the RPV beltline region--including all weldments--must undergo a complete nondestructive volumetric examination in accordance with the requirements of Section XI of the Code. Second, additional tests must be performed to determine the actual RPV material response to neutron radiation, using archive material, accelerated irradiation, and measured properties such as dynamic fracture toughness. Third, a conservative fracture analysis of the RPV must be performed, including allowance for all uncertainties, to demonstrate the existence of adequate margin during continued operation. If an adequate safety margin cannot be demonstrated by performing the above three-step procedure, continued operation would be contingent upon the successful completion of a thermal anneal to recover sufficient material toughness.

The inspection step may require revision to the inservice examination schedule, with related loss in availability, but it presents no new problems. However, most surveillance specimens are V-notch Charpy bars (a few are small fracture mechanics specimens); therefore, the second step is difficult. The principal problems are (1) interpretation of Charpy data and (2) inadequate testing techniques for the fracture mechanics specimens. In a later section, a fracture mechanics correlation with Charpy data is proposed based on TAP A-11 work; other efforts are under way to resolve both difficulties.

Several years ago it was recognized that the 10 CFR 50 requirements--while reasonable in principle and in intent--would create a dilemma in practice because of inadequacies in accepted fracture mechanics analyses. Experimental evidence showed that violations of the 10 CFR 50 toughness requirements occur because of radiation-induced decreases in Charpy USE to less than 50 ft-lb; thus, the indicated arena for RPV safety margin analysis was marked out as high temperature. Specifically, that would be from as much as 350F° below the typical reactor operating temperature (about 200°F) up to and including the high temperatures which might occur during or as a result of an accident (about 650°F). Within that temperature range, the RPV materials--including plates, forgings, and weld metals (even the high copper content welds)--which exhibit Charpy V-notch energies of the order of 50 ft-lb are tough enough that the prefracture crack tip plastic zone would exceed the boundary conditions

assumed in an LEFM analysis. The resulting dilemma is that, whereas a fracture analysis is required by Section V.C of Appendix G, an LEFM solution would be incorrect, and no elastic-plastic fracture mechanics analyses were available with sufficient accuracy and reliablity for nuclear RPV safety margin calculations.

The above considerations resulted in the identification of the task of providing a viable high temperature elastic-plastic fracture mechanics analysis for the RPV upper shelf problem as the goal of TAP A-11. The resources of TAP A-11 were organized to provide an engineering methodology, generally acceptable to the NRC, which could be employed to satisfy the third requirement (that is, analysis) of Section V.C of Appendix G to 10 CFR 50.

4 PROBLEM DEFINITION

The issue was to establish the means of assessing the safety margin in RPVs which contain steels with 50 ft-lb or less of C_V energy at upper shelf temperatures. The problem area was limited to the beltline region, where neutron flux and radiation sensitivity (especially in some weld metals with relatively high copper content) both were high. The goal was to utilize the current theories of elastic-plastic fracture to develop an engineering method for calculating failure conditions and for evaluating safety margins in operating nuclear reactors.

The low upper shelf mode of failure, which is the principal concern of TAP A-11, requires some definition. It concerns predicting the burst pressure of a reactor vessel with a beltline flaw of considerable depth at temperatures too high for cleavage fracture to occur. One pressure limit relates to the onset of plastic instability in the ligament beneath the flaw. Neutron radiation will raise the pressure required for plastic instability by the flaw stress elevation. However, radiation also reduces the tearing resistance and, if the pressure is to induce full ligament plastic instability, the crack must remain stable as that pressure is applied. When preceded by such a scenario, the final fracture is called the low upper shelf mode of failure.

The A-11 Technical Team agreed that the J-integral provides the best basis for an engineering method of elastic-plastic fracture analysis. This means that the crack extension parameter should be either the J-integral itself or a parameter analytically relatable to the J-integral. To ensure an appropriate solution to the problem, the recommended method should consider the actual flaw geometry involved, should include an analysis of the uncracked structure in terms of load and the related strain, and should reduce smoothly to the LEFM solution for linear elastic conditions. From practical considerations, the method of analysis should not require a computerized numerical solution for each individual problem, although it may be based on existing numerical solutions. In addition, the results of calculations should be presentable in a form that has direct physical significance with respect to the safety margin determined for both load and flaw size.

5 PROBLEM SOLUTION

To make efficient use of resources, it was decided to base the solution on available elastic-plastic fracture mechanics concepts. The foundation for a rational theory of elastic-plastic fracture was built from the concept of the Rice J-integral, the Hutchinson-Rice-Rosengren (HRR) analysis for the stress strain fields in the vicinity of a crack,[9] and materials J-resistance curves (known as J-R curves) based on data in the form of: $J = f(\Delta a)$. A method for applying the J-Integral fracture theory was developed by Prof. Paul C. Paris under NRC sponsorship (Appendix B and References 1, 10, 11, 12, and 13). The theoretical aspects are discussed in Appendix C; their application to the RPV problem is discussed in Appendix H. At the same time, an experimental procedure was needed to obtain material fracture parameters in a form compatible with the theoretical concepts. The single specimen unloading compliance method was adapted and further developed for tests of irradiated specimens in hot cells at the U.S. Naval Research Laboratory (NRL).[14] Materials properties are discussed in Appendix D.

The value of J is a measure of the intensity of the stress-strain field (in terms of total work, elastic plus plastic) in the vicinity of a crack. Comparison of J for a structure with the corresponding J for the material of construction leads to a statement of crack equilibrium. The tearing modulus, T, is proportional to the derivative of J with respect to the crack size or, equivalently, to the second derivative of the mechanical energy in the system. Analytical methods of stable crack growth applicable to nuclear pressure vessel steels must be based on the premise that material J-R curves are continuously nonlinear.

It has been shown that crack extension depends on the relative value of the J-integral and that the stability of the ensuing fracture depends on the relative value of T. Thus, crack extension would be expected for values of J_{appl} greater than a characteristic J_{matl}, say J_{Ic}. The fracture would proceed by stable tearing (under rising load), so long as $T_{appl} < T_{matl}$; it would become unstable when the two values reach equality. The conditions were easily visualized by plotting curves of the related structural and material parameters on a single J-T graph. Details are given in Appendix B.

The distinguishing feature of the methods of analysis applied in this report is the use of a resistance curve that shows the fracture resistance as a function of the extent of ductile crack growth. As shown in Figure 5.1, up to the point of instability, the applied value of J is less than the critical material J-integral and

$$J_{appl} = J_{mat} \tag{5-1}$$

at the point of tearing instability. An increase in crack size would cause the applied value of J to increase by more than the related increase in the material J-integral. The failure criterion for tearing instability is (Equation 5-1), combined with [14,15]

$$\frac{dJ}{da} = \frac{dJ_m}{da} \tag{5-2}$$

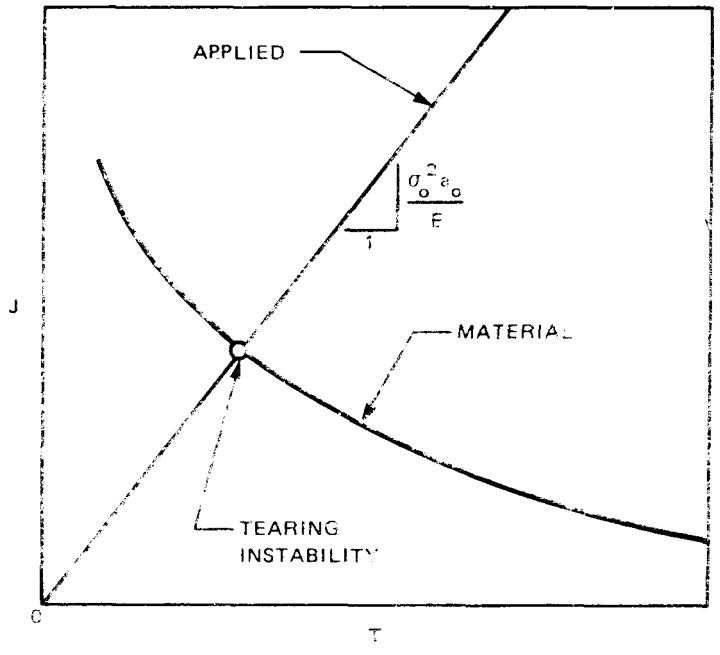

Figure 5.1 Schematic Curves of J=f(T) Illustrating the Material and Structural (Applied) Curves, the Intersection Denoting Instability.

The J-R curves shown in Figures 5.2 and 5.3 show no trend which would suggest a size effect at either the 77 or 302°F (25 or 200°C) test temperature. This result was surprising in view of the likelihood that the fractures occurred beyond the accepted limit of J-control. It suggested that small specimens may be more useful than previously assumed by providing the R-curve trends of larger specimens. Figure 5.4 compares J-R curves for irradiated A 533-B weld metal obtained from two different size CT specimens (0.5 T and 1.6 T).[14] The J-R curves are similar for small crack extensions (Δa less than 1.5 mm). As in Figures 5.2 and 5.3, these data suggest that the small specimen J-R curve is no less conservative than that derived from a larger specimen.

Resistance-curve analysis has been applied by Paris and others[1] to develop a method for estimating the onset of ductile crack instability at limit load under specified boundary conditions. The analysis uses the slope of the resistance curve to determine the nondimensional parameter T, the tearing modulus

$$T = \frac{dJ}{da} \cdot \frac{E}{\sigma_o^2} \qquad (5\text{-}3)$$

where E is the elastic modulus and σ_o is the flow stress (the average of the tensile yield and ultimate strengths), assumed to govern the magnitude of the fully plastic limit load.

The tearing modulus approach was used to solve two specific pressure vessel fracture problems, namely the simple cylindrical shell with (1) a surface crack and (2) a through-wall crack. The next sections present the following topics: (1) the two fracture problem solutions; (2) a comparison of the approximate (tearing modulus) surface crack solution with a detailed, three-dimensional finite element solution; (3) verification of the solutions by application to (a) the HSST ITVs* and (b) large surface-cracked tensile

*HSST: heavy-section steel technology research (NRC) program; ITV: intermediate-size test (pressure) vessels.

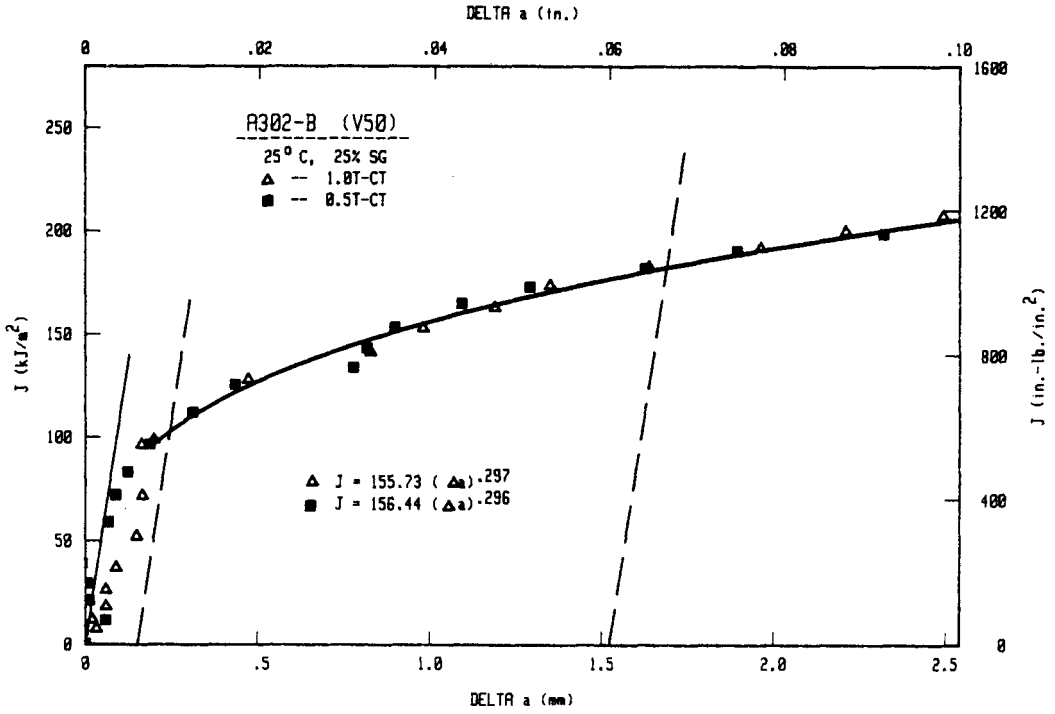

Figure 5.2 J-R Curves From a Low USE A-302B Steel Showing No Size Effects Between 0.5T and 1T CT Specimens at 25°C.

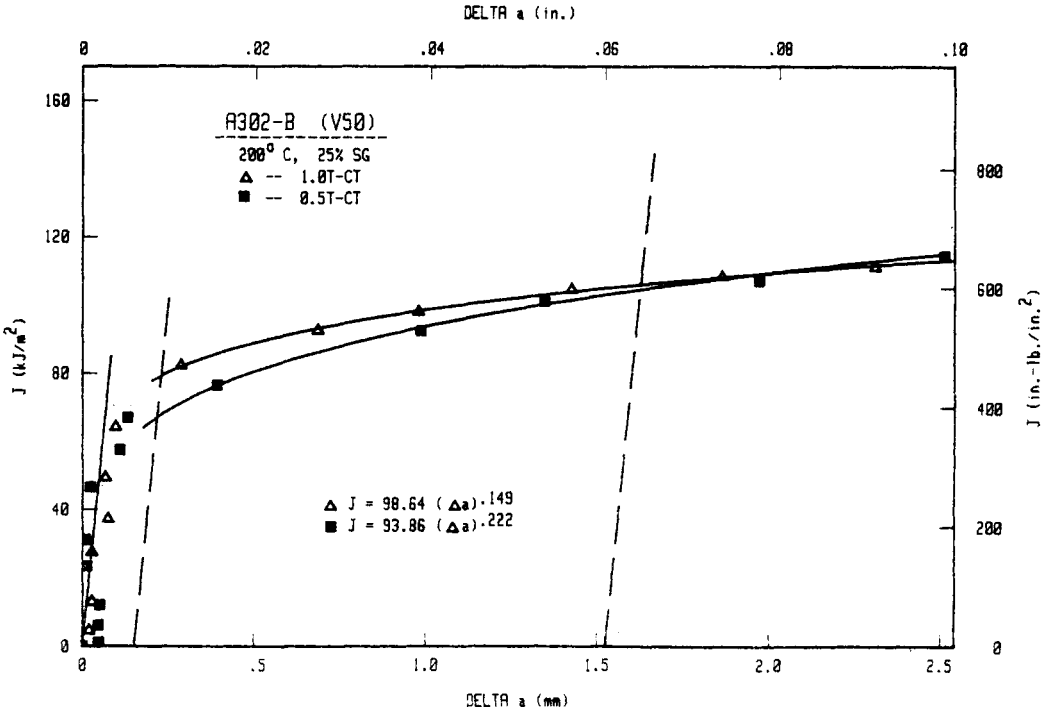

Figure 5.3 The Same as Figure 5.2, for Tests at 200°C, Also Showing No Size Effects.

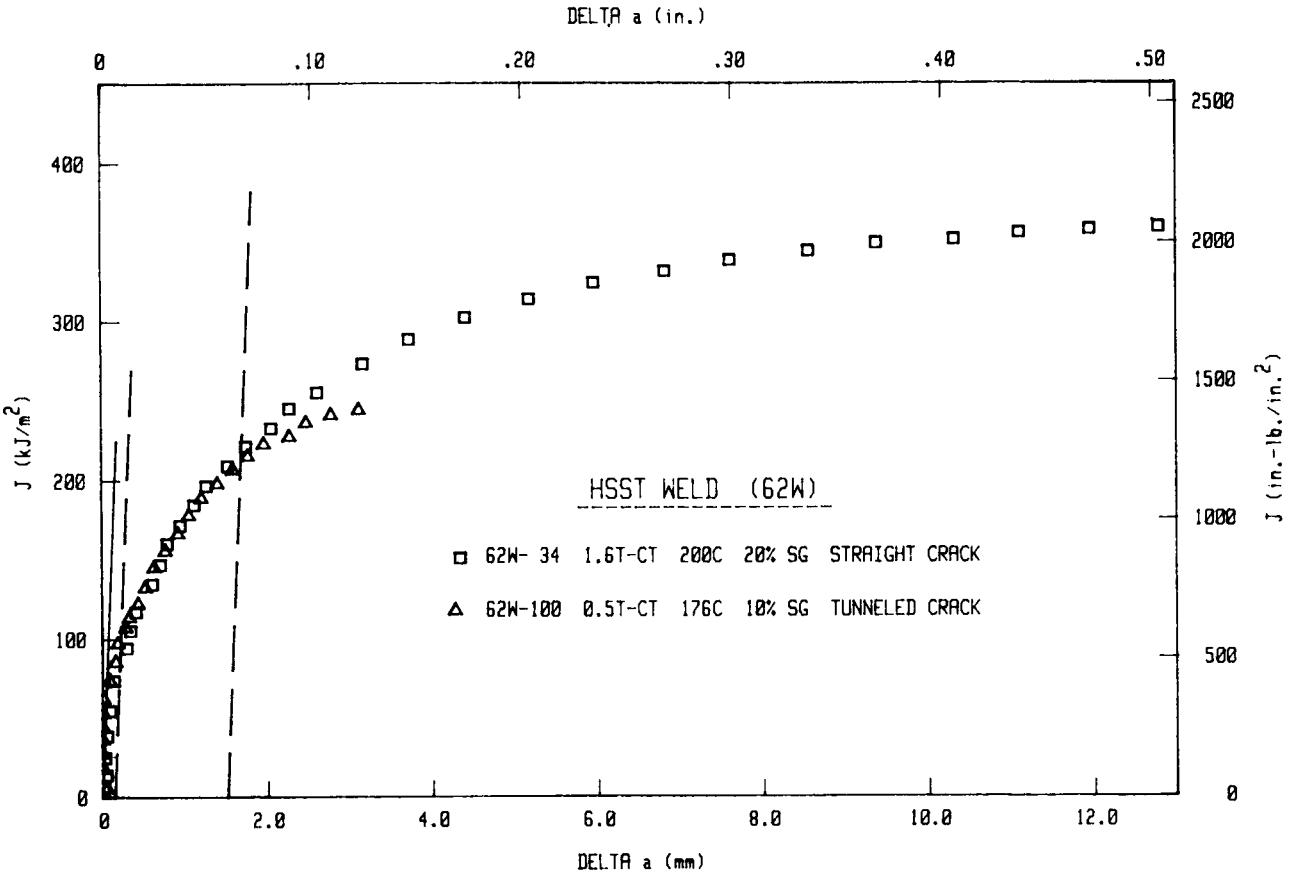

Figure 5.4 J-R Curves from an Irradiated A-533B Submerged Arc Weld Deposit Using 0.5T and 1.6T CT Specimens.

fracture specimens and, in both cases, comparison of the calculated and observed failure conditions; (4) the results of a sensitivity study showing the effect of variability in the underlying mechanical property parameters on the results; and (5) comparison of the tearing modulus approach with other EPFM fracture predictions. Finally, the report addresses the situation where an analysis is necessary, but specific EPFM mechanical property data are unavailable. An alternative is proposed based on a correlation between C_V impact test data and conservatively established values of the J-integral for pressure vessel steels covering a spectrum of metallurgical conditions.

The elastic-plastic analyses of vessel cracks are more easily understood if one first follows through a simple elastic derivation: Consider a wide plate under a uniform tensile stress, σ. Introduce a through-thickness crack of total length 2a normal to the tensile load. The associated stress intensity factor, K, is given by [15]

$$K = \sigma(\pi a)^{\frac{1}{2}} \tag{5-4}$$

In addition to assuming that an LEFM analysis is proper, one also may ignore geometrical differences and apply the equation to a pressure vessel. In the more detailed analyses, done as part of TAP A-11, shell correction factors were derived and were shown to play an important role. From LEFM

$$G = K^2/E \tag{5-5}$$

where G is the elastic strain energy release rate for a virtual crack extension; that is, $G = \partial U/\partial a$. In the absence of significant prefracture crack tip plastic deformation, the J-integral reduces to G, so

$$J = G = K^2/E = \pi a\sigma^2/E \tag{5-6}$$

for the wide-plate elastic approximation to the vessel with a through-wall crack. It will be seen later that the plasticity correction factors derived from the TAP A-11 solution also played an important role.

Differentiating Equation 5-6: $dJ/da = \pi\sigma^2/E$, and using Equation 5-3

$$T = \frac{\pi\sigma^2}{E} \cdot \frac{E}{\sigma_o^2} = \pi\left(\frac{\sigma}{\sigma_o}\right)^2 \tag{5-7}$$

Finally, combining Equations 5-6 and 5-7

$$\frac{J}{T} = a\sigma_o^2/E \tag{5-8}$$

The relationship provides a pressure vessel loading curve approximation which, on a graph of $J = f(T)$, will be a straight line except for crack extension. In a large structure with a relatively small initial crack size under slow, stable crack growth (by a ductile tearing mechanism), the straight line will be a good approximation. In combination with a materials curve of $J_{matl} = f(T_{matl})$, as on Figure 5.1, Equation 5-8 would allow a determination of unstable (that is, rapid or catastrophic) fracture conditions.

The elastic-plastic fracture analyses for pressure vessels with through-wall or part-through cracks are reported in detail in Appendices B and C of this report. An abbreviated presentation follows.

For a pressure vessel with a through-wall crack of 2a total length, LEFM considerations suggest

$$J = K^2/E \tag{5-9}$$

and $$K = \sigma\sqrt{\pi a} \cdot Y(\lambda) \tag{5-10}$$

where Y is a geometrical shell correction factor, a function of $\lambda = a\sqrt{Rt}$.

In turn, R = vessel radius, and t = shell (wall) thickness. So

$$J = \frac{\sigma_o^2 a}{E} \left\{\frac{\pi\sigma^2}{\sigma_o^2}\right\} (Y^2) \tag{5-11}$$

where the convention is adopted that

{ } = the stress bracket (yielding correction factor)

( ) = the geometry bracket

Operating on Equation 5-11

$$T = \left\{\frac{\pi\sigma^2}{\sigma_o^2}\right\} \cdot (Y^2 + 2\lambda Y \cdot Y') \tag{5-12}$$

where the prime signifies $\frac{d}{d\lambda}$. Thus

$$\frac{J}{T_{appl}} = \frac{\sigma_o^2 a}{E} \left[\frac{1}{1 + 2\lambda Y'/Y}\right] \tag{5-13}$$

As was the case in the simplified previous example, if $\Delta a = 0$, the loading line is a linear curve. In Appendix B, Paris develops graphical values of Y. Also, consideration of plasticity corrections on { } led to the same final result and the conclusion that the same loading line equation applies whether a crack tip plastic zone size correction is used or not. Because the evaluation of the geometry bracket in Equation 5-13 showed that ( ) = 0.5 to 1.0, it was concluded that the simple elastic result of Equation 5-8 was a good first-order approximation.

For a pressure vessel with a part-through (surface) crack of depth a and total (surface) length 2c, LEFM analysis suggests

$$K = \frac{\sigma\sqrt{\pi a}}{\Phi\left(\frac{a}{c}\right)} \cdot f\left(\frac{a}{c}\right) \cdot g\left(\frac{a}{t}\right) \tag{5-14}$$

where Φ is the complete elliptic integral of the second kind (a function of the aspect ratio, a/c) and f and g are geometric correction factors for the front surface and back surface, respectively. From Equation 5-9:

$$J = \frac{\sigma_o^2 a}{E} \left\{\frac{\pi\sigma^2}{\sigma_o^2}\right\} \cdot F\left(\frac{a}{c}\right) \cdot G\left(\frac{a}{t}\right) \tag{5-15}$$

where: $F\left(\frac{a}{c}\right) = \left(f\left(\frac{a}{c}\right)/\phi\left(\frac{a}{c}\right)\right)^2$, $G\left(\frac{a}{t}\right) = \left(g\left(\frac{a}{t}\right)\right)^2$

and, according to Equation 5-3

$$T = \left\{\frac{\pi\sigma^2}{\sigma_o^2}\right\} F\left(\frac{a}{c}\right)\left[G\left(\frac{a}{t}\right) + \frac{a}{t} \cdot G'\left(\frac{a}{t}\right)\right] \qquad (5\text{-}16)$$

In deriving Equation 5-16, F' was ignored because it would result in a small change (zero to slightly negative) for an increase in a relative to c; the result is to make the evaluation of T somewhat conservative. Finally

$$\frac{J}{T}_{appl} = \frac{\sigma_o^2 a}{E}\left[\frac{1}{1 + \frac{a}{t} \cdot G'/G}\right] \qquad (5\text{-}17)$$

The similarity with the equation for the through-wall crack, Equation 5-13, should be obvious on inspection. Taking a well-known approximate relation,

$$G\left(\frac{a}{t}\right) = \sec\frac{\pi a}{2t},$$

the geometry bracket from Equation 5-17 becomes $\left[\frac{1}{1 + \frac{\pi a}{2t}\tan\frac{\pi a}{2t}}\right]$,

and for $0 \leq \frac{a}{t} \leq \frac{1}{2}$; $1 \leq [\ ] \leq 0.57$.

Analyses of plasticity effects relative to the influence on the stress bracket, { }, did not alter the conclusion. Thus, for pressure vessels with significant cracks in the beltline (cylindrical) region

$$\left(\frac{J}{T}\right)_{appl} = \frac{\sigma_o^2 a}{E}\left[\Gamma\right] \qquad (5\text{-}18)$$

where $0.5 \leq \Gamma \leq 1.0$ for most examples of interest.

The General Electric Company conducted a detailed three-dimensional elastic-plastic finite element analysis of a typical pressurized water reactor (PWR) vessel containing a 1/4 T beltline axial flaw.[17] Vessel geometry and modelling details are illustrated in Figure 5.5. Because this problem is very relevant to TAP A-11, it was decided to compare these results to the approximate,

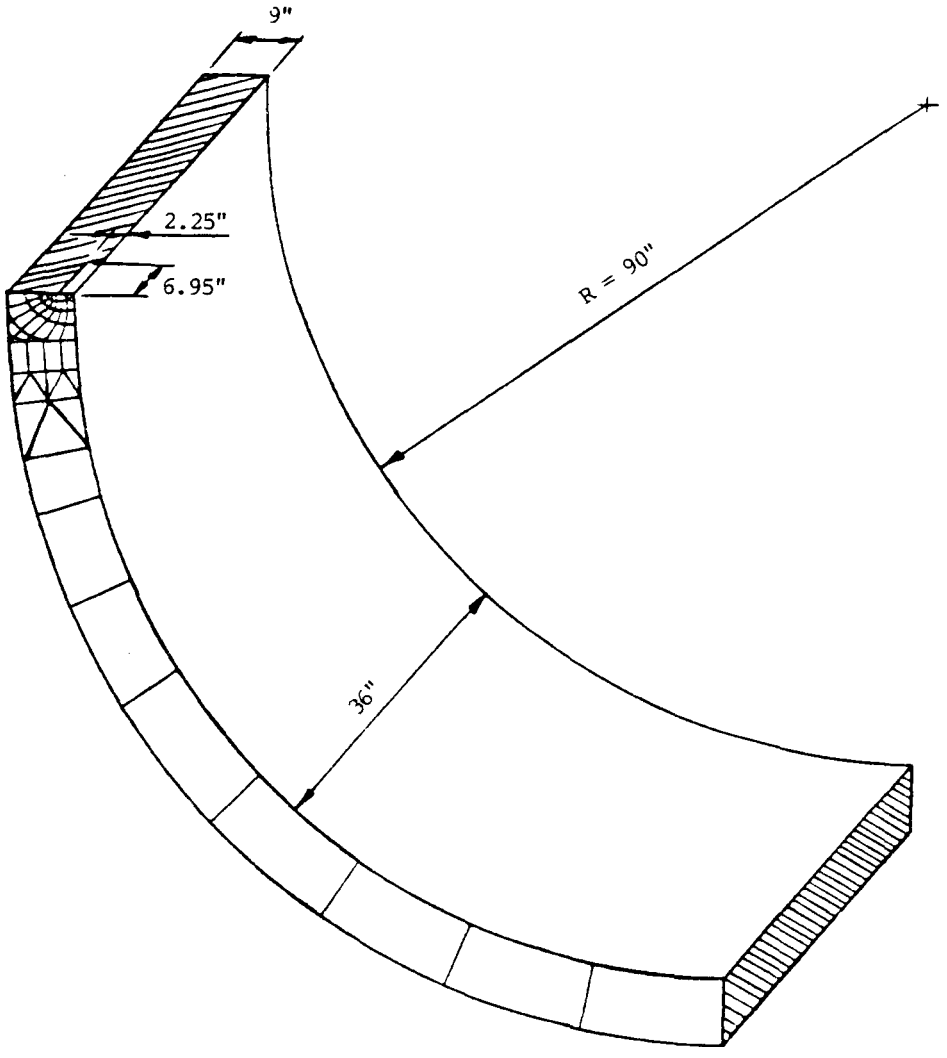

Figure 5.5 Finite Element Model of Vessel with Beltline Axial Flaw

part-through flaw methodology using J/T curves. The estimated J-values from the approximate surface flaw analysis listed in Table 5.1 were plotted in Figure 5.6, along with the three-dimensional, finite element results. The agreement between the two approaches is excellent for the entire range of pressure over which the finite element calculations have been performed. Moreover, the approximate analysis has been carried beyond this point to values of $\sigma/\sigma_0 > 1$, and the extension of the analysis looks reasonable also. This agreement further verifies the approximate surface flaw methodology developed under TAP A-11 for application to the RPV beltline region. It also

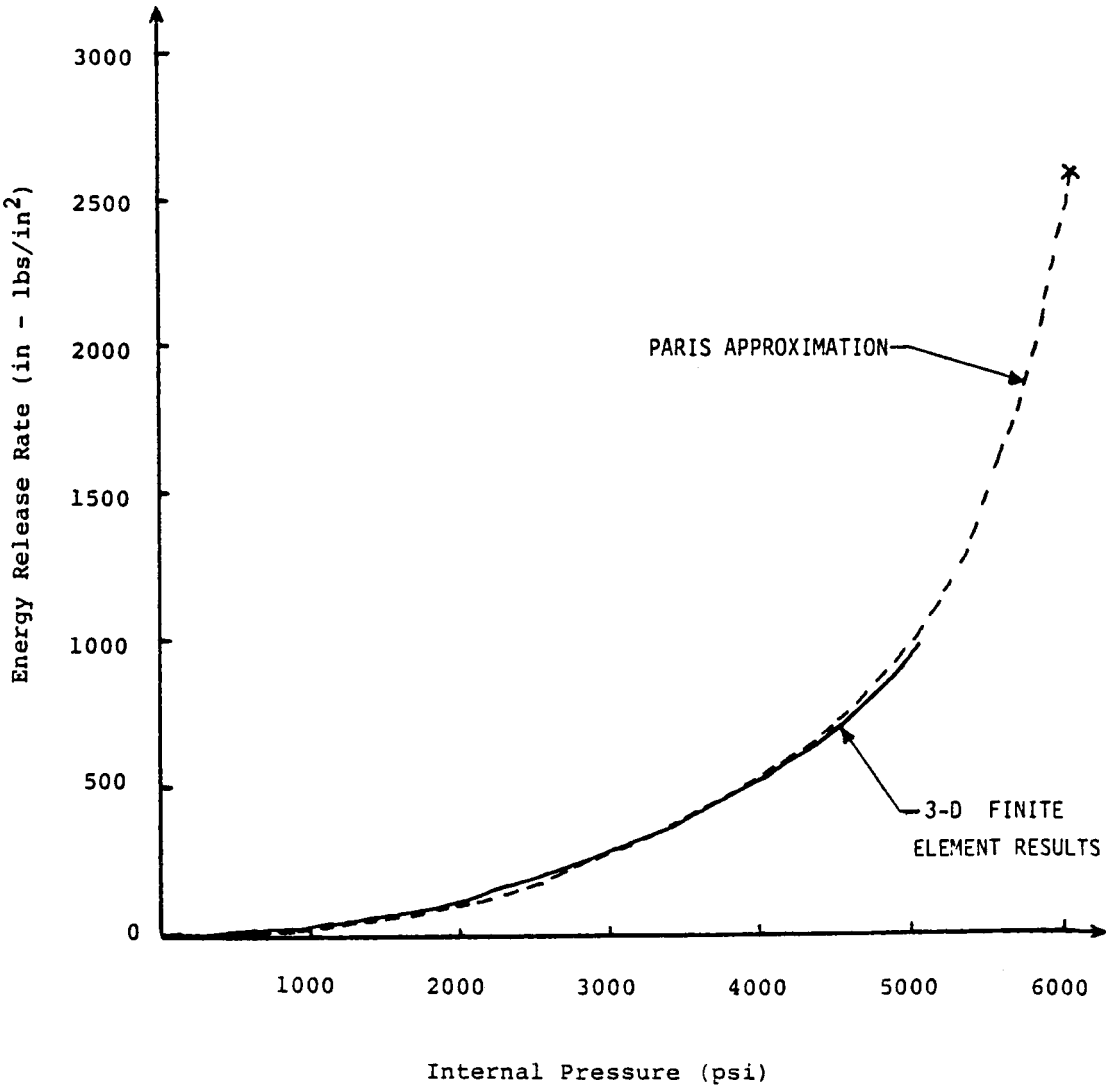

Figure 5.6 Variation of Energy Release Rate with Internal Pressure.

Table 5.1 J-Integral as a function of internal pressure

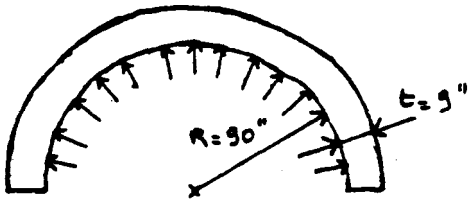

$\sigma_o = 60{,}000$ psi

$\varepsilon_o = 0.002$

$E = 30 \times 10^6$ psi

$\sigma_\theta = \frac{PR}{t} = 10P$

$$\varepsilon = \varepsilon_e + \varepsilon_p = \frac{\sigma_\theta}{E} + \varepsilon_p\,(\sigma_\theta)$$

$$\frac{\varepsilon}{\varepsilon_o} = \frac{\sigma_\theta}{E\varepsilon_o} + \frac{\varepsilon_p(\sigma_\theta)}{\varepsilon_o}$$

$$\frac{\varepsilon}{\varepsilon_o} = \frac{\sigma_\theta}{\sigma_o} + 1.4\,(\frac{\sigma_\theta}{\sigma_o})^{8.6}$$

P	σ_θ	σ_θ/σ_o	$\varepsilon_\theta/\varepsilon_o$	$F(\sigma/\sigma_o)$	J
1000	10,000	.17	.17	---	---
2000	20,000	.33	.33	---	---
3000	30,000	.5	.503	.82	261
4000	40,000	.67	.71	1.5	478
5000	50,000	.83	1.11	3.0	956
6000	60,000	1.0	2.4	8.0	2549
7000	70,000	1.17	6.51	24.5	7806

indicates a lack of sensitivity of the stress correction $F(\sigma/\sigma_0)$ to the particular stress-strain law, because it has now been demonstrated for two different stress-strain laws.

Further evaluation of the analyses was done by comparing calculated failure conditions to observations. A series of ITVs were constructed and tested under the HSST program. Very large cracks were introduced artificially; then the vessels were pressurized to failure at various test temperatures ranging from the lower transitional to the upper shelf for the specific low alloy steels used. The magnitude and diversity of the ITV program test results provided an opportunity to verify the application of the tearing modulus concepts developed for TAP A-11.

Table 5.2 summarizes the results of the tearing modulus analysis of the surface flawed ITVs. Estimates of J_{appl} and T_{appl} for ITVs V1, V2, V3, V4, and V6 were obtained using an approximate elastic-plastic analytical procedure for part-through flaws in tension presented in detail in Appendix H in Volume II of this report. For vessels V2 and V4, which were tested in the transitional regime, the failure prediction was based on $J = J_{Ic}$ (1200 in.-lb/in.^{2}).

Table 5.2 Comparison of actual and predicted failure conditions for vessels 1 to 4, and 6

Vessel	Test Temp (°F)	Regime	Actual Failure Conditions		Tearing Instability Calculations			Plastic Instability Check	Predicted Failure Conditions	
			P (ksi)	ε (%)	J_{crit}	ε_{crit} (%)	P_{crit} (ksi)	P (ksi)	P (ksi)	ε (%)
V2	32	Transition	27.9	0.19	1200	0.21	27.5	N/A	27.5	0.21
V4	75	Transition	27.0	0.17	1200	0.18	27.2	N/A	27.2	0.18
V1	130	Upper Shelf	27.6	0.92	5000	0.71	27.6	28.0	27.6	0.71
V3	130	Upper Shelf	31.0	1.47	8000	1.06	28.6	30.2	28.6	1.06
V6	190	Upper Shelf	31.9	2.0	8000	1.59	30.4	32.2	30.4	1.59

Entering the curves of Figure 5.7 at the J value of 1200 in.-lb/in.^{2} (=J_{Ic}) yields outer surface surface hoop strain predictions of 0.21 and 0.18, in excellent agreement with the actual failure strains. Failure pressure predictions obtained from the pressure/strain curve of Figure 5.8 were also in excellent agreement with the test results. For vessels V1, V3, and V6, which were tested on the upper shelf, values of J_{crit} for instability of 5000, 8000, and 8000 in.-lb/in.^{2}, respectively, were chosen. This was based on the intersection of the best estimate material curves and the J/T applied bands in Figure 5.9. Entering Figure 5.7 at the above J values yielded failure strain predictions of 0.71, 1.06, and 1.59, respectively, for vessels V1, V3, and V6. Once again, failure pressures were obtained from Figure 5.8. The predicted failure conditions all were reasonably conservative underpredictions of the actual experimental failure conditions. Considering some of the approximations used in the analysis, the favorable comparisons were highly encouraging.

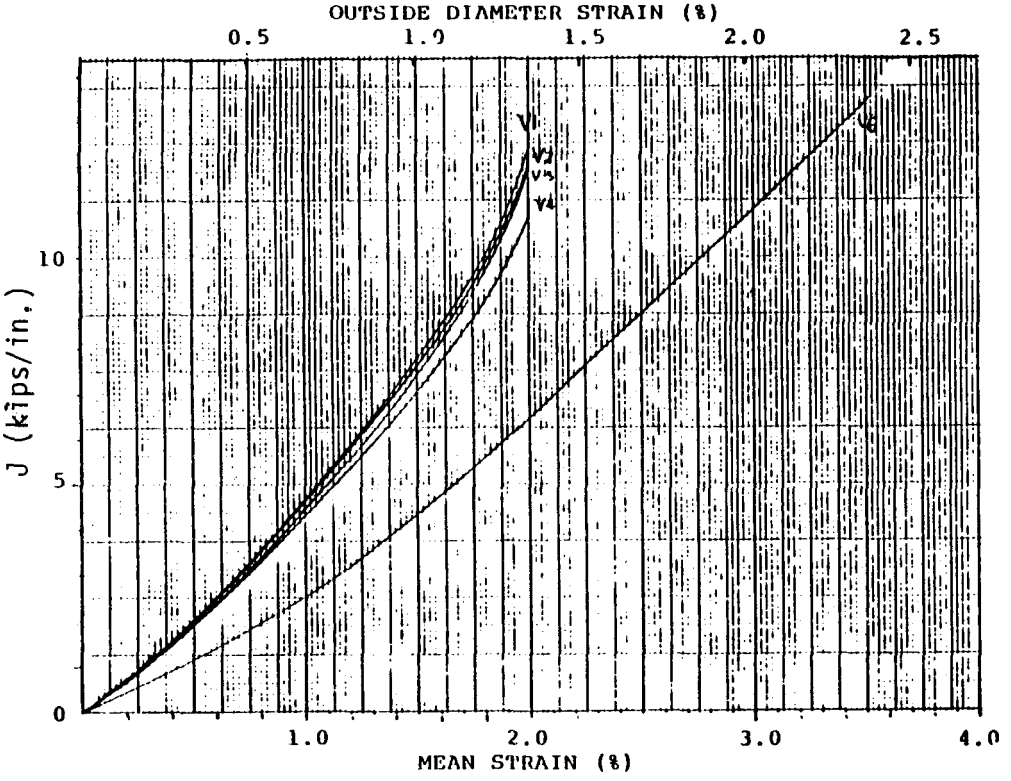

Figure 5.7 J Vs. Mean and Outside Strain for Test Vessels.

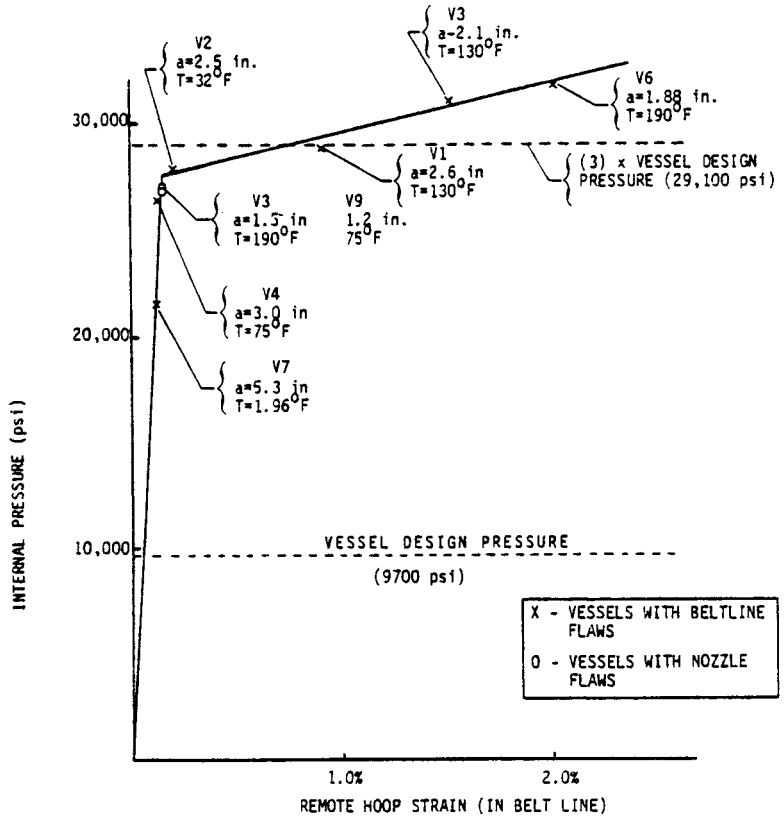

Figure 5.8 HSST Intermediate Pressure Vessels Test Data

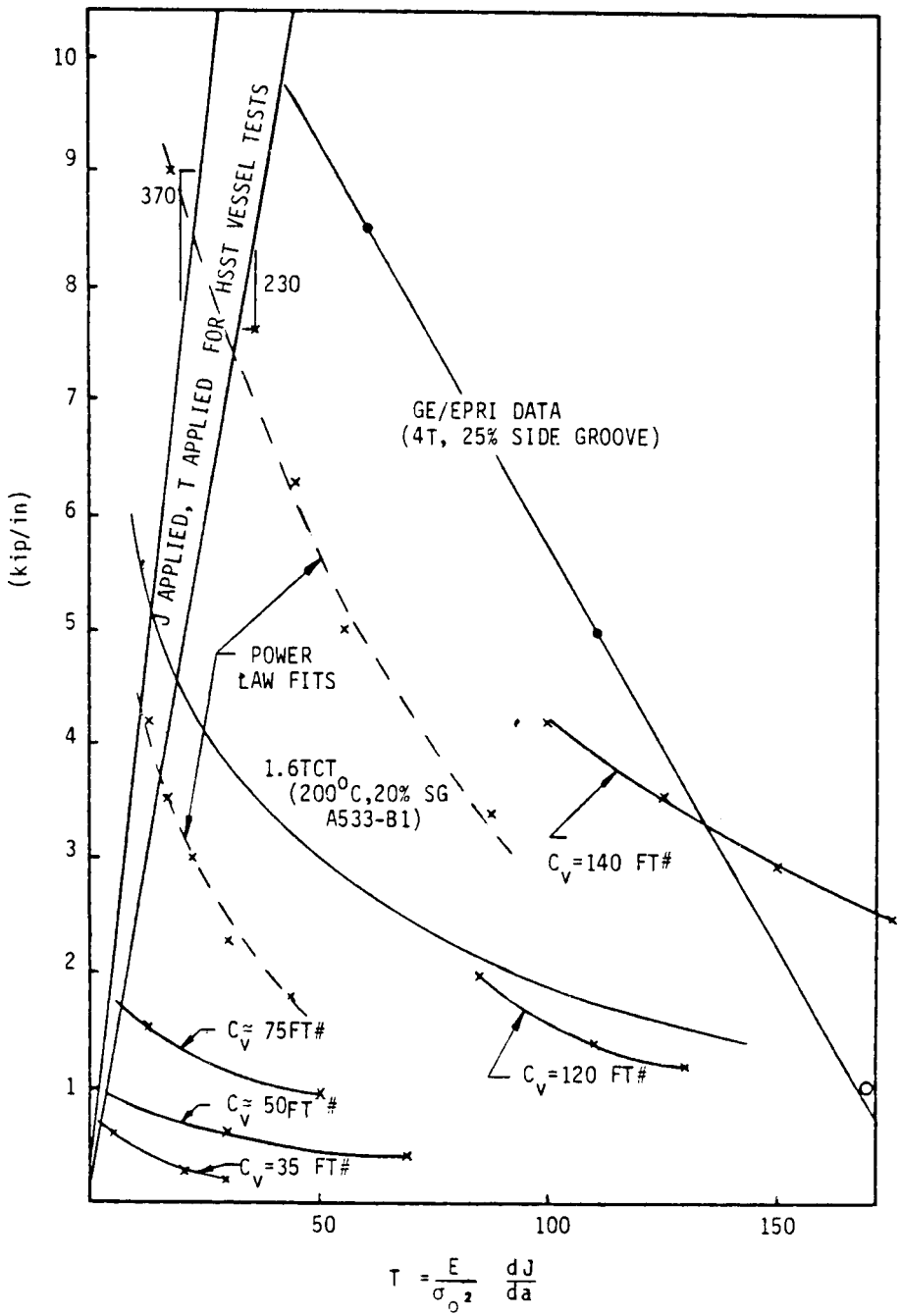

Figure 5.9 J_{mat} Vs. T_{mat} Curves of Figure B-8, Appendix G

Vessel V7 contained a 5.3-in. deep flaw, which is almost a through-thickness flaw for the 6-in. wall. During the test, the flaw propagated through the wall and caused a leak, but it did not propagate further. Therefore, in the case of vessel V7, the analysis should predict that a through-wall flaw is stable at the peak test pressure.

Vessel 7 was tested at 190°F (88°C); therefore, the critical value of J was approximately 11 kip/in. Entering this value in Figure 5.10 yielded a failure strain at the outside surface of 0.16%. The measured peak strain was actually 0.12% and no failure occurred; therefore, the analysis correctly predicted the vessel behavior.

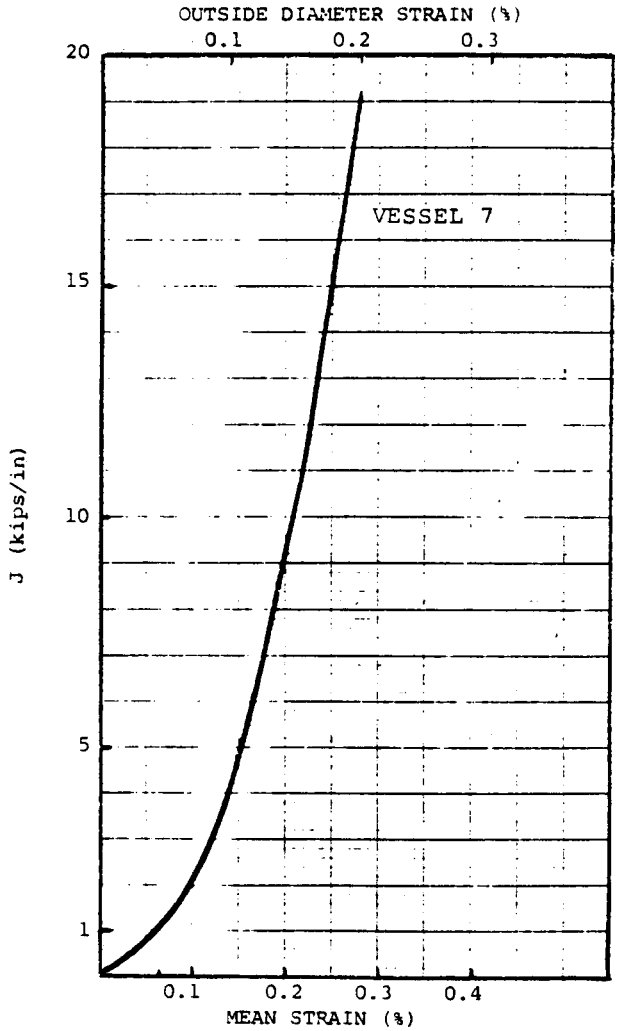

Figure 5.10 J Vs. Mean and Outside Surface Strain for Test Vessel V7

The same analysis was used to estimate J_{appl}/T_{appl} curves for a series of large, surface-cracked tensile specimens. However, the analysis neglected the effect of specimen bending induced by the presence of the crack; therefore, it was valid only as a first approximation. Tables 5.3 and 5.4 list geometry parameters and J/T values for the various tests performed. As discussed above, the approximate analysis developed by Paris (which yielded the values of ($F\ \sigma/\sigma_0$) listed in Table 5.3) was used to develop curves of J as a function of ε for the tensile specimens tested. The curves were drawn in Figure 5.11.

Table 5.3 Crack dimensions after sharpening

Specimen	a(in.)	B(in.)	J/T (lb/in.)
1	2.375	6.598	280
2	2.16	6.0	255
3	2.05	8.37	242
4	2.05	8.20	242
5	2.53	8.26	299
6	3.37	9.53	398
14	2.55	7.85	301

Table 5.4 Crack dimensions at ultimate load

Specimen	a(in.)	B(in.)	J/T (lb/in.)
1	----	----	----
2	2.86	5.91	338
3	2.05	8.37	242
4	3.45	8.02	407
5	2.53	8.26	299
6	4.33	10.25	511
14	2.90	7.85	342

The resulting J_{appl}/T_{appl} calculations were compared to the material properties (J_{matl} and T_{matl}) to predict the failure stresses and strains for the specimens. The predicted fracture strains were conservative estimates of the ultimate strains, except for test 6. This test was performed at 100°F, which is about the limit between transitional and upper shelf regimes. To account for the plane stress conditions, Paris suggested* that the J_{matl}/T_{matl} curves should be modified by coupling the J values. The modified curve is shown on Figure 5.12, with the J_{appl}/T_{appl} curve. The critical value of J is somewhere between 8 and 19 kips/in. Taking J_c as 18 kips/in. yielded new predicted strains at the ultimate; these are listed in Table 5.5 and were in better agreement, although higher than, the experimental ultimate strains.

Table 5.5 Comparison of predicted and actual strains at failure

Specimen	Strain (%) at ultimate	Strain (%) at fracture	Test Temp, °F	Predicted Strain (%) J_c=8kip/in.	Predicted Strain (%) J_c=18kip/in.
1	---	8.50	215	2.3	3.6
2	3.83	9.60	220	2.6	4.5
3	0.24	0.24	50	0.28	---
4	4.10	7.90	100	2.0	3.3
5	0.35	0.35	75	0.28	---
6	0.48	0.48	100	1.60	2.7
14	1.81	4.22	200	1.70	2.9

As part of TAP A-11, EG&G Idaho performed a sensitivity analysis, verified correction terms, and performed calculations of critical conditions using alternate analytical techniques. The sensitivity analysis and verification of correction terms were associated with the equation

$$J = \sigma_{ys}\ \varepsilon_{ys}\ a\ \{F(\frac{\sigma}{\sigma_{ys}})\}\ [\frac{M^2}{Q}] \qquad (5\text{-}19)$$

*In a private communication with P. Ricardilla, as cited in Appendix H to this report.

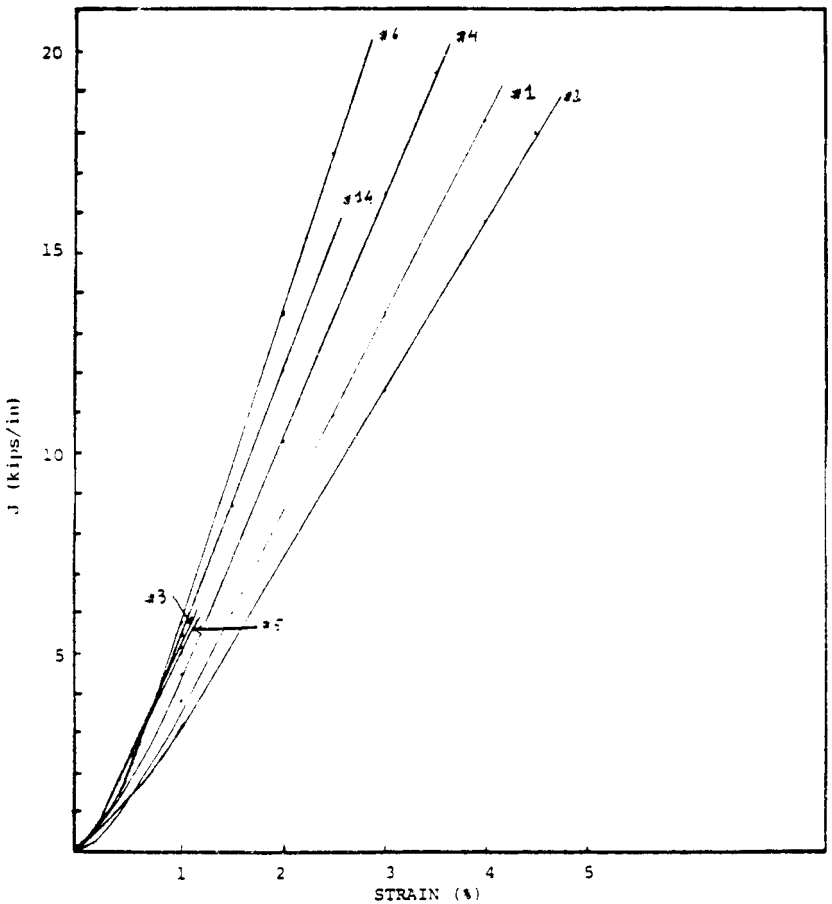

Figure 5.11 $J_{applied}$ Vs. Strain for the Large Tensile Specimens

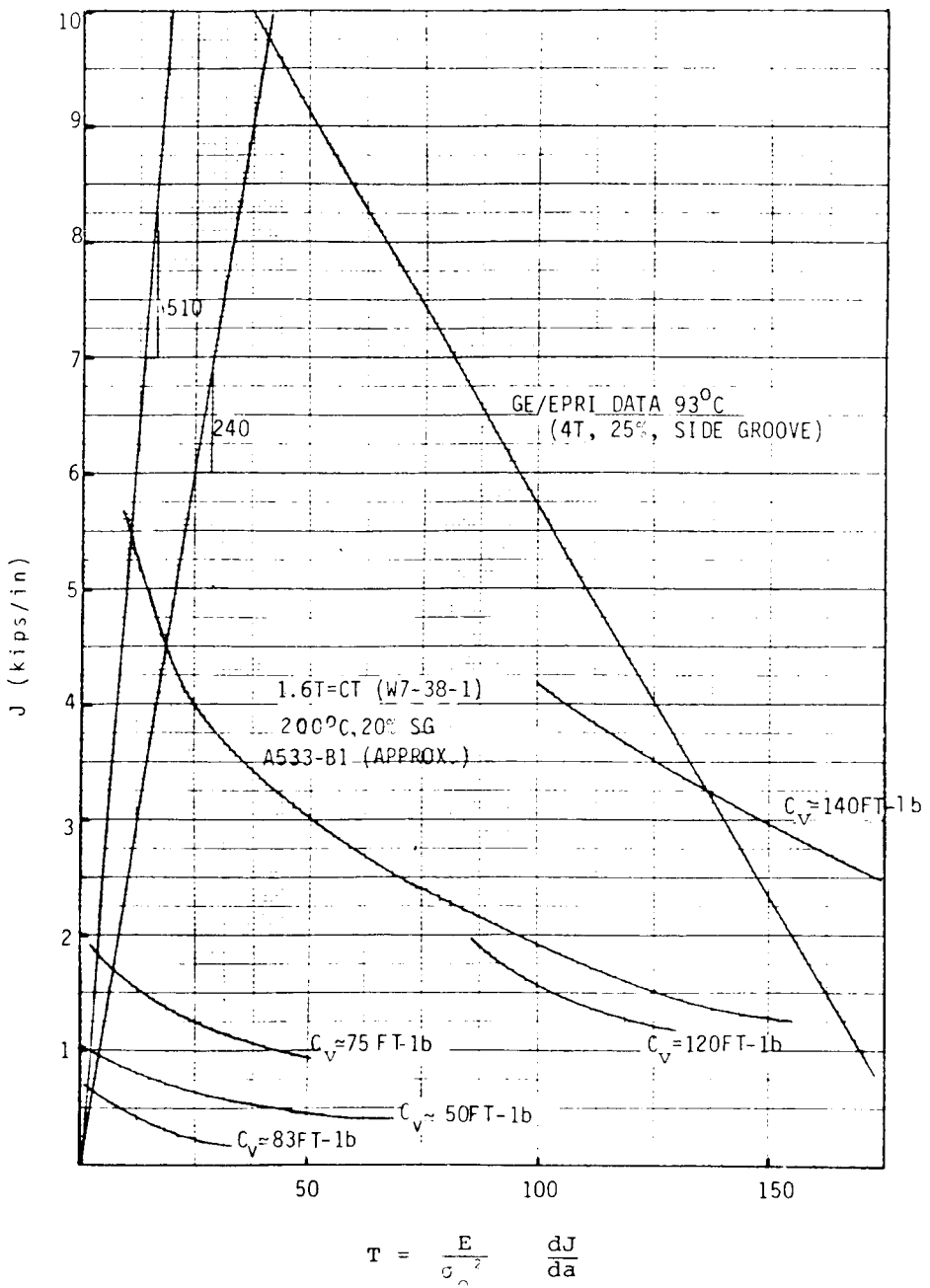

Figure 5.12 J Vs. T Curves for the Large Tensile Specimens Corrected for Plane Stress

The stress function $\{F(\frac{\sigma}{\sigma_{ys}})\}$ consists of constants for the elastic and the plastic components of stress. The sensitivity analysis was conducted to evaluate the dependence of the constants on the values of the stress-strain curve parameters. For plane-strain conditions, a relationship has been developed between $(\frac{\varepsilon}{\varepsilon_{ys}})$ $\{F(\frac{\sigma}{\sigma_{ys}})\}$.

The relationship appears to be consistent, regardless of material or experiment conditions. This relationship should be used to estimate the stress term.

The geometry correction term in Equation (5-19) included the parameters M^2 and Q. The variability of several solutions for M was evaluated for the surface flaw. For a standard (Appendix G) flaw with a/t = 0.25 and a/c = 0.17, a total variability of 11% was observed for M. A similar observation was made for Q. Therefore, the use of the correction factors M and Q obtained from Section XI of the Code will provide conservatively high values of J_{appl}. M and Q had to be evaluated for use under plasticity conditions because they were developed for elastic conditions. Experimental results were used to show that M and Q are useful in the plastic region as long as a suitable stress correction term is applied.

The effect of deleting the geometry correction term from $\delta J/\delta a$ on the calculated value of T was determined. Comparison of $\delta J/\delta a$ calculated without the geometry term compared to $\delta J/\delta a$ with the term resulted in an overestimate of 24%. The deletion would result in an overestimate of T_{matl} by 24%.

The method for reactor pressure vessel analysis based on the J-integral and tearing modulus concepts was compared with other EPFM approaches (Appendix I). Generally, the J-T method provided similar results, but its range of applicability was second to none. It was concluded that EPFM analysis using the structural and materials J-T curves provided a satisfactory basis for the resolution of the safety issue of low USE RPV steels at relatively high temperatures.

An alternate approach available through the British Standards Institute (BSI)[18] was used to calculate the maximum allowable stresses for an Appendix G-type of

defect. This approach requires that $J_{appl} \leq 0.7\ J_{crit}$. Depending on the value of C_v energy (35 or 50 ft-lb) and σ_{ys} (80 or 97 ksi), the maximum allowable circumferentially oriented stress varied from 24.5 to 28.8 ksi. A comparison of calculated maximum allowable stresses was conducted using the BSI approach and the elastic-plastic equations for J and T previously presented, after first multiplying the EPFM allowable stresses by 0.7 to bring both to a similar factor of safety. A ratio of the maximum allowable stress from the first to the second approaches varied from 1.12 to 1.03. The closeness of the two approaches is surprising, because in addition to the difference in fundamental approaches, different correlations were used relating C_v to K or J. It was concluded that the elastic-plastic fracture mechanics analysis using the structural and materials J-f(T) curves provided a satisfactory basis for the resolution of the safety issue of low USE RPV steels at relatively high temperatures.

Some RPVs have neither specimens which could be used to generate J-R curves nor available archival material from which the curves could be made. Even if such a situation applies to only one material of construction (for example, one of the welds), it would be enough to create an impasse relative to using the foregoing elastic-plastic analysis. Therefore there is a need for an indirect means of determining the relevant mechanical parameters for the irradiated steel in question. By pulling together several observations which grew out of the TAP A-11 work, it was possible to produce a potentially useful correlation between values of J which would provide a conservative estimate of unstable fracture and the corresponding C_v USE. The nature of the correlation is described in the following paragraph.

Fracture tests based on the single specimen unloading compliance procedure resulted in J-R curves which exhibited continuously changing slope, not unlike the familiar true-stress/natural-strain tensile curves. On that basis: (1) the tearing modulus, T, would be a continuously changing parameter and (2) data reduction to curves of J = f(T) would result in an hyperbola. Most importantly, the hyperbolic materials curves were observed to form a family of parametric curves, generally increasing in magnitude with the USE from C_v tests of the same material. Loading curves of $(J/T)_{appl}$ for RPVs with cracks

were determined to be straight lines out of the origin with slopes of the order 500 in.-lb/in.^{2} Thus, a loading curve of slope J/T = 50 in.-lb/in.^{2} would be a very conservative estimate of the cracked RPV behavior. Most of the hyperbolic material curves would cross the slope = 50 loading line within the range of valid experimental measurements, whereas either extrapolation or small values of ω would be met in order to reach loading lines of slope = 500, or so. When values of J at the intersections of the hyperbolic material curves with the J/T = 50 in.-lb/in.^{2} loading line were plotted against the corresponding C_V USE, a reasonably narrow, generally parabolic, scatter band was obtained (shown in Figure 5.13). The lower bound curve of the scatter band was populated with data from all varieties of material: plates, forgings, and welds, both irradiated and nonirradiated. In the absence of J-R curves for the actual RPV material(s), the lower bound of Figure 5.13 can be used to obtain a conservative value of J to be used in fracture instability calculations, along with T = J/50. As additional data become available, it may be necessary to modify the lower bound curve.

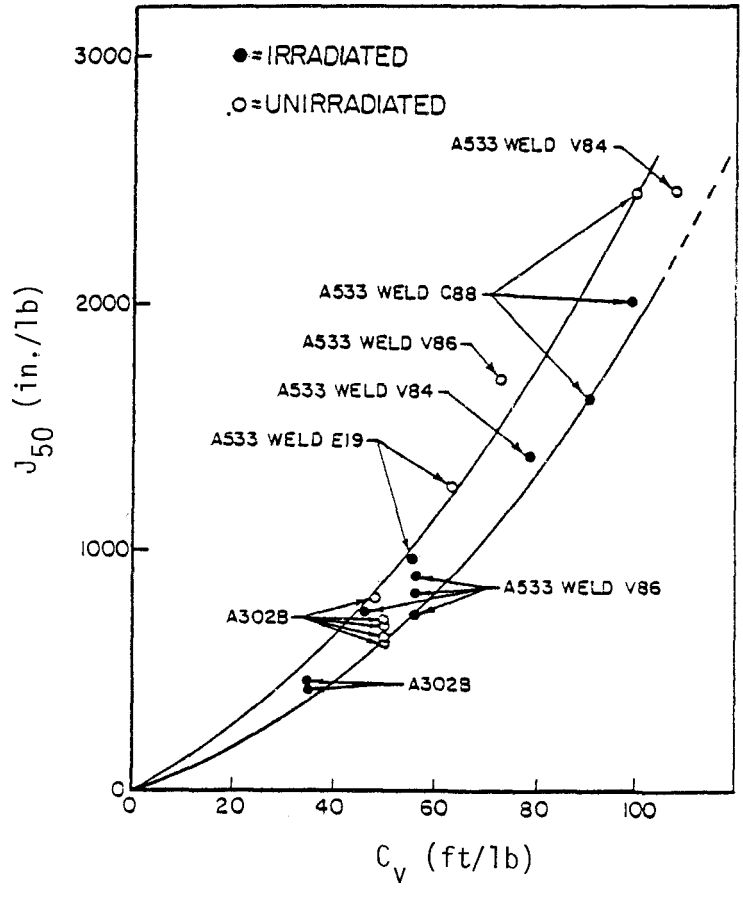

Figure 5.13 J Vs. C_V Correlation for Leak-Before-Break

Underlying the problem of discovering useful correlations between mechanical property data is the larger issue of the applicability of data obtained under laboratory conditions on small specimens to full-scale pressure vessels under operating conditions. Clearly, experiments on compact tension (CT) specimens come closer to modeling RPVs than do C_v tests, yet the latter have been accepted by the design, operating, and regulatory communities. The majority of the J-R curves used in resolving the TAP A-11 issue were obtained from CT specimens with 20% side grooves.* Results for A 533-B steel have shown that 20% side grooves are required to produce a straight crack front extension. If properly side grooved specimens approximate plane strain tearing behavior, they should be directly applicable to problems involving propagation of a surface flaw in the thickness direction of a pressure vessel wall until the crack approaches the back surface and to a longitudinal propagation direction near the midthickness of a pressure vessel wall.

*Grooves with Charpy V-notch dimensions were cut to 10% of the thickness on each side, giving a total thickness reduction of 20%.

6 LICENSING ASPECTS

The staff concludes that the approach and methodology described in the following paragraphs provide an acceptable means for all commercial nuclear power reactor licensees to meet the requirements of 10 CFR 50, Appendix G, with regard to the need to demonstrate adequate margins for continued operation when the requirements of Section V.B. (of Appendix G) cannot be satisfied.

First, all plants should establish J-T curves for all materials in the RPV, either from experimental J-R curves or by correlation with the lower bound J (at J/T = 50) = f(USE) curve. Second, the USE at the plant-specific end of life (EOL) should be established in accordance with 10 CFR 50 and the ASME Code. If the EOL USE $\geq$ 50 ft-lb, the RPV is acceptable (other factors, detailed in 10 CFR and in the Code, remain in force). If the EOL USE $\leq$ 50 ft-lb, either an EPFM analysis should be performed in accordance with the concepts and examples in the Appendices to this report, or a thermal anneal should be performed to restore the RPV material toughness.

If the EPFM analysis is performed, the safety factor should be compared with the following recommendations to determine the RPV acceptability. To determine the safety factor, failure conditions must be calculated conservatively from the J and T values at the intersection of the relevant $[J=f(t)]_{matl}$ curve and the loading line of slope: J/T=50. For normal and upset conditions (Levels A and B), the margin between failure and operating conditions must be equivalent to the margin now required by Appendix G. For emergency and faulted conditions (Levels C and D), the value of T_{appl} must be no more than one-half the value of T at the above-named curve intersection. The evaluation must recognize flaw growth at $J > J_{Ic}$. If the safety margin for some operating conditions is unacceptable, the licensee may opt to modify the plant system, plant operations, or both, to ensure that potentially damaging conditions are avoided.

The schedule for implementation of these actions for operating plants will be established concurrently with the issuing of this NUREG report in final form. With publication of NUREG-0744, the need to modify Appendix G to 10 CFR 50 (and possibly, Appendix H) will be established. The responsibility for these modifications and the timing of that task will be established by NRC.

The procedures of Appendix G of the ASME Code are applicable only to normal and upset operating conditions (Levels A and B). With respect to Levels C and D, Section III states:

> The possible combinations of loadings, defect sizes, and material properties which may be encountered during Level C and Level D limits are too diverse to allow the application of definitive rules and it is recommended that each situation be studied on an individual case basis.

One of the major reasons for not including such rules was the recognized need to consider relevant upper shelf material properties and analytical methods which were unavailable in 1972. Obviously this is a situation which has not been fully covered; further discussion is presented in Appendix J of this report.

Appendix G to 10 CFR 50 essentially adopts the ASME Code Appendix G, with additional restrictions related to the presence of fuel or of criticality. The additional restrictions will not be discussed here because they apply in the lower region of the brittle-ductile transition. However, 10 CFR 50, Appendix G, extends the applicability of the design rules to operations, and fluence effects must be considered. Because the resulting pressure/temperature limitations must be included in the Technical Specification which controls plant operation, the 10 CFR 50 Appendix G rules apply to all operating plants, not just those to which Appendix G of the ASME Code applies.

Because normal and upset conditions are limited by both Section III, Appendix G, and Section XI rules, a planned operation can be controlled in a manner which contributes to safety. In contrast, events which may occur during the initial stages of an emergency or a faulted condition are, by definition, out of control. It is not practical to try to limit operating procedures by brittle fracture prevention considerations; there are many other reasons for limiting the operation so that these events do not occur. However, it may be useful to limit plant recovery operations, such as limiting the system repressurization following a main steam line break (MSLB) by having the operator take action

10 or so minutes after initiation of the event. The most important goal of limitations on emergency or faulted conditions is assurance that the plant can be shut down and maintained in a shutdown condition. Additionally, for emergency conditions, it is desirable that the damage resulting from the event be repairable.

The need to include rules for emergency and faulted condition control in the ASME Code, Section III, Appendix G, is not clear. The Section III rules are of value only to the extent that they influence the construction (that is, materials, design, fabrication, examination, testing, and certification), and it is not apparent that such rules would have that effect. Although material selection might be influenced, indications are that the current acceptance criteria are satisfactory in that they provide adequate lifetime fracture resistance. Any major changes in the criteria would eliminate materials with which there is about 1000 reactor years of operating experience. Therefore, application of Task A-11 concepts to new plants should confirm existing procedures for material selection and qualification.

In contrast, inclusion in Section XI is essential for inservice flaw indication evaluations and to account for the effect of fluence on material properties. Such an action also has the advantage of utilizing the actual material properties for all evaluations, a possibility which Section III does not provide. It appears advisable, therefore, to include rules for evaluation of emergency and faulted conditions in nonductile failure prevention only in Section XI.

7 ANCILLARY ASPECTS

7.1 Neutron Fluence

The mechanical properties which are used in calculating high temperature safety margins of RPVs with relatively low USE are known to depend on exposure to neutron radiation. Therefore, it is necessary to know the fluence as a function of location in the vessel. However, there are some disturbing aspects to this problem both with respect to the theoretical calculations (neutronics) and the experimental determinations (dosimetry). A large, long range effort is under way, sponsored by the NRC Office of Reactor Research (RES). The solution to the neutronics/dosimetry problem is beyond the scope of TAP A-11; however, it is recognized that establishing the relevant fluence in an RPV, like the task of determining the relevant stress, must be performed by the licensee with all the accuracy and reliability warranted by the state of the art, because both become inputs to the solution to the TAP A-11 problem.*

Reactor physics codes have been written to predict the neutron spectrum and flux level in reactor surveillance and vessel wall environments. Methods, materials, and equipment are available to measure the instantaneous neutron flux and subsequent time-integrated fluence that impinge on a surveillance capsule. The predictive codes and dosimetry measurement methods, however, have been developed independently over the years and when used together in analyses they do not necessarily give accurate answers. With reasonable effort, the calculational and experimental methods can be internally consistent and calibrated to yield an accuracy not less than ± 15%. Neutron dosimetry predictions and measurements for application to surveillance programs are being upgraded and standardized. A comprehensive, vigorous research program under NRC sponsorship already has provided significant improvements. Some of the activities in the program include the following:

(1) Reactor physics calculations have been certified by referencing to benchmark flux or spectrum calculations.

*The material presented in the following paragraphs is discussed in detail in Appendix G.

(2) Dosimetry counting measurement certification procedures have been established through satisfactory comparison of counts from a test set of dosimetry foils, used as standards, to the results from surveillance capsule foils.

(3) The improvement from using displacement per atom (dpa) as an exposure or damage parameter rather than fluence >1 MeV has been demonstrated.

(4) The value of using exvessel dosimetry (between the vessel wall and the biological shield) in conjunction with surveillance programs.

(5) Existing ASTM standards have been improved and the development of new ones undertaken in a general plan to provide the means for accurate, reliable reactor vessel neutron surveillance dosimetry.

Calculations of RPV margins require material property values as inputs which, in turn, depend on the exposure to neutron radiation. The problem of ensuring proper radiation values is beyond the scope of Task A-11. It is expected that licensees and others who apply the recommended fracture mechanics engineering analyses will couple the effort with state-of-the-art fluence determinations.

7.2 Pressure Vessel Data

Because material property data are necessary for evaluating RPV integrity, TAP A-11 included a subtask of developing a computer-based program for storage and retreival of operating RPV data and a computerized system to accomplish the storage and retrieval. The program is called the materials surveillance information computer system (MATSURV) and is described in Reference 20.

The system can cross-reference between RPV materials, surveillance materials, and irradiated and unirradiated data, allowing quick identification of the limiting materials in any operating RPV and correlation of those materials with pertinent surveillance program specimens and test results.

MATSURV also includes data on operating RPV materials of fabrication, surveillance specimen materials and types, and results of pre- and postirradiation tests of surveillance specimens. General information for each plant includes plant name and unit number, the nuclear steam supply system vendor, the RPV manufacturer, reactor type, EOL fluence and fluence rate, RPV design conditions, and RPV base metal specifications. Typical examples of the data stored for RPV plates, forgings, and welds are the manufacturer's identification, steel producer, heat numbers, weld wire specification, flux type and grade, location in the RPV, EOL fluence, fluence rate, RT_{NDT}, heat treatment sequence, and chemical composition.

The staff intends to ensure the correctness and completeness of the MATSURV data, to provide the software necessary to perform safety-related RPV calculations using the MATSURV data, and to provide access to MATSURV for the nuclear industry or other interested segments of the public.

7.3 Pressure Vessel Annealing

Also at issue is the question of how an operating plant should be annealed. Details can be found in Appendix F; only brief comments are appropriate here.

Appendix G of 10 CFR 50 identifies thermal annealing as one method that may be used to restore material toughness to acceptable levels for continued operation. However, little field experience and few research results are available to help define precisely the variables that will result in the most efficient and safe annealing process. Nonetheless, although test results are limited, they are sufficient to indicate that annealing at 650°F and 750°F can restore upper shelf fracture toughness and maintain the levels above those required to comply with 10 CFR 50.

Programs sponsored by the NRC and Electric Power Research Institute (EPRI) have established that in situ RPV annealing is feasible. At the same time, the conditions (for example, maintaining 750°F for one week) suggest a difficult, costly operation. The decision to anneal will demand a thorough, indepth, engineering study. The evaluation must include the constraints imposed on the

licensee to achieve worker radiation protection at the reactor site. Environmental protection considerations will be important because to effect a 750°F anneal, the vessel internals must be removed, plant modifications may be necessary, and radioactive particulate matter may be dislodged and become airborne because there will be no primary coolant (water) present (only air or some other gas). In addition to ensuring that plant personnel and the general public are protected from accidental releases of radioactive fission and corrosion products during the annealing process, adequate consideration must be given to occupational radiation exposure, radioactive waste processing, radioactive material decontamination, and radioactive waste shipments which result from the reactor vessel annealing operation.

A single generic annealing process cannot be defined. The annealing process which would restore adequate upper shelf toughness most effectively depends on many variables and must be designed for each individual plant after a thorough engineering and safety evaluation. The variables that must be considered include the neutron fluence level at annealing, the desired period of subsequent operation, personnel exposure, fuel storage capacity, system heat removal capacity, protection of safety-related systems during annealing, the time period the annealing process will remain effective under subsequent irradiation, and verification of the annealing effectiveness. Whatever method is chosen by the licensee, it must be performed under the guidelines of keeping releases of radioactivity to the atmosphere as low as reasonably achievable (ALARA guidelines) and according to the procedures contained in Regulatory Guide 8.8.

8 REFERENCES

Documents marked with an asterisk are available from the NRC/GPO Sales Program, Washington, DC 20555, and/or the National Technical Information Service, Springfield, VA 22161. Except as specifically noted, all other documents cited are available in public technical libraries.

(1) U.S. Nuclear Regulatory Commission, "A Treatment of the Subject of Tearing Instability," USNRC Report NUREG-0311, July 1977.*

(2) U.S. Code of Federal Regulations, Title 10, Energy, Part 50, "Domestic Licensing of Production and Utilization Facilities."

(3) U. Potapovs and J.R. Hawthorne, "The Effect of Residual Elements on 550°F Irradiation Responses of Selected Pressure Vessel Steels and Weldments," NRL Report 6803, U.S. Naval Research Laboratory, Washington, D.C. (available from NTIS only).

(4) J.R. Hawthorne, "Demonstration of Improved Radiation Embrittlement Resistance of A 533-B Steel Through Control of Selected Residual Elements," NRL Report 7121, U.S. Naval Research Laboratory, Washington, D.C. (available from NTIS only).

(5) U.S. Nuclear Regulatory Commission, Regulatory Guide 1.99, "Effects of Residual Elements on Predicted Radiation Damage to Reactor Vessel Materials," Revision 1, April 1977.*

(6) American Society of Mechanical Engineers, Boiler and Pressure Vessel Code, Sections III and XI.

(7) J.G. Merkle, G.D. Whitman, and R.H. Bryan, "An Evaluation of the HSST Program Intermediate Pressure Vessel Tests in Terms of Light-Water Reactor Pressure Vessel Safety," Oak Ridge National Laboratory Report ORNL-T-5090, November 1975 (available for inspection and copying for a fee in the NRC Public Document Room, 1717 H St., NW, Washington, DC 20555).

(8) American Society of Mechanical Engineers, "PVRC Recommendations on Toughness Requirements for Ferritic Material," WRC Bulletin 175, by the PVRC ad hoc Task Group on Toughness Requirements, August 1972.

(9) J. W. Hutchinson, Journal of the Mechanics and Physics of Solids, Volume 16, 1968, pp. 13-31; J. R. Rice and G. F. Rosengren, Journal of the Mechanics and Physics of Solids, Volume 16, 1968, pp. 1-12.

(10) P. C. Paris and H. Tada, "Further Results on the Subject of Tearing Instability," USNRC Report NUREG/CR-1220, Volume I, January 1980; H. Tada and P. C. Paris, "Further Results on the Subject of Tearing Instability," USNRC Report NUREG/CR-1220, Volume II, January 1980.*

(11) H. Tada and P. C. Paris, "Tearing Instability Analysis Handbook," USNRC Report NUREG/CR-1221, January 1980.*

(12) H. A. Ernst and P. C. Paris, "Techniques of Analysis of Load-Displacement Records by J-Integral Methods," USNRC Report NUREG/CR-1222, January 1980.*

(13) P. C. Paris, "CSNI Specialists Meeting on Plastic Tearing Instability," USNRC Report NUREG/CR-0010 (also CSNI Report No. 39), January 1980.*

(14) F. J. Loss, ed., "Structural Integrity of Water Reactor Pressure Boundary Components, Quarterly Progress Report, April-June 1980," USNRC Report NUREG/CR-1783, February 1981 (also NRL Memorandum Report 4400).*

(15) P. C. Paris, H. Tada, A. Zahoor, and H. Ernst, "The Theory of Instability of the Tearing Mode of Elastic-Plastic Growth," in Elastic-Plastic Fracture, ASTM STP 668, 1979.

(16) J. E. Srawley and W. F. Brown, Jr., Fracture Toughness Testing and Its Applications, ASTM STP 381, American Society of Testing and Materials, 1965.

(17) V. Kumar and others, "Estimation of Techniques for the Components of Nuclear Systems, Semi-Annual Report," EPRI Contract RP-1237-1, to be published (draft copies available from EPRI).

(18) British Standards Institute, "Guidance on Some Methods for the Derivation of Acceptance Levels for Defects on Fusion Welded Joints," PD-6493:1980, BSI, London, 1980.

(19) J. Strosnider and C. Monserrate, "Computerized Reactor Pressure Vessel Materials Information System," USNRC Report NUREG-0688, October 1980.*

APPENDIX A

Task A-11

1. DESCRIPTION OF PROBLEM

Because the possibility of failure of nuclear reactor pressure vessels designed to the ASME Boiler and Pressure Vessel Code is remote, the design of nuclear facilities does not provide protection against reactor vessel failure. Prevention of reactor vessel failure depends primarily on maintaining the reactor vessel material fracture toughness at levels that will resist brittle fracture during plant operation. At service times and operating conditions typical of current operating plants, reactor vessel fracture toughness properties provide adequate margins of safety against vessel failure; however, as plants accumulate more and more service time, neutron irradiation reduces the material fracture toughness and initial safety margins.

Results from reactor vessel surveillance programs indicates that up to approximately 20 operating PWRs will have beltline materials with marginal toughness, relative to the requirements of Appendices G and H of 10 CFR Part 50, after comparatively short (approximately 10 EFPY) periods of operation. The specific requirement which may be violated is that of paragraph V.B, Appendix G, 10 CFR Part 50. For vessels which fail to satisfy that requirement, paragraph V.C.3, Appendix G, 10 CFR Part 50, must be satisfied (along with the rest of V.C); that is, perform an analysis which demonstrates the existence of adequate operational safety margins against fracture. For plants currently under licensing review, reactor vessels generally have acceptable fracture toughness. However, a few plants under licensing review have reactor vessels that have been identified as having the potential for marginal fracture toughness within their design life; these vessels will have to be reevaluated in the light of the new criteria for long term acceptability.

The fundamental goal of Task A-11 is to provide an engineering method to assess the safety margin for failure prevention in nuclear reactor pressure vessels. The method will employ the most advanced fracture mechanics concepts presently available. Although linear elastic fracture mechanics analyses may be applicable at low temperatures, the amount of crack tip plastic deformation accompanying fracture at high temperature will be relatively large, even in pressure vessel steels of low toughness. Therefore safety will be evaluated by comparing some measure of fracture resistance to a structural parameter, both being based on elastic-plastic fracture mechanics concepts. The concepts set forth in NUREG-0311, "A Treatment of the Subject of Tearing Instability," will be utilized to develop the required engineering method. Adequate margin will require that the structural parameter remain sufficiently below the measure of fracture resistance but the quantitative relationship may depend on the reactor plant conditions. For example, a much larger margin would be required for normal/upset conditions than for low probability accident events.

2. PLAN FOR PROBLEM RESOLUTION

The determination of appropriate licensing criteria for low toughness reactor vessel materials and the evaluation of material degradation resulting from neutron irradiation demands an interdisciplinary effort encompassing several aspects of materials and fracture technology. The plan for development of suitable licensing criteria for low toughness reactor vessel materials, including the effects of neutron irradiation damage, includes the following tasks.

A. Identify and measure the mechanical properties which control tearing instability types of fractures.

B. Develop a method for analyzing structural members that incorporates postulated flaws, under conditions which could lead to tearing instability fractures.

C. Using the results from Subtasks A and B, define reactor vessel safety criteria to avoid failure by tearing instability fracture, to supplement existing criteria for other failure modes.

D. Evaluate the feasibility of in-place reactor vessel annealing to regain toughness.

E. Evaluate actions which could lessen the severity of actual neutron radiation damage or improve the accuracy of calculations of such damage.

F. Establish a computer information system for storage and retrieval of reactor pressure vessel materials data.

Each subtask is discussed briefly in the rest of this section.

A. Evaluate Material Fracture Resistance

The measurement of fracture toughness for reactor vessel and other materials at temperatures corresponding to the upper shelf region is complicated by the presence of significant pre-fracture plastic flow. Current toughness testing methods based on linear elastic fracture mechanics are not adequate to account for plastic flow. New toughness testing techniques have been developed to allow evaluation of low toughness in reactor vessel materials for normal, upset and accident conditions.

It is widely recognized that the J-integral provides a valid, general solution to the problem of crack tip singularity fields under large-scale yielding, even up to fully plastic conditions for some geometries. Moreover, J_{IC} has been shown to provide a good indication of small-scale crack extension, although the ASTM has not yet established a standard test method for its measurement. More advanced work at Washington University, St. Louis, Missouri, under NRC funding, has resulted in the development of the tearing modulus, T, which is

proportional to dJ/da. An experimental method, developed under the Office of Nuclear Regulatory Research funding apparently can be used routinely to provide curves of J = f (Δa), the so-called J-R curves. From such data, both J_{Ic} and T_{matl} can be determined. The former has proven adequate as a general fracture parameter; the latter provides a criterion for tearing instability where a large value of T_{matl} indicates ductile tearing and a small value indicates fast fracture.

The goal of this subtask is to provide the relevant materials mechanical property data for the evaluation of reactor vessel margin against fracture at temperatures above the ductile-brittle transition (beyond the range of linear elastic fracture mechanics applicability). Task A-11 will use data provided by the RES (NRC)-funded HSST Program which will include the effects of material condition, temperature and neutron radiation.

B. Develop Structural Analysis Methods

Application of the tearing modulus concept to a reactor vessel failure evaluation requires the development of a method for determining load carrying capacity. Factors to be included in the analytical method must include the following. The geometry of the component must be a basic consideration, including postulated flaw size, shape and orientation, in a parametric way. Crack initiation and propagation will be characterized by J-integral and tearing modulus, T_{appl}, parameters. Loading conditions will include time dependence and the role of structural compliance. Temperature is a consideration to the extent that the instability analysis is applicable only above the ductile-brittle fracture mode transition. At relatively low temperatures the well-developed linear elastic fracture mechanics methods will be applicable.

The problem to be faced when considering reactor pressure vessel welds of marginal toughness is that neutron radiation can decrease the toughness, as represented by the Charpy upper shelf energy, below that required by current regulations. Because of the dominant role of radiation-induced embrittlement, the elastic-plastic response of the reactor pressure vessel beltline region will be controlling and will be the calculation used for the purpose of meeting the Task A-11 goal.

Completion of this subtask will depend on a Technical Assistance contract, funded by NRC and managed by ORNL.

Additional effort is available from existing Technical Assistance contracts with Washington University, St. Louis, Missouri and the Naval Research Laboratory.

This subtask will provide elastic-plastic fracture mechanics formulations, applicable to reactor pressure vessel beltline regions, with which relevant structural parameters can be calculated for

comparison to material properties (Subtask A) in order to evaluate failure margins.

C. Define Safety Criteria

To ensure adequate margins against failure for plants with marginal toughness materials in the reactor vessel beltline region, it will be necessary to establish suitable safety criteria for the vessels which fail to satisfy the requirements of Section V.B, Appendix G, 10 CFR Part 50. The solution is to employ the elastic-plastic fracture concepts set forth in NUREG-0311. The relevant materials mechanical properties will be those developed in Subtask A, above. The reactor vessel beltline region will be analyzed with the methods developed in Subtask B, above. The material parameters, such as J_{Ic} and T_{matl} can be compared to the structural parameters, such as J and T_{appl}. Comparison, as was done in the report "A Preliminary Fracture Analysis on the Integrity of HSST Intermediate Test Vessels" by A. Zahoor, P.C. Paris and M.P. Gomez, is expected to show that crack extension occurs when J is the order of J_{Ic} and that the fracture mode depends on the relative mass of T_{matl} and T_{appl} (where fast fractures can be avoided by keeping T_{appl} to values well below T_{matl}). This subtask will provide more realistic criteria for evaluating vessel fracture margins under normal, upset or faulted conditions at higher temperatures than the currently available linear elastic fracture mechanics. The required margin of safety will depend on analyses of available fracture data (such as the HSST vessels) and on the severity of the given operating conditions.

D. Evaluate Vessel Annealing Feasibility

Thermal annealing to recover the toughness lost by neutron radiation was recognized as a theoretically possible method to regain toughness margins. Studies are underway through contracts funded by the NRC and EPRI. The feasibility studies will assess the practicality of reactor vessel recovery annealing. Engineering guidance will be developed to help licensees determine the relative merits of vessel annealing to regain toughness.

E. Radiation Damage Abatement

The root cause of the reactor vessel toughness problem is neutron radiation. There are at least three aspects of neutron radiation which will be examined to determine their potential for reducing the severity of pressure vessel embrittlement or improving the accuracy of embrittlement calculation. The thrust of this subtask is to determine the amount of decrease in calculated mechanical property degradation which could be attained, while maintaining safety margins, by more exact neutron radiation calculations and to evaluate the potential for mitigating the problem through minor design changes.

(1) The neutron fluence through the vessel wall is calculated. Some conservatism is purposely put into the calculations. However, for marginal material, small decreases in calculated fluence could delay the point in time when the current code limits would be violated and, in some cases, could eliminate the problem altogether. The Office of Nuclear Regulatory Research, NRC, has an ongoing program which includes evaluation of neutron flux calculations and measurements. Although the program will not be completed within the term of Task A-11, early results may be used to assess the accuracy and margin of conservatism of vessel embrittlement calculations.

(2) Pre-service estimates of changes in reactor pressure vessel mechanical properties per unit fluence are based on relevant data, including those from test reactor experiments. Vessel surveillance programs, required by 10 CFR Part 50, provide closer approximation from encapsulated specimens close to the vessel wall in the same reactor environment. Surveillance data, as well as some long-term basic radiation experiments, can be used to modify relationships between fluence, inferred from calculation and measurement, and mechanical properties so that the predicted changes will be more realistic. However, test reactor neutron radiation is significantly different from that through the vessel wall, particularly with respect to dose rate and spectrum. The extent to which such results are applicable to vessel steels with marginal toughness will be examined as part of this subtask.

(3) To the extent that neutron fluence reductions can significantly reduce the rate of embrittlement, thereby delaying the advent of code violation, it is worthwhile to consider actions which would diminish the actual flux at the vessel. Shielding, for example, might be inserted between the core and the vessel. Another possibility being considered by some European operators is replacing corner fuel assemblies with dummies thus reducing the azimuthal neutron peaks.

F. Establish a Vessel Data Information System

Because of the large number of possible combinations of reactor vessel and surveillance materials and the large number of variables involved in evaluating these materials, it is necessary to develop an information system for the storage and retrieval of these data. This system will be utilized particularly to maintain up-to-date, accurate data for the generic and plant specific evaluation of operating facilities. This subtask is part of a program funded by DOE/NPD, managed by Sandia, Albuquerque, and is complete.

3. BASIS FOR CONTINUED PLANT OPERATION AND LICENSING PENDING COMPLETION OF TASK

As discussed in Section 1, the safety issue addressed by this task is the reduction of reactor vessel material fracture toughness as a result of

neutron irradiation. The operational temperature range includes the transition temperature region, where material toughness increases significantly with increasing temperature, and the upper shelf temperature region, where material toughness reaches a relatively constant maximum value. The task will develop licensing criteria to ensure that adequate margins of safety, relative to flaw-induced fracture, are maintained during normal operating and postulated accident conditions for reactor vessels containing beltline (that part of the reactor vessel directly opposite the core) material with reduced toughness after prolonged irradiation.

For most plants now in the licensing process, current criteria, together with the materials currently employed, are adequate to ensure suitable safety margins for the reactor vessels throughout their design lives. For currently operating plants, and for several plants in late stages of licensing that may have marginal toughness materials, the safety margins required by Appendix G to 10 CFR Part 50 in the transition temperature region are, or will be, maintained during normal operating conditions by appropriate shifts in the operating pressure-temperature limitation. Various analyses of accident conditions indicate that adequate material toughness in the transition temperature region will continue to be available to ensure adequate safety margins for time periods significantly in excess of that required to complete this task.

A few PWRs have reactor vessel beltline materials whose upper shelf energies may fall below levels required by Appendices G and H to 10 CFR Part 50 within the next few years. An interim assessment* was made of the safety margins with respect to flaw-induced fracture for operating vessels with low upper shelf beltine materials. The evaluation indicated that adequate margins of safety can be maintained in the interim period prior to completing this task or the postulated stress and flaw conditions specified in Appendix G to Section III of the ASME Code and required by Appendix G to 10 CFR Part 50.

Pending completion of this task, the safety margins required by Appendix G to 10 CFR Part 50 for operation in the transition temperature region can be maintained during normal operation by appropriate shifts of the operating pressure-temperature limits as dictated by the material surveillance program results and Regulatory Guide 1.99. Initial analyses submitted by some NSSS vendors and our preliminary review indicate that adequate toughness margins can also be maintained in the transition region for postulated accident conditions for up to approximately 20 years of neutron irradiation, or significantly beyond completion of this task.

Appendix G to 10 CFR Part 50 requires licensees of those plants where the beltline material upper shelf energy is predicted to fall below 50 ft-lb to conduct a 100% volumetric examination of the low toughness

*Memorandum, V.S. Noonan to D.G. Eisenhut, "Reactor Vessels with Marginal Toughness Properties," July 19, 1979.

beltline material. This examination provides added assurance that very large flaws are not present in the reactor vessel beltline region.

Should the results of this task indicate that in the future adequate margins of safety for the reactor vessels of operating plants cannot be demonstrated for both normal operation and postulated accident conditions, one or more of the following alternative measures can be taken.

(1) Reactor vessel annealing to regain material toughness in the beltline region.

(2) Increased beltline inspections using improved in-service inspection (ISI) techniques, as they become available with demonstrated required reliability, leading to a justified decrease in postulated flaw size.

(3) Modifications to the vessel internals or core design to modify the neutron flux and reduce subsequent material degradation.

(4) System modifications to limit the severity of loading (stress levels) of the reactor vessel during postulated emergency or accident conditions.

In summary, the staff considers that in the interim period the safety margins are adequate to ensure the safety of reactor vessels in currently operating plants. The current licensing criteria and the materials used for reactor vessel fabrication provide assurance that reactor vessels for those plants now in the licensing process will also have adequate margins of safety relative to flaw-induced failure. Accordingly, we conclude that while the task is being performed, continued operation and plant licensing can proceed with reasonable assurance of protection to the health and safety of the public.

4. NRR TECHNICAL ORGANIZATIONS INVOLVED

A. Engineering Branch, Division of Operating Reactors. Has overall lead responsibility in the identification of relevant reactor vessel material in licensed plants, evaluation of operating experience with neutron irradiation damage, determination of the associated degradation in reactor vessel material toughness and the evaluation and determination of an appropriate safety criterion for low toughness reactor vessel materials.

Manpower Estimates: 2.0 man-years FY 1980, 0.5 man-year FY 1981

B. Materials Engineering Branch, Division of Systems Safety. Has lead responsibility for review of experimentally determined materials fracture resistance as a function of neutron radiation, for developing the NRC position on in-place reactor vessel annealing and for evaluation of information developed during the evaluation of material toughness in licensed facilities for possible inclusion into material

toughness criteria currently used for facilities not yet licensed for operation, where appropriate.

Manpower Estimates: 0.25 man-year FY 1980, 0.1 man-year FY 1981

C. Reactor Safety Branch, Division of Operating Reactors. Has lead responsibility for review of neutron fluence calculation methods. Will advise EB/DOR with respect to the application of the results from the RES radiation damage program to the problem of predicting reactor vessel damage and the advisability of recommending shielding or core modifications to mitigate neutron damage.

Manpower Estimates: 0.2 man-year FY 1980, 0.1 man-year FY 1981

D. Environmental Projects Branch 2, Division of Site Safety and Environmental Analysis. Has lead responsibility for defining licensing criteria related to effluent and personnel exposure control during reactor vessel annealing operations.

Manpower Estimates: 0.04 man-year FY 1980

5. TECHNICAL ASSISTANCE

Technical assistance from organizations outside the NRC will be required to complete Tasks A through F in Section 2, Plan for Problem Resolution, i.e., all aspects of the Task Action Plan. The contractors assisting in these tasks are as follows:

A. Contractor: ORNL (EB/DOR)

Funds Required: $80K FY 1980

The scope of this program includes three tasks. The first is material evaluation wherein available experimental results will be revised to establish relevant fracture mechanics parameters and the effect of size and neutron radiation on them. The second is reactor vessel analyses wherein existing plastic-elastic fracture mechanics concepts will be used to develop a crack instability predictive method applicable to the reactor vessel beltline region and compared to available vessel test data. The third is evaluation wherein the results of the other two tasks will be compared to the criteria of existing codes (ASME and 10 CFR 50). Details of the program are currently being developed by ORNL. This may reveal the need for more funds to complete the work than the current $80K allocation.

B. Contractor: Washington University (EB/DOR)

Funds Required: $80K FY 1980

This program is directed specifically at Tasks 2-A, 2-B, and 2-C. The results of the program will allow advanced fracture mechanics techniques to be used to establish a technical basis for NRC's

development of a suitable licensing criterion for low toughness materials. Associated with this is the determination of simplified analytical techniques to evaluate normal operating conditions, postulated accident conditions and assistance in plant specific analyses.

C. Contractor: Naval Research Laboratory (EB/DOR, MTEB/DSS)

Funds Required: $75K FY 1980

This program will investigate neutron irradiation of reactor vessel steels and is directed specifically at Task 2D, Evaluate Vessel Annealing Feasibility. The results should provide improved means to quantitatively describe the effects of material microstructure, chemical composition, neutron spectra and dose rate and allow suitable evaluation, prediction and monitoring of irradiation damage to reactor vessel steels. Included in this program is a study of the feasibility of in-place annealing of reactor vessels to restore fracture toughness to levels that will provide adequate safety margins.

D. Contractor: Brookhaven National Laboratory (RS/DOR)

Funds Required: $5K FY 1980

This program will provide independent neutron flux (fluence) calculations including the effects of core and structural configurations and energy spectra.

6. INTERACTION WITH OUTSIDE ORGANIZATIONS

A. Licensees

Intermittent interaction with licensees is expected for the purpose of obtaining required materials data.

B. NSSS Vendors

Some plant specific analyses have been conducted by the NSSS vendors. Review of the portions of these analyses relevant to completion of the generic task will be required. Some NSSS vendors have first-hand knowledge of fabrication and materials data relevant to low material toughness; review of these data will be required.

C. EPRI

EPRI is currently funding a number of programs related to reactor vessel materials toughness. These programs include studies for neutron irradiation damage of pressure vessel steels and the development of fundamental failure criteria based on elastic-plastic fracture mechanics. Interaction with EPRI to remain informed on the direction and results of these programs and to ensure that appropriate NRC licensing concerns are addressed will be required.

D. ACRS

This task is closely related to one of the generic items identified by the ACRS and, accordingly, will be coordinated with the Committee as the task progresses.

E. Sandia (Albuquerque)/DOE

A program in support of Task A-11 was funded by DOE and managed by Sandia, Albuquerque, during FY 1979. The program had two stated goals: (1) develop an information system to complete Subtask F and (2) develop an analysis for assessing the fracture failure margin of reactor vessel beltline regions using elastic-plastic concepts as described in Subtask B. Contracts were let for both goals. The contractor given the job of developing a computer program for storage and retrieval of reactor pressure vessel data completed the work; the contractor given the job of developing an elastic-plastic vessel analysis could not complete the work within the limits of available time and money.

7. ASSISTANCE REQUIREMENTS FROM OTHER NRC OFFICES

A. Office of Nuclear Regulatory Research, Division of Reactor Safety Research, Metallurgy and Materials Branch.

RES is funding a major experimental research program (Heavy Section Steel Technology, HSST) through Oak Ridge National Laboratory to determine the fracture toughness of reactor vessel steels and the safety margins for reactor vessels. At the request of NRR, RES modified this program to include materials with low toughness, representative of those at operating facilities. (Subtask A)

At the request of NRR, RES is supporting a program to verify experimentally the application of the tearing stability concept as a failure criterion for beltline materials with marginal fracture toughness. (Subtask A)

RES initiated a comprehensive research program to experimentally validate neutron irradiation damage in pressure vessel steels and the associated calculational schemes used to predict radiation damage. This effort is to be part of an overall program being conducted in cooperation with research groups in the US and Europe. (Subtask E)

B. Office of Standards Development, Division of Engineering Standards, Structures and Components Standards Branch.

SD is assisting NRR in the study of the effects of neutron irradiation and the evaluation of low toughness reactor vessel steels. (Subtask C)

C. Office of Management Information and Program Control, Division of Regulatory Information Systems, Processing and Programming Branch.

MIPC provides assistance to NRR toward the goal of establishing a computer-based information system for the storage and retrieval of materials surveillance data. (Subtask F)

8. POTENTIAL PROBLEMS

The technical information required to complete Subtasks A (experimental) and B (analytical) must be developed by advancing the elastic-plastic fracture mechanics state-of-the-art. Therefore, although the contractors and their corresponding NRC Technical Contacts estimate that the work can and will be completed on schedule, unforeseen additional works needs and delays in completion may be encountered as was the case in 1979.

APPENDIX B

A METHOD OF APPLICATION OF ELASTIC-PLASTIC FRACTURE MECHANICS TO NUCLEAR VESSEL ANALYSIS

By Paul C. Paris
Professor of Mechanics
Washington University
St. Louis, Missouri

Manuscript Submitted: January 1981

A report produced under
subcontract K-8195 for
EG&G Idaho, Inc. By Del
Research Corporation
- FIN A-6419 -

Blank Page

ABSTRACT

The primary purpose of this work was to provide analytical methods for assessing the safety of nuclear reactor pressure vessels against fracture when the material Charpy upper shelf energy may fall below 50 ft-lb because of neutron radiation damage. The approach made use of "tearing instability" concepts under "J-controlled growth" conditions for the crack stability criterion. The above purpose was served by developing fracture mechanics methods of wider applicability than previously available for analysis at upper shelf conditions (above transition temperature). Elastic-plastic fracture mechanics was used to extend recognized linear elastic fracture mechanics flaw analysis equations for through-the-thickness flaws and surface flaws into the plastic range. The approach also made use of J-R curve characterization of the material fracture resistance.

A crack stability diagram in the form of J as a function of T plot was shown to be useful in demonstrating safe levels of loading (applied J) by comparison to the material J-R curve, plotted on the same diagram. Limits of applicability also are readily assessed on the diagram. Consequently, a safe level of applied load, J_{50} (for J/T = 50), was suggested and the possibility of its correlation with upper shelf Charpy energy values discussed.

Blank Page

CONTENTS

FIGURES

ACKNOWLEDGEMENTS

This analysis has been developed and this report produced under a subcontract (K-8195) between the author and EG&G, Idaho (Nuclear) Incorporated. The encouragement of R. Johnson of (NRC) and R. Gamble (formerly with NRC, now with EDS Nuclear) is gratefully acknowledged as essential to this work. Their continued guidance, experienced perspectives, and earlier direct technical support has been most effective and is due utmost thanks. The financial support of other programs at Washington University (St. Louis) by NRC contributed effectively to the origins of the analysis herein. The use of J versus T diagrams, as further developed here, was originated in earlier unpublished work with Societe Technigaz.

APPENDIX B

A METHOD OF APPLICATION OF ELASTIC PLASTIC FRACTURE MECHANICS TO NUCLEAR VESSEL ANALYSIS

INTRODUCTION

The ASME Boiler and Pressure Vessel Code for nuclear reactor pressure vessels has for some time permitted the use of linear-elastic fracture mechanics (LEFM), specifically in Appendix A of Section XI. This has allowed clear and conservative evaluations of any potential danger due to flaws found in inspections of reactor vessels. However, LEFM, as incorporated in the Code, has a limited range of direct applicability without large and perhaps undue conservatism. Moreover, the Code version of LEFM makes use of the K_{Ic} - K_{Id} concept of impending failure (little or no crack growth), instead of the more advanced concepts of flaw or crack stability permitting limited stable flaw growth. Under the use of LEFM, the Code itself acknowledges ranges of inapplicability such as well above the transition temperature where LEFM cannot produce applicable quantitative results. Appendix A provides no specific criteria for upper shelf toughness; the situation was discussed in Reference 1. In Title 10 of the Code of Federal Regulations Part 50 (10 CFR 50), a lower limit is imposed on the Charpy upper shelf energy (USE), namely 50 ft-lb. For materials of less USE, unspecified methods must be used to assure safety. On the other hand, the current ASME Code provisions using fracture mechanics have served very well in cases of appropriate quantitative applicability.

In recent years, a great deal of progress has been made in J-Integral-based elastic-plastic fracture mechanics (EPFM). In particular, a more advanced crack stability criterion has been developed[2,3] and widely accepted[4,5] which depends on the whole J-Integral R curve for material characterization (rather than a single value such as K_{Ic}, which is more limited). These and other advances in EPFM make possible the suggestion of new methods for application to nuclear vessels.

The new methodology presented in this report is proposed on its own merit but is phrased with the existing Code in mind in order to supplement it with alternative methods in areas such as upper shelf conditions where the existing Code seems lacking. Indeed, the most realistic postulated vessel failure conditions are usually well within the elastic range for gross section stresses but may include occasional cases of large scale yielding. Therefore, only modest modifications of current methods of vessel flaw stress analysis will be suggested. On the other hand, more ductile, perhaps fully plastic, failures are characterized by significant amounts of stable flaw growth. Therefore, a more advanced (R-curve) stability concept will be suggested, especially for material property evaluation purposes. The new methodology can be considered as an extension of the existing Code methods, written in terms of J-Integral EPFM, for which LEFM is simply a special case.

Indeed, the only really new embellishment to be presented herein is the use of a J versus T diagram to assess crack instability. It is simply a new diagramatic representation of J-R curve material representation and applied J-T curves from established methods. It is proposed to clarify situations which will lead to crack instability, to simply delineated regions of rigorous applicability of the analytic concepts, to clearly demonstrate safety margins for approaching instability, and so forth. However, the use of J versus T diagrams involves no new assumptions; it is just a new representation method which clarifies many matters. One further result, which will be demonstrated, is that the limiting allowable J values suggested herein to avoid crack instability on the J versus T diagram have, so far, shown good correlation with Charpy upper shelf energies. This can be of great practical significance where only Charpy data are available.

THE PLANE-STRAIN J-INTEGRAL R CURVE

According to developments by Hutchinson[6] and Rice and Rosengren,[7] the value of the J-Integral (or $J_{applied}$) can be seen to be a parameter characterizing the intensity of the plastic stress-strain field surrounding the crack tip. Their results lead to the following form for the stress-strain field; that is, the HRR field

$$\sigma_{ij} = \sigma_0 \left(\frac{J}{r\varepsilon_0\sigma_0}\right)^{\frac{1}{n+1}} \bar{\Sigma}_{ij}(\theta, n)$$

$$\varepsilon_{ij} = \varepsilon_0 \left(\frac{J}{r\varepsilon_0\sigma_0}\right)^{\frac{n}{n+1}} \bar{E}_{ij}(\theta, n) \qquad (1)$$

plus higher order terms (negligible near a crack tip). The coordinates r and θ are the usual cylindrical coordinates measured from the crack tip. The analysis was based on adopting a deformation theory of plasticity for a stress-strain curve whose latter portion (well beyond the elastic range) can be represented by a power law or

$$\frac{\varepsilon}{\varepsilon_0} = \left(\frac{\sigma}{\sigma_o}\right)^n \qquad (2)$$

then $\bar{\Sigma}_{ij}$ and $\bar{E}_{ij}$ are particular specified functions for the distribution of stresses and strains surrounding the crack tip.

The above approach assumes that two different cracks in the same material will have identical stress-strain fields surrounding the crack tips if loaded to the same intensity, J. It follows that if the stress and strain fields for the two cracks are identical then what happens within them is identical, such as increments of extension, Δa of the tips of the cracks. Hence, it is argued that a plot of J versus Δa, the J-R curve, is a unique plot of a material's crack extension characteristics. Indeed, this is the very same argument upon which LEFM is based for K-controlled crack tip fields. Though the logical basis of the J-R curve is equivalent to that of LEFM, the assumptions, conditions, and limitations should be clearly specified because they are less familiar than those for LEFM. Unless otherwise specified, they are

(1) that conditions in the material's crack tip fracture process zone are plane-strain

(2) that conditions which disrupt the HRR field are avoided, such as avoiding concentrated slips direct from the crack tip to nearby boundaries or cross-slip (slip at 45° through the thickness)

(3) that crack growth does not disrupt the HRR fields

(4) that cleavage does not intercede on the J-R curve.

Indeed, J-R curves produced by the types of test conditions proposed by ASTM Committee E-24 for standards at least attempt to be sufficient to avoid conditions (1) and (2) as problems. Indeed, condition (4) is thought not to be a problem at temperatures exceeding 100°C above the transition temperature (beginning of upper shelf); but, more data on this point may be needed. Finally, (3) is not a problem under conditions proposed by Hutchinson[3] which are

$$\omega = \frac{dJ}{da}\,\frac{b}{J} >> 1$$

and (3)

$$\Delta a << b$$

Hutchinson[3] showed by differentiating (1), obtaining the increments of the strain, $d\varepsilon_{ij}$, that these increments $d\varepsilon_{ij}$ are sufficiently proportional to ε_{ij} to ensure appropriate use of deformation theory. The use of J itself here is also based on having conditions sufficiently appropriate for deformation theory. Hence equations (3) also ensure sufficient conditions for the definitions of J in its integral forms to follow. [It should be noted that sufficient conditions are distinct from necessary conditions, and therefore equations (3) may not always be required for appropriate use of J.]

Therefore, under the given conditions the applicability of "strict deformation theory" is appropriate, the conditions for so called "J-controlled crack growth" are met, and J may be defined with equal validly either by its contour integral or compliance counterparts which are, according to, Reference 8 (see also Reference 9 for details):

$$J = \int_{\Gamma} W dy - T_i \frac{\partial u_i}{\partial x} ds$$

(Γ is any contour around the crack tip)

or

$$J = -\int \frac{\partial P}{\partial a} d\sigma_p = \int \frac{\partial \sigma_p}{\partial a} dp \qquad (4)$$

Consequently, the "plane strain J-R curve," as shall be adopted here, is assumed to be produced under appropriate conditions as discussed under the four conditions stated above. J should be measured by a method consistent with applying equations (4), including crack length change, Δa, corrections. The J-R curve is then a plot of J versus Δa points as loading progresses on a cracked sample of the material at a given temperature.

Further, the J-R curves available may not always have been produced under ideal conditions (often undersized test specimens). This will not rule out their use if they can be shown to be conservative. For example, slightly subsized samples and/or the use of side grooves with appropriate data reduction methods have been shown to give conservative J-R curves for bending-type tests. As used here, conservatism is taken with respect to safety when the test results are used to evaluate applications by the methods developed later in this report.

THE TEARING INSTABILITY CRITERION

In equations (1) above it was noted that J is the intensity of the crack tip stress and strain field. Moreover, with proportional straining as guaranteed by meeting the conditions of equations (3), it can be argued that appropriate use of "strict deformation theory" and "J-controlled crack growth" will result. Therefore, at least under these conditions, the second definition of J in equations (4) implies that

$$J_{applied} = \frac{dU}{da} \tag{5}$$

where U is pseudo-elastic energy per unit thickness stored (that is, for the nonlinear elastic analogue to an elastic-plastic material) by applying loads or deformation to the cracked body of interest. Regarding crack length change, da, as a displacement, $J_{applied}$ takes on the connotation of a generalized force and $J_{material}$ may be regarded as the material's resistance to that force.

Consequently, a statement of equilibrium with respect to crack extension is

$$J_{applied} = J_{material} \tag{6}$$

The stability of the equilibrium expressed by equation (6) can be found by examining the second derivative of system energy. Using equation (5), the stability criterion can be written

$$\frac{d^2U}{da^2} = \frac{dJ_{applied}}{da} \begin{matrix} < \\ = \\ > \end{matrix} \frac{dJ_{material}}{da}. \tag{7}$$

For convenience, the tearing modulus, T, is defined as

$$T = \frac{dJ}{da}\frac{E}{\sigma_o^2} \tag{8}$$

where E is elastic modulus and σ_o is flow stress. Then the stability criterion, equation (7), may be expressed in nondimensional terms by

$$T_{applied} \begin{matrix} < \\ = \\ > \end{matrix} T_{material} \begin{matrix} \text{(stable)} \\ \text{(indifferent)} \\ \text{(unstable)} \end{matrix} \tag{9}$$

Now, $J_{applied}$ may be found from the stress analysis solution for the cracked body, applying equations (4) to make the determination. Consequently, $J_{applied}$ will depend on applied loads, P, or deformations, Δ, and crack size, a; hence

$$J_{applied} = J_{applied}\ (P, a)$$

or

$$= J_{applied}\ (\Delta, a) \tag{10}$$

On the other hand, $J_{material}$ depends on the material's resistance or its J-R curve, which is a plot of J versus Δa, characterizing the material's resistance to crack extension. Consequently,

$$J_{material} = J_{material}\ (\Delta a) \tag{11}$$

Therefore, when derivatives $\frac{d}{da}$ are taken of equations (10) and (11) to form $T_{applied}$ and $T_{material}$ as indicated in equation (8), it should be noted that $T_{material}$ may be formed from the slope of the J-R curve, $\frac{dJ_{material}}{da}$, taken at a given level of J. That is to say,

$$T_{material} = T_{material}\ (J) \tag{12}$$

On the other hand,

$$\frac{dJ_{applied}}{da} = \frac{\partial J_{applied}}{\partial P} \cdot \left(\frac{\partial P}{\partial a}\right) + \frac{\partial J_{applied}}{\partial a}$$

or

$$= \frac{\partial J_{applied}}{\partial \Delta} \cdot \left(\frac{\partial \Delta}{\partial a}\right) = \frac{\partial J_{applied}}{\partial a} \tag{13}$$

where the partial derivatives of $J_{applied}$ on the right sides of equations (13) are found from $J_{applied}$ solutions in the form of equations (10). The other ( ) partial derivatives in equations (13) depend on the load application system compliance and must be evaluated accordingly. Furthermore, assuming that the quantities in equations (13) are properly evaluated, it is observed that

$$T_{applied} = T_{applied}\ (P, a)$$

or

$$= T_{applied}\ (\Delta, a) \tag{14}$$

Regarding equations (10) and (14) as parametric equations for $J_{applied}$ and $T_{applied}$, the loading parameter P or Δ may be eliminated between them. Making use of the statement of equilibrium from equation (6)

$$J_{applied} = J_{material} = J$$

then

$$T_{applied} = T_{applied}\ (J,\ a) \tag{15}$$

The result is that both $T_{applied}$ and $T_{material}$ in equations (12) and (15) may be thought of as functions of J, where increasing J is viewed as the variable indicating increasing load or deformation applied to the body. Moreover, the crack size, a, in equation (15) may be regarded as an initial crack size, a_0, plus the change in crack size, Δa, from the increase in J as determined from equation (11) or the material's J-R curve. That is to say that

$$a = a_0 + \Delta a$$

where

$$\Delta a = \Delta a\ (J) \tag{16}$$

is determined by the J-R curve (or Δa may be negligible compared to a_0 in some cases). Therefore, as loading progresses and J increases, $T_{applied}$ may be computed by equation (15) with (16) and $T_{material}$ by equation (12) then compared, according to equation (9), to determine the first value of J or the loading which causes instability.

This approach to determining instability will be exploited graphically in the next section where J versus T diagrams will be used as a method of exploring crack instability problems.

THE J VERSUS T STABILITY DIAGRAM

Consider a schematic representation of $J_{material}$ and $T_{material}$ on a J versus T diagram, using a side-by-side plot of the material's J-R curve (Figure 1). Given the material's J-R curve, the left-hand diagram of Figure 1, at any J

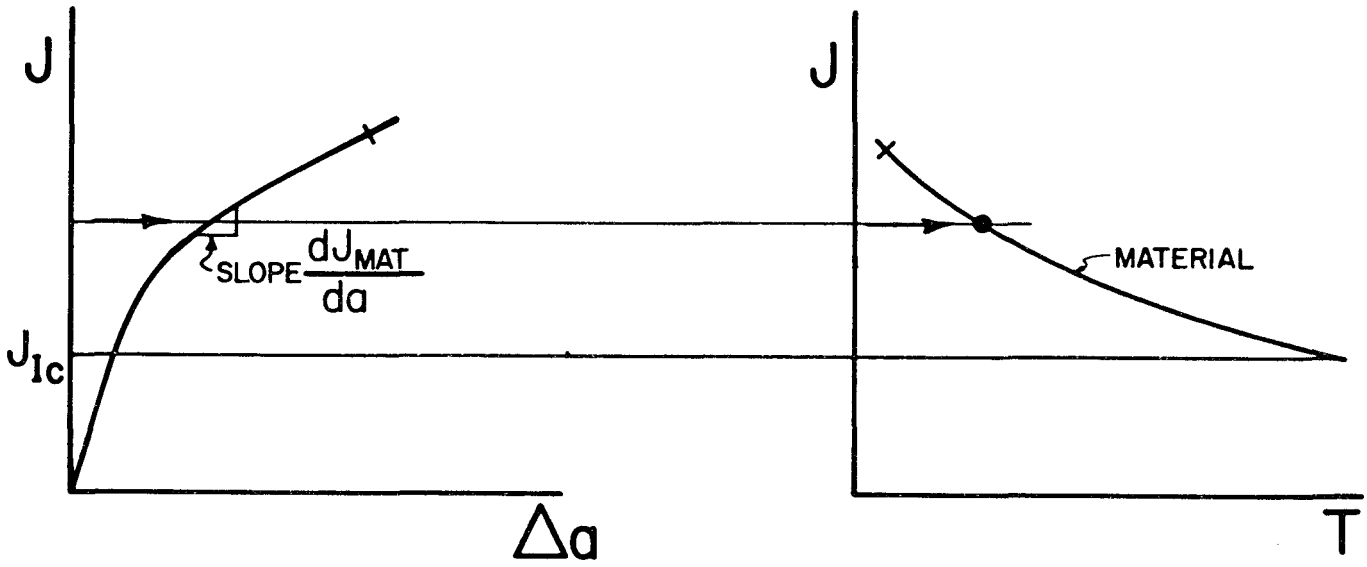

Figure 1 A material's J-R curve replotted on a J-T diagram

such as indicated by the arrow, the slope, $\frac{dJ_{material}}{da}$, may be determined. As defined by equation (8), then

$$T_{material} = \frac{dJ_{material}}{da} \frac{E}{\sigma_o^2} \tag{17}$$

which establishes a point on the J versus T diagram on the right in Figure 1. Repeating the procedure at various J values will result in the J versus T material curve. Note that below J_{Ic} no crack extension takes place so $T_{material}$ is very large (that is, off scale). In this way, J-R curves can be transformed directly into J versus T-mat. curves.

In a typical J-R test, the remaining uncracked ligament, b, is the proper dimension to determine ω as defined by equations (3).

Therefore, dividing $J_{material}$ by $T_{material}$

$$\frac{J}{T}_{material} = \frac{J \sigma_o^2}{\frac{dJ}{da} E} = \frac{\sigma_o^2 b}{E \omega} \tag{18}$$

Consider the conditions of assured validity, equations (3). As shown on Figure 1, a crack extension limit ($\Delta a << b$) may be placed on the R curve, with a corresponding mark at the same J level on the J versus T-mat. curve. Another limit (from equations (3)) can be represented in Figure 2 by a line of slope $\frac{\sigma_o^2 b}{E \omega}$

representing equation (18). The actual material properties (σ_o and E), specimen size (b), and smallest acceptable ω (perhaps 5 or smaller) determine the slope and, therefore, the intersection with, and the ω limit of, the materials curve. Therefore, the J versus T-mat. curve may be doubtful above the lower of these two limits. (It is presumed that all other J-R curve test requirements and practices are met satisfactorily.)

All J versus T material curves which have been plotted to date have shown concave upward behavior. Physical reasons why this should be observed will be omitted here. Accepting this empirically observed behavior, the material curve, at least from below the limit marks, could be extrapolated upward as a straight line extension of the valid curve to determine a safe J versus T loading region as shown on Figure 3. That is to say that if a cracked sample of the same material is loaded to a certain J-level, and the applied ($J_{applied}$, $T_{applied}$) point is in the "safe region" as shown in Figure 3, then for that J-level, $T_{applied} < T_{material}$ and the crack is stable according to equation (9).

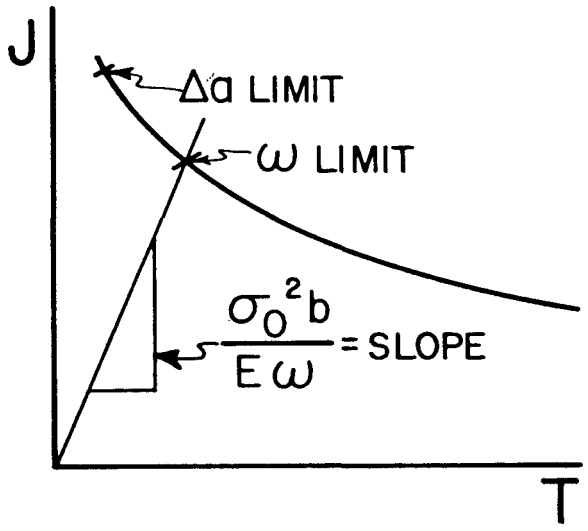

Figure 2 Assured validity limits noted on a J-T diagram

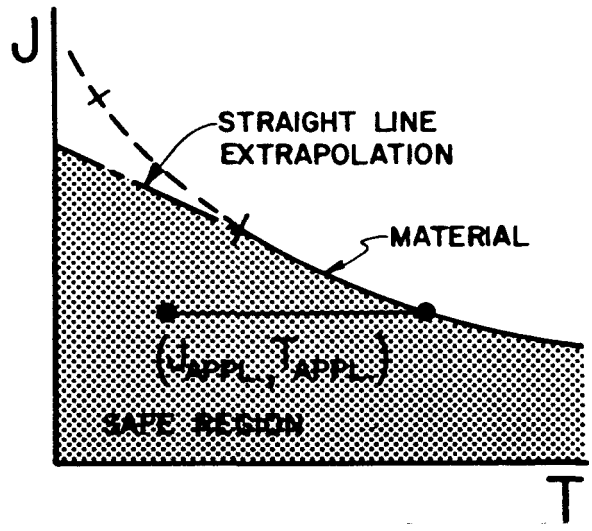

Figure 3 The safe region (J_{appl}, T_{appl}) for a given material

It remains to determine the trace of the ($J_{applied}$, $T_{applied}$) points for $T_{applied}$ (J)-curve, as loading or J increases, starting with no load. However, it is sufficient to observe that for the applications to be considered here*, the $T_{applied}$ curves always increase monotonically with J whereas the $T_{material}$ curves decrease monotonically with J, so the intersection of the two curves uniquely indicates the onset of instability; that is, no prior instabilities (intersections) can occur. This is illustrated on Figure 4.

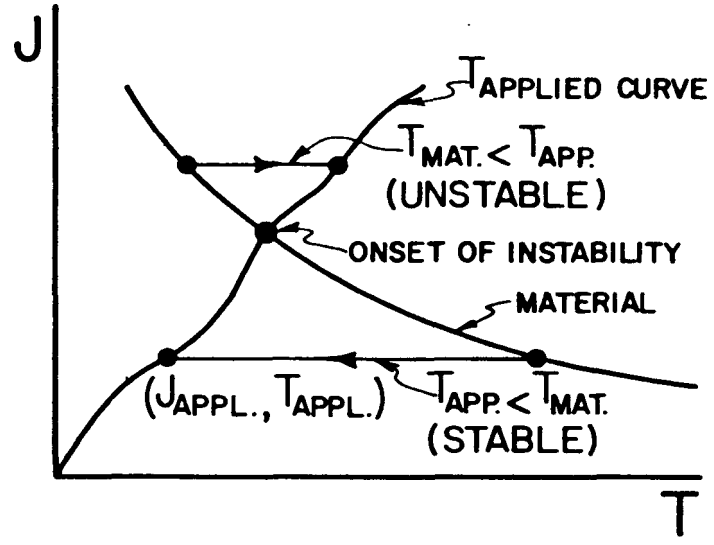

Figure 4 A schematic T-applied curve extending to instability

Analysis of typical $T_{applied}$ curves for the applications of interest will follow to demonstrate the monotonic increasing J versus $T_{applied}$ behavior. On the other hand, there are other applications such as testing for which always stable conditions are sought (in bending where $T_{applied}$ = negative). These are treated in earlier studies[2] sufficiently for the objectives of this current work. Nevertheless, it is noted and the reader is warned that other relevant considerations must be made where widely different loading conditions and crack configurations exist, such as plastic bending of nuclear piping with through-wall cracks. However, for the normal conditions and postulated flaws for pressure vessels, the J versus $T_{applied}$ behavior will follow a consistent pattern, as will be shown.

*Cracks in pressure vessel walls primarily loaded with internal pressure are considered here.

ANALYSIS OF J VERSUS T APPLIED CURVES FOR THROUGH CRACKS IN PRESSURE VESSEL WALLS

Under the actual pressures expected in nuclear pressure vessels, the shell stresses remain linear elastic and LEFM conditions apply. At a temperature high enough to be well into the Charpy upper shelf region and for flaw sizes of interest, it may take stresses approaching yield or higher to cause actual crack instabilities. Moreover, in assessing measured crack instabilities in model or full scale vessel tests, the necessary pressures resulted in stresses near or exceeding the yield of the material. Therefore, along with the previously developed J versus T diagram, stability analysis, and material characterization, it is necessary to develop analytical equations for $J_{applied}$ and $T_{applied}$ which are accurate when applied in the LEFM range and which also can be applied in the range where stresses exceed the yield strength. Thus factors of safety and/or results of vessel tests may be assessed at least approximately.

A. Linear-Elastic Format

In the linear-elastic range it is noted that

$$J = \frac{K^2}{E} \tag{19}$$

where for a cylindrical shell or radius, R, and thickness, t, with a through crack of length, 2a, the applied stress intensity factor, K, may be written

$$K = \sigma \sqrt{\pi a} \cdot Y(\lambda) \tag{20}$$

where $\lambda = a/\sqrt{Rt}$, and Y is a geometrical correction factor for the effect of shell curvature and bending. Substituting equation (20) into (19) and rearranging leads to a convenient form.

$$J_{applied} = \frac{\sigma_o^2 a}{E} \left\{ \frac{\pi \sigma^2}{\sigma_o^2} \right\} [Y^2] \tag{21}$$

where we define

{ } = the stress bracket

[ ] = the geometry bracket

for the purposes to follow. For examining crack stability under constant pressure or load (that is, σ constant), the first form of equation (13) applies with $\partial P/\partial a = 0$; hence, following the definition of equation (8)

$$T_{applied} = \frac{dJ_{applied}}{da}\frac{E}{\sigma_o^2} = \frac{\partial J_{applied}}{\partial a}\frac{E}{\sigma_o^2} \qquad (22)$$

putting equation (21) into (22) leads to

$$T_{applied} = \frac{\pi\sigma^2}{\sigma_o^2} \cdot [Y^2 \times 2\lambda Y \cdot Y'] \qquad (23)$$

which contains the same stress bracket as equation (21) but a new geometry bracket. To identify the implied $J_{applied}$ versus $T_{applied}$ curve on a J versus T diagram by eliminating load or σ, simply divide equation (21) by (23) to obtain

$$\frac{J_{applied}}{T_{applied}} = \frac{\sigma_o^2 a}{E} \cdot \left[\frac{1}{1 + 2\lambda Y'/Y}\right] \qquad (24)$$

For constant crack size, a, and for a given material, the ratio of $J_{applied}$ to $T_{applied}$ is a constant according to equation (24), which can be represented as a straight line through the origin on a J versus T diagram as in Figure 5.

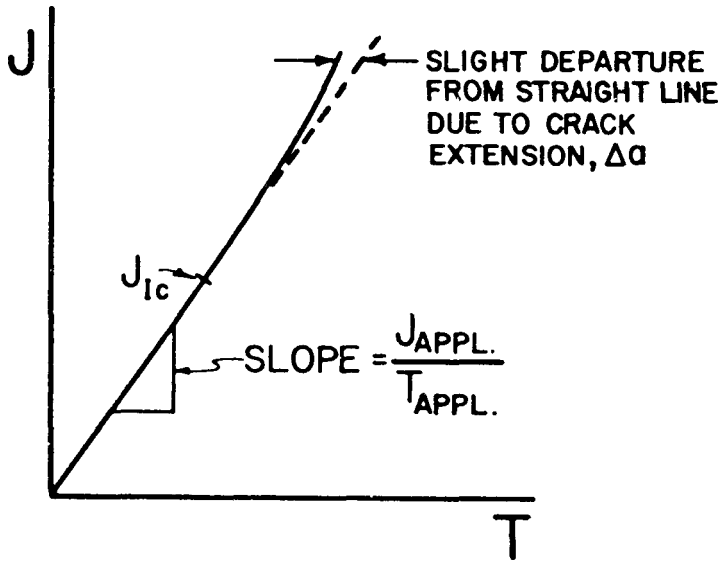

Figure 5 A typical J versus T applied curve, almost straight

As loading occurs (that is, stress σ is applied) from equation (21), $J_{applied}$ starts from zero (the origin of Figure 3) and proceeds to increase with the square of the applied stress. If J exceeds J_{Ic} crack extension, Δa (actual) begins to occur so the trace of $J_{applied}$ versus $T_{applied}$ would depart slightly from a straight line. But the crack length changes prior to the onset of instability are likely to be small in heavy sections so this slight departure will be neglected for the moment.

It remains to show how the $J_{applied}$ versus $T_{applied}$ curve behaves as stresses exceed the range of applicability of LEFM. But first it is relevant to establish values for the geometry brackets as given in equations (21), (23), and (24).

B. Shell Correction Factors or Geometry Brackets for Through Cracks in Cylindrical Shells With Internal Pressure

The shell correction factors for longitudinal through cracks in shells as developed first by Folias[10] and modified by Erdogan and Kibler[11] and verified by Krenk[12] are perhaps most conveniently shown in Rooke and Cartwright's work.[13] For the longitudinal crack, they can be empirically expressed over the range of interest by the approximations (± 1%):

$$Y = (1 + 1.25\lambda^2)^{\frac{1}{2}} \text{ for } (0 \leq \lambda \leq 1)$$

$$= (0.6 + 0.9\lambda) \text{ for } (1 \leq \lambda \leq 5) \qquad (25)$$

where, as before

$$\lambda = \frac{a}{\sqrt{Rt}}$$

Similar expressions may be developed for circumferential cracks (again see Reference 13), but are of lesser interest since the applied longitudinal stresses are a factor of 2 less than the hoop stresses, which favors cracking.

Using expressions such as equations (25) or curves from Reference 13, the geometry brackets required in equations (21), (23), and (24) have been computed and are given here graphically in Figures 6, 7, 8, and 9 for both longitudinal and circumferential through cracks.

In the following discussion, it will be of special interest to note that the geometry bracket associated with equation (24) (dashed curves on Figures 6 to 9) is always a number smaller than 1 and greater than 1/3. Indeed for most vessels, R/t ≅ 10 and the usual leak-before-break assumption of a = t gives λ ≅ 0.31 and the [ ] is between 1 and 0.8; that is, always nearly 1 in equation (24).

C. Plastic Zone Corrected LEFM Conditions

Historically the first attempts to extend LEFM toward the elastic-plastic range included correcting the crack length for the plastic zone at the crack tip to obtain an effective crack size, a_{eff}; that is:

$$a_{eff} = a + r_y$$

where

$$r_y = \frac{1}{\beta\pi}\left(\frac{K^2}{\sigma_o{}^2}\right) = \frac{JE}{\beta\pi_o{}^2} \qquad (26)$$

where $\beta \cong 2$ (for plane stress)
$\cong 6$ (for plane strain)

In applying the plastic zone correction to equation (21), for example, the crack size, a, might be replaced by $a_{eff.}$, both where it appears explicitly and in Y. However, its use here shall be restricted to relatively low nominal stress levels (for example, $\frac{\sigma}{\sigma_o} < \frac{2}{3}$ so r_y << a) and its effect on the value of the geometry bracket [Y^2] and others will be small enough to be neglected. Correcting only the explicit appearance of a in equation (21) and rearranging gives the result

$$J_{applied} = \frac{\sigma_o{}^2 a}{E}\left\{\frac{\pi\left(\frac{\sigma}{\sigma_o}\right)^2}{1 - \frac{Y^2}{\beta}\left(\frac{\sigma}{\sigma_o}\right)^2}\right\}[Y^2]. \qquad (27)$$

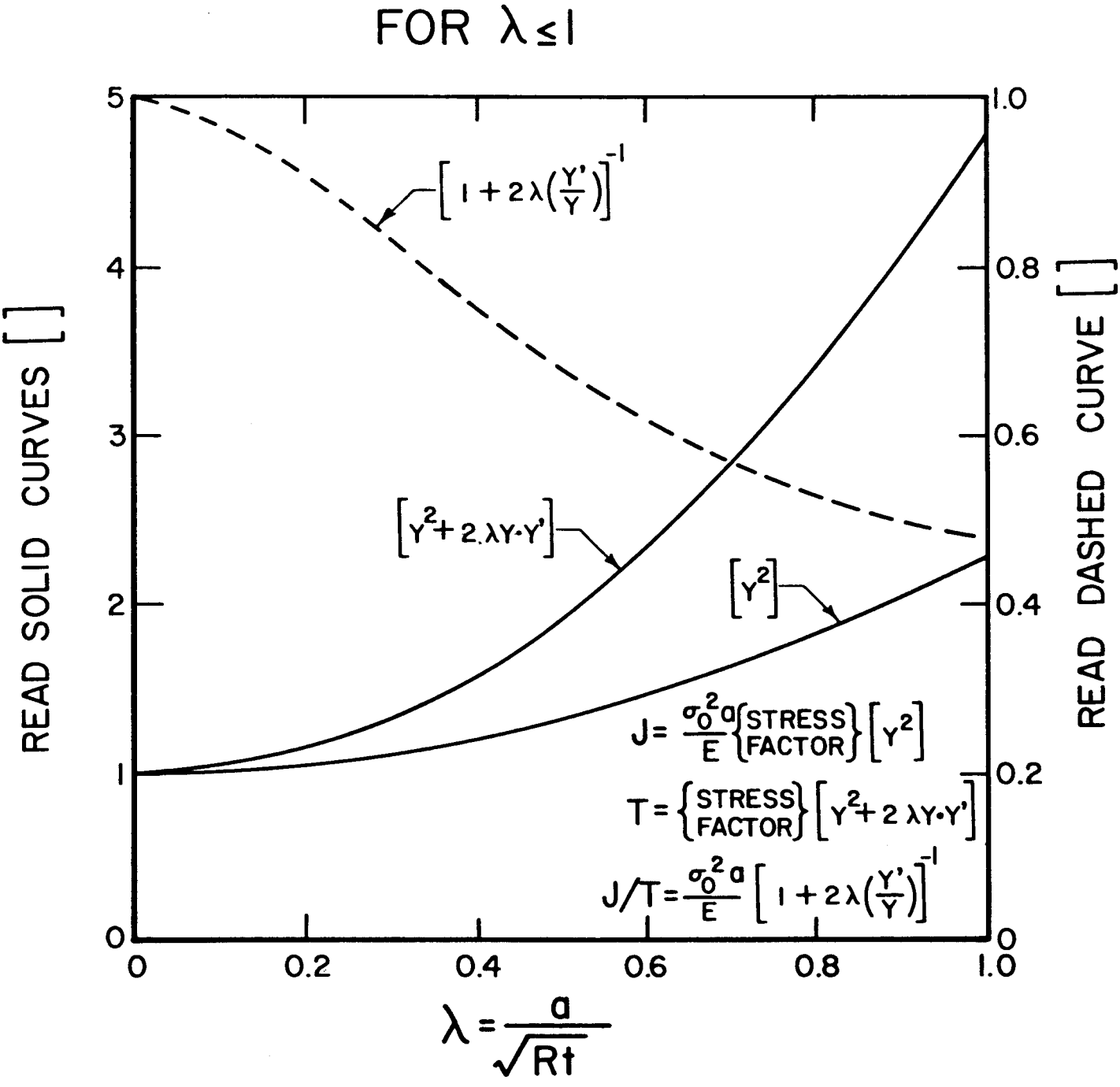

Figure 6 Shell correction factors for longitudinal cracks in cylinders (for low λ)

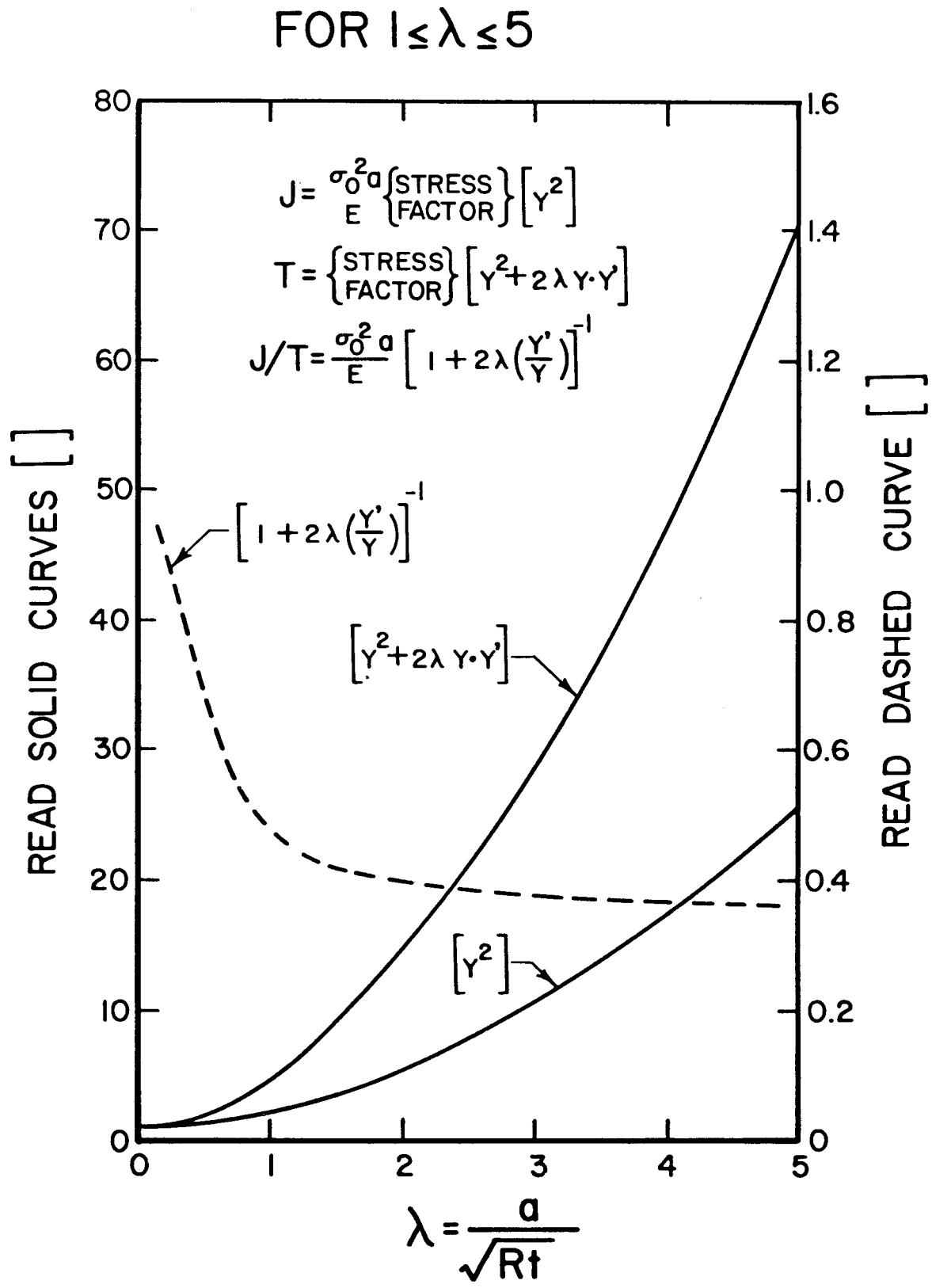

Figure 7 Shell correction factors for longitudinal cracks in cylinders (for high λ but with $\sigma/\sigma_0 \le 0.67$)

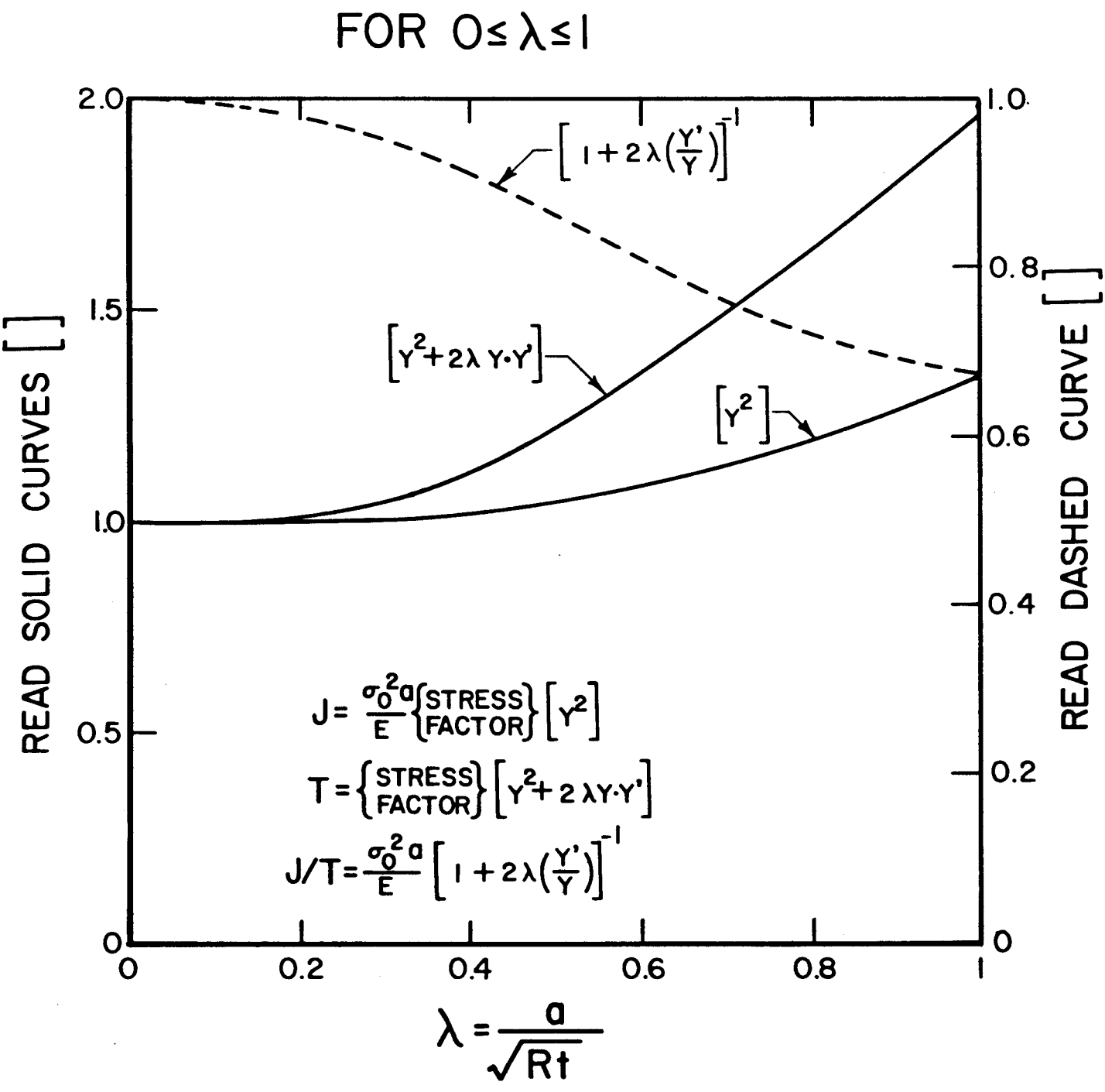

Figure 8 Shell correction factors for circumferential cracks in cylinders (for low λ)

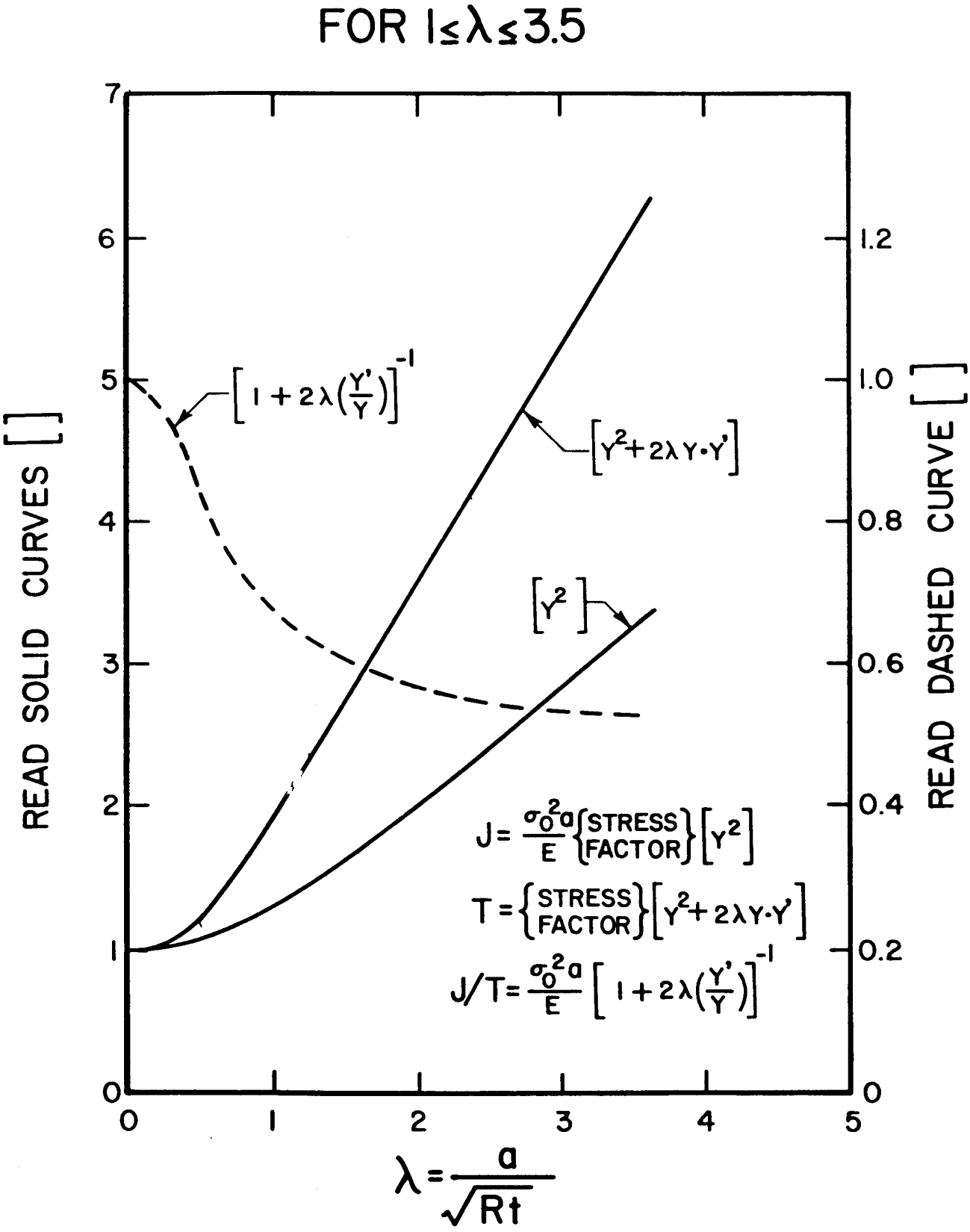

Figure 9 Shell correction factors for circumferential cracks in cylinders (for high λ but with $\sigma/\sigma_0 \leq 0.67$)

For through cracks in nuclear vessels, where instability is approached at stress levels of 2/3 yield or less, the crack tip plastic zone stress state will be closer to plane strain than plane stress. Hence, to simplify the stress bracket in equation (27), taking $Y^2 \cong 1$ (but using the actual values from curves) and $\beta = 2$ (plane stress thus conservative), a conservative estimate of $J_{applied}$ is achieved:

$$J_{applied} = \frac{\sigma_o^2 a}{E} \left\{ \frac{\pi \left(\frac{\sigma}{\sigma_o}\right)^2}{1 - \frac{1}{2}\left(\frac{\sigma}{\sigma_o}\right)^2} \right\} [Y^2]. \qquad (28)$$

Indeed, most often the 1/2 in the stress bracket might be too conservative, but it can be no less than 1/6. For the range of interest, Figure 10 shows a plot of these extremes for the stress bracket. Using the conservative value 1/2 also compensates for the slight underestimate of the geometry bracket, $[Y^2]$, by neglecting the plastic zone correction in it.

Finally, it is noted that the simplifying assumptions leading to equation (28) not only result in a good (perhaps slightly conservative) approximation for $J_{applied}$, but most importantly result in an especially convenient format. The stress bracket and geometry brackets in equation (28) completely separate the stress and geometry effects on $J_{applied}$ into independent factors. Because of the separation and, operating on equation (28), following the analysis represented by the sequence: equation (21) to equations (23) and (24), the results are:

$$T_{applied} = \frac{\sigma_o^2 a}{E} \left\{ \frac{\pi \left(\frac{\sigma}{\sigma_o}\right)^2}{1 - \frac{1}{2}\left(\frac{\sigma}{\sigma_o}\right)^2} \right\} [Y^2 + 2\lambda YY'], \qquad (29)$$

and

$$\frac{J_{applied}}{T_{applied}} = \frac{\sigma_o^2 a}{E} \left[\frac{1}{1 + 2\lambda Y'/Y} \right] \qquad (30)$$

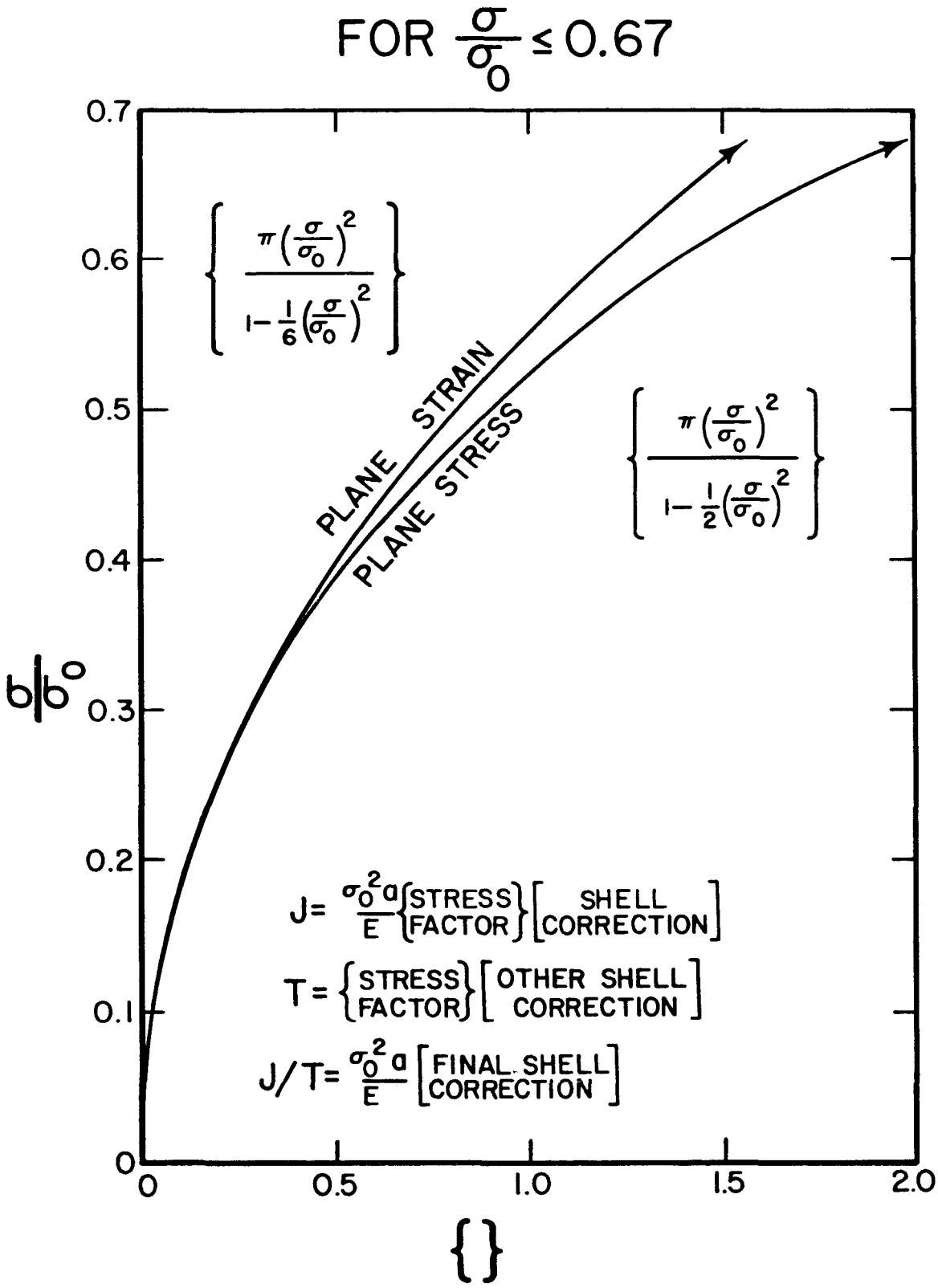

Figure 10 Stress correction factors for J and T for low stress ($\sigma/\sigma \leq 0,67$)

It should be noted that the final result, equation (30), is identical to equation (24), which implies that on the J versus T diagram, Figure 5, the same $J_{applied} - T_{applied}$ trace or loading line is followed, whether the plastic zone correction is used or not! Consequently, as discussed earlier, the loading line is a straight line through the origin of the J versus T diagram of a slope given by

$$\underline{\text{slope}} = \frac{J_{applied}}{T_{applied}} = \frac{\sigma_o^2 a}{E} \text{ [order of 1]} \cong \frac{\sigma_o^2 a}{E} \tag{31}$$

D. A Note on Further Extrapolation of the Stress Bracket

The analysis of actual nuclear vessels at nominal stress levels above 2/3 yield is not realistically associated with any known operating or even faulted conditions. However, for the purpose of comparison of analytical methods with test results from model vessel tests pressurized to crack instability, extrapolation of the above methods to obtain fair approximations is relevant.

Moreover, at stress levels higher than 2/3 yield, interest becomes centered on rather short through cracks, $a << t$, so that $\lambda << 1$ and the geometry correction effects become small. Under such conditions, the separation as in equation (28) to independent stress brackets and geometry brackets is no less justified; thus it need not be discussed further here. For the stress bracket functions derived below, it must be noted that they should be applied only for low λ ($\lambda < 1$) so Figures 6 and 8 will be relevant but Figures 7 and 9 should be excluded.

E. The Strip Yield Model Stress Bracket

Using the so-called Dugdale strip yield model to develop the stress bracket, the development of the function follows equations (21), (23), and (24), or equally well by equations (28), (29), and (30), repeated here for emphasis:

$$J_{applied} = \frac{\sigma_o^2 a}{E} \left\{ \right\} [Y^2]$$

and

$$T_{applied} = \left\{ \right\} [Y^2 + 2\lambda YY']$$

and (32)

$$\frac{J_{applied}}{T_{applied}} = \frac{\sigma_o^2 a}{E} \left[\frac{1}{1 + 2\lambda Y'/Y} \right]$$

where

$\left\{ \right\}$ = the stress bracket

From the solution for the strip yield model for a center through-cracked plate (for example, see Reference 14) and comparing results with the first of equations (32), the stress bracket <u>for strip yielding</u> is

$$\left\{ \right\} = \left\{ \left(\frac{8}{\pi\gamma}\right) \ln \sec \left(\frac{\pi}{2} \frac{\sigma}{\sigma_o}\right) \right\} \quad (33)$$

where

0.7 (for plane strain) $\leq \gamma \leq 1$ (for plane stress).

This stress bracket might be used for stress levels from 2/3 yield up to (but not including) the yield strength (it assumes elastic perfectly plastic non-hardening material). It is appropriate to go on to hardening solutions for extrapolation of the stress bracket for stresses at or above the yield strength.

F. The Power Hardening Stress Bracket

For a power hardening approximation of a material's stress strain curve by

$$\frac{\varepsilon}{\varepsilon_0} = \bar{\alpha} \left(\frac{\sigma}{\sigma_o}\right)^n \tag{34}$$

the numerical solutions for center-cracked plates under both plane stress and plane strain have been presented by Hutchinson and coworkers.[15] Their results were compiled and applied to develop tearing instability parameters by Zahoor[16] and tabulated by Tada.[17] Taking their plane stress results in the same form as the first of equations (32), the stress bracket becomes

$$\{\ \} = \left\{ \bar{\alpha} f^* \ \left(\frac{\sigma}{\sigma_o}\right)^{n+1} \right\} \tag{35}$$

where

$f^* = \pi \ (n = 1)$ $= 0.88 \ (n = 7)$
$= 2.22 \ (n = 3)$ and so forth
$= 1.25 \ (n = 5)$

The power hardening model, equation (34), is a fair approximation only above yield for nominal stresses. Therefore, its use is limited. However, if only the above yield range is of interest in certain applications, some further simplifications may be invoked. Dividing equation (35) by (34) and rearranging:

$$\{\ \} = \left\{ f^* \left(\frac{\sigma}{\sigma_o}\right) \ \left(\frac{\varepsilon}{\varepsilon_o}\right) \right\} \tag{36}$$

Above yield the stress is always near the yield stress $\sigma \cong \sigma_o$ (or equation (34) can be adjusted). Hence, in the above-yield range the stress bracket is almost proportional to the strain, or more properly the stress times the strain. Substituting equation (36) into the first of equations (32)

$$J_{applied} = f^* \sigma \varepsilon a [Y^2] \tag{37}$$

Noting that in this relationship $J_{applied}$ varies approximately linearly with nominal stress, σ, with nominal strain, ε, and with crack size, a, is of

considerable assistance in intuitively understanding the roles of loading deformation and geometry (size) as variables affecting $J_{applied}$.

However, the simple power hardening model of a material's stress-strain curve, equation (34), is inadequate to represent the detailed behavior of both the elastic range and the hardening range. A better representation is found through the Ramberg-Osgood approximation.

G. The Ramberg-Osgood Stress Bracket

The Ramberg-Osgood representation of a material's stress-strain behavior is

$$\frac{\varepsilon}{\varepsilon_o} = \frac{\sigma}{\sigma_o} + \bar{\bar{\alpha}} \left(\frac{\sigma}{\sigma_o}\right)^n \tag{38}$$

Again from Hutchinson's results[15] as compiled by others,[16,17] comparing terms in the same form as the first of equations (32), the stress bracket may be written:

$$\{\ \} = \left\{ \psi^* \left(\frac{\sigma}{\sigma_o}\right)^2 + \bar{\bar{\alpha}}\ G^* \left(\frac{\sigma}{\sigma_o}\right)^{n+1} \right\} \tag{39}$$

The parameters ψ^* and G^* vary in a complex way with $\bar{\bar{\alpha}}$ and n which can be determined from analysis in References 16 and 17. The limiting case for elastic material, $\bar{\bar{\alpha}} = 0$ is $\psi^* = \pi(G^* \neq \infty,\ n \neq \infty)$. Thus equation (39) is seen to reduce to a form proper for insertion in equation (21). At the other limit, with the stress above yield, $\sigma > \sigma_o$, the ψ^* term is negligible and then $\bar{\bar{\alpha}}\ G^* \cong \alpha f,^*$ which produces agreement with equation (35).

It would be cumbersome to present stress-strain curve fitting considerations using equation (38), as well as corresponding determinations of ψ^* and G^* for all materials here. More to the point is to consider a typical material, A533B, at 93°C, for which Shih[18] obtained the following curve-fitting results:

σ_o = 60 ksi
E = 29 x 10^3 ksi
$\bar{\bar{\alpha}}$ = 1.115
n = 9.7

Following References 16 and 17 for plane stress and using these results, one obtains

$$\psi^* = 4.3$$
$$\bar{\bar{\alpha}}G^* = 11.8$$

which, when substituted in equation (39), gives

$$\left\{\ \right\} = \left\{4.3\ \left(\frac{\sigma}{\sigma_o}\right)^2 + 11.8\ \left(\frac{\sigma}{\sigma_o}\right)^{10.7}\right\} \qquad (40)$$

for a typical nuclear vessel material. Plotting the stress bracket, equation (40), for $\frac{2}{3} < \frac{\sigma}{\sigma_o} < 1$, and fairing it into the stress bracket from equation (28) for $\frac{\sigma}{\sigma_o} < \frac{2}{3}$ resulted in the curve of Figure 11. Again, the reader is reminded that the curve in Figure 11 is appropriate only for situations where $\lambda << 1$, so the elastically determined geometry brackets must not be used inappropriately in the fully plastic range.

SUMMARY ON THROUGH-CRACK ANALYSIS

In summary, a method has been developed to analyze through cracks in nuclear pressure vessels to determine $J_{applied}$, $T_{applied}$ and $J_{applied}/T_{applied}$. Neglecting both a plastic zone correction to the geometry factor and geometry correction to the stress factor forced a separation of effects which was compensated by developing stress factors for plane stress (conservative). For application at stress levels below 2/3 yield or at low values of λ ($\lambda << 1$), the method is accurate and slightly conservative. At stresses above 2/3 yield or with high λ ($\lambda > 1$), but not both, the method will give good approximations. This permits comparison of analytical predictions with many test results. (The method is not intended to treat long through cracks ($\lambda > 1$), concurrent with high nominal stresses (approaching or above yield), but this combination is never encountered in nuclear vessel analysis.)

The resulting equations for all cases were reduced to equations (32). The geometry brackets were given in Figures 6, 7, 8, and 9, and the stress brackets in Figure 11 (and 10).

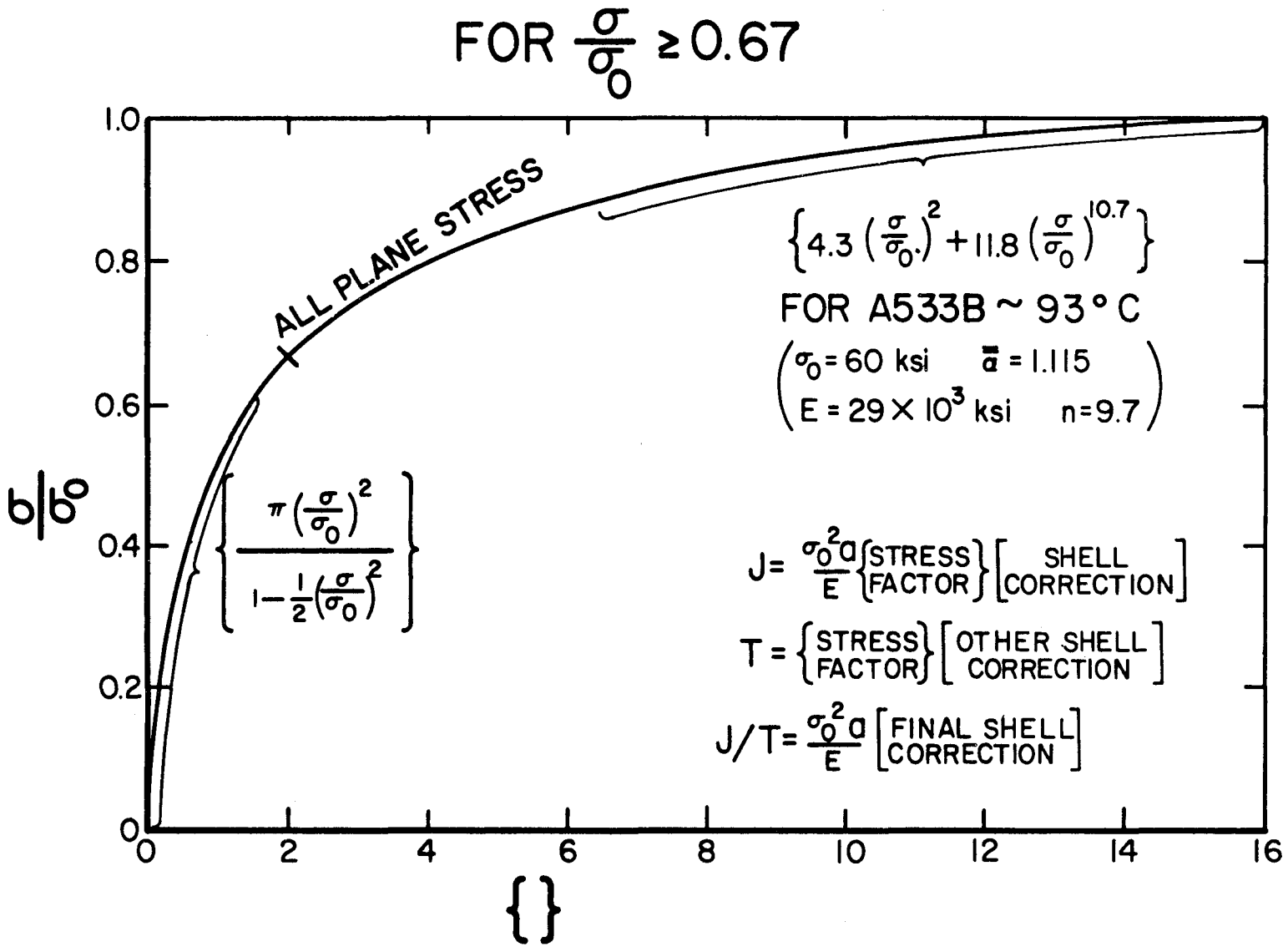

Figure 11 Stress correction factors for J and T extended to high stress

Finally, the loading line on a J versus T diagram for the trace of $J_{applied}$ versus $T_{applied}$ is effectively a straight line through the origin of slope equal to

$\frac{\sigma_o^2 a}{E}$ times a factor which ranges from 0.5 to 1. This result is independent of the stress bracket model employed.

SURFACE FLAW ANALYSIS

For a surface flaw of depth, a, and length, 2c, in a vessel wall of thickeness, t, the form of the elastic solution for K is often given as

$$K = \frac{\sigma\sqrt{\pi a}}{\phi_o\ (\frac{a}{c})}\ f(\frac{a}{c})\ \cdot\ g(\frac{a}{t}) \qquad (41)$$

where ϕ_o is the elliptical shape factor as computed from the complete elliptic integral of the second kind [19]:

$$\phi_o = \int_0^{\pi/2} [1 - \frac{c^2 - a^2}{c^2} \sin^2\theta]^{\frac{1}{2}}\ d\theta$$

and where;

$f(\frac{a}{c})$ = a front surface correction factor;

$g(\frac{a}{t})$ = a back surface correction factor.

One may combine ϕ_o and f into F by

$$F(\frac{a}{c}) = \left(\frac{f(\frac{a}{c})}{\phi_o(\frac{a}{c})}\right)^2$$

A. LEFM Surface Flaw Equations

Writing $J_{applied}$ directly from the above

$$J_{applied} = \frac{K^2}{E} = \frac{\sigma_o^2 a}{E} \left\{ \pi \frac{\sigma^2}{\sigma_o^2} \right\} F(\tfrac{a}{c}) \cdot G(\tfrac{a}{t}) \qquad (42)$$

where $G(\frac{a}{t}) = [(\frac{a}{t})]^2$ and $G'(\frac{a}{t}) = \frac{dG}{d(\frac{a}{t})}$, and so forth.

Differentiating under constant pressure stress, σ, as before to obtain $T_{applied}$ gives

$$T_{applied} = \left\{ \right\} F(\tfrac{a}{c}) \left[G(\tfrac{a}{c}) + \tfrac{a}{t} G'(\tfrac{a}{t}) \right] \qquad (43)$$

where the derivatives of F are neglected since they are slightly negative for increasing a compared to c. This gives a conservative result for $T_{applied}$. Proceeding as before, dividing equation (42) by equation (43)

$$\frac{J_{applied}}{T_{applied}} = \frac{\sigma_o^2 a}{E} \cdot \left[\frac{1}{1 + \frac{a}{t} \cdot G'/_G} \right] \qquad (44)$$

Notice that the form of this result is identical to those for through flaws. Indeed, taking G to be the often employed "secant correction"[14] or

$$G(\tfrac{a}{t}) = \sec \frac{\pi a}{2t}$$

the geometry bracket in equation (44) is given by:

$$[\ \ ] = \left[\frac{1}{1 + \frac{\pi a}{2t} \tan \frac{\pi a}{2t}} \right] \qquad (45)$$

which for $0 \leq \frac{a}{t} \leq 1/2$ takes on values which range from 1 to 0.57. Hence, as before, the geometry bracket in equation (44) is slightly less than but nearly equal to 1 for cases of interest. This result is also independent of adjustment to the stress bracket, does not enter equation (44), and is independent of the crack shape aspect ratio (that is, does not include the function $F(\frac{a}{c})$. This elastic analysis should be tentatively restricted to avoid yielding of the uncracked remaining ligament, t-a, behind the crack. It is certainly acceptable if

$$\frac{\sigma}{\sigma_o} < (1 - \tfrac{a}{t}).$$

For additional reasons associated with correctness of the form of the above elastic analysis, it is prudent to restrict its use to a/t values equal to or less than 1/2.

B. The Surface Flaw With Yielding Remaining Ligament

Consider the case where a/t is greater than 1/2 and where

$$1 > \frac{\sigma}{\sigma_o} > (1 - \frac{a}{t}).$$

The ligament behind the crack will surely yield, but the uncracked regions of the vessel wall will be elastic. Following the analysis of the yielded ligament behind a surface flaw as in Reference 2 (that is, as an elastic through crack with the remaining ligament supplying distributed closing forces equal to the flow stress over the net section area), the displacement at the center of the crack is taken to be equal to the crack opening stretch, δ, or

$$\delta = \gamma \frac{J}{\sigma_o} = \frac{2\sigma_{eff}\ (2c)}{E} = \frac{4c}{E}\ [\sigma - \sigma_o\ (1 - \frac{a}{t})]. \tag{46}$$

Solving for $J_{applied}$ gives

$$J_{applied} = \frac{\sigma_o{}^2 a}{E} (\frac{4c}{\gamma a}) (\frac{\sigma}{\sigma_o} - 1 + \frac{a}{t}). \tag{47}$$

Note that stress and geometry effects are necessarily mixed here. However, $T_{applied}$ can be computed again by differentiating with constant nominal pressure stress or:

$$T_{applied} = \frac{4c}{\gamma t}\ . \tag{48}$$

This result was found in Reference 2. Continuing, we divide equation (47) by (48), resulting in

$$\frac{J_{applied}}{T_{applied}} = \frac{\sigma_o{}^2 a}{E} (\frac{t}{a})\ \ (\frac{\sigma}{\sigma_o} - 1 + \frac{a}{t}). \tag{49}$$

Under the conditions stated above, the final parenthesis in equation (49) is positive but less than a/t. Therefore, the product of the final two parentheses is less than, but nearly equal to, 1. Hence, comparing the form of equation (49) to equation (44) and earlier results (such as the last of equation (32)) shows that all can be described by

$$\frac{J_{applied}}{T_{applied}} = \frac{\sigma_o{}^2 a}{E} \quad [\sim 0.5 \text{ to } 1]. \tag{50}$$

Figure 12 shows the values of the [ ] factor from equation (49) and equation (45) faired together from high a/t to low a/t respectively, consistent with the limitations of these equations.

The discussion has established that equation (50) applies to surface flaws, as well as through flaws. However, the analysis is recommended currently only for reasonably shallow surface flaws, that is, $a/t \leq 1/2$. Moreover, for good precision over a wide range of stress levels, the stress bracket should be further developed.

C. The Stress Bracket for the Surface Flaw

The geometry correction for the surface flaw (that is, $F(\frac{a}{c})$ and $G(\frac{a}{t})$ in equation (42)) is adequately represented by the curves in Appendix A of Section XI of the Nuclear Pressure Vessel Code. The curves for $\frac{\sigma}{\sigma_o} = 0$ are uncorrected for plastic zone effects and are most appropriate here (not overly conservative), since the plastic zone correction and other higher stress level effects shall be treated by modifying the stress bracket.

First, consider a plastic zone correction for the surface flaw formula, equation (42). As noted previously, since $F(\frac{a}{c})$ diminishes with increasing a, its effect somewhat cancels the increase in $G(\frac{a}{t})$. Thus a small plastic zone correction will have little effect on the values of the combined geometry correction terms. On the other hand, the explicit appearance of a in equation (42) can be plastic

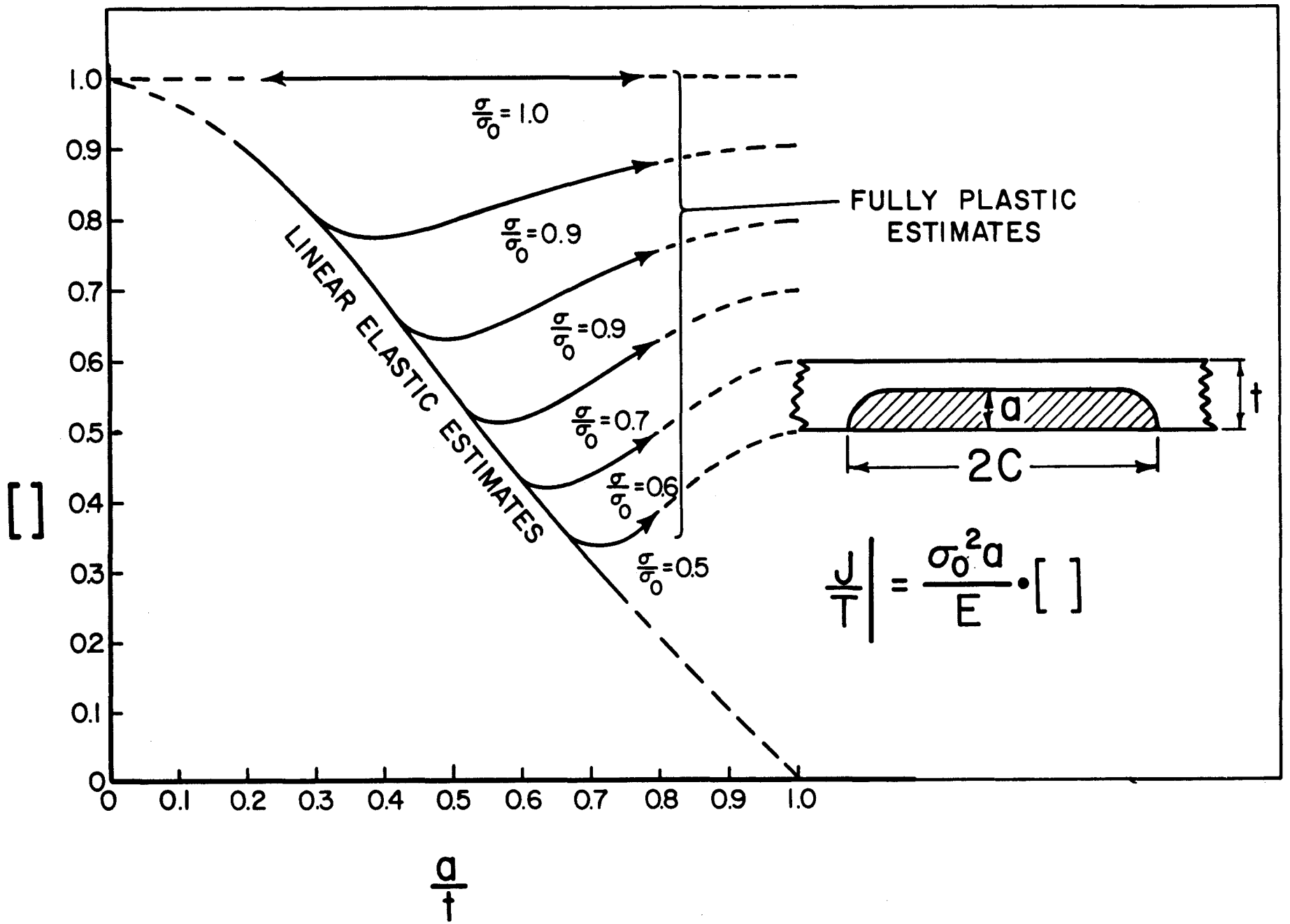

Figure 12 The J/T geometry correction [ ] for surface flaws for elastic and plastic ligaments

zone corrected, using equation (26) for plane strain. Up to stress levels of 2/3 of yield, this can be accomplished by adopting the plane-strain stress bracket correction as plotted on Figure 10, or

$$\left\{ \quad \right\} = \left\{ \frac{\pi \left(\frac{\sigma}{\sigma_o}\right)^2}{1 - \frac{1}{6}\left(\frac{\sigma}{\sigma_o}\right)^2} \right\}. \tag{51}$$

The (1/6) coefficient in the stress bracket could be corrected for geometry effects, but, in the stress range of applicability and for $a/t \leq 1/2$, this correction is small and applies to a term of small influence; thus, it well may be neglected, especially since it is a greater convenience to avoid mixing stress and geometry factors.

As was done before for through-thickness flaws, the stress bracket correction approach may be accomplished most appropriately for higher stress levels by employing the hardening results of Hutchinson and coworkers.[15] In this case, plane strain Ramberg-Osgood hardening analysis was employed. Indeed, for very shallow ($a/t << \frac{1}{2}$) but long ($a/c << 1$) surface flaws, their results for center-cracked plates are accurately appropriate. Hence, for $a/t \leq 1/2$ and $a/c \leq 1$, their results will give fair approximations for the high stress level range, that is, $\frac{\sigma}{\sigma_o} > 2/3$.

Following the same Ramberg-Osgood analysis associated with equations (38) and (39) but for plane strain and again adopting Shih's[18] parameters for A533B steel at 90°C (that is, $\sigma_o = 60$ ksi, $E = 30 \times 10^3$, ksi $\bar{\bar{\alpha}} = 1.115$, and $n = 9.7$) resulted in

$$\{ \} = 3.30 \left(\frac{\sigma}{\sigma_o}\right)^2 + 3.5 \left(\frac{\sigma}{\sigma_o}\right)^{10.7} \tag{52}$$

Fairing the stress bracket, equation (52), together with the former equation (51) near $\sigma/\sigma_o = 2/3$ provided the results in the "Plane Strain" column in Table 1. The "Plane Stress" column gives tabular results for through cracks for comparison. The Table 1 results were consistently similar even though the plane stress values eventually deviated from the plane strain values; therefore, the methodology was extended to surface flaws in uniform stress fields in vessel walls.

D. Analysis of Surface Flaws into Nonuniform Stress Fields

Though the pressure stresses in a nuclear vessel wall induce (almost) uniform unperturbed stress fields, secondary stresses such as residual stresses, thermal transient stresses, faulted conditions, and so forth, result in high stress gradients through the wall. The secondary stresses are of great concern only in combination with pressure stresses; they cause yielding locally (at the surface of the wall). The above methods are inadequate to handle this situation accurately, and other analytic methods are not available currently to develop a method of equal accuracy. However, an approximate and conservative method may be advanced (as suggested to this author by Riccardella (see Appendix H of NUREG-0744)).

As noted with equation (37), $J_{applied}$ is roughly proportional to applied strain. Consequently, if thermal stresses (or other secondary stresses) are solved for by elastic analysis, the stress values are much too high (yielding should have occurred), but the implied strains are nearly correct. Therefore, computing implied strains, averaging them over the crack area of a surface flaw, then transforming them back to equivalent stresses by the Ramberg-Osgood relation, equation (38), for insertion into the preceeding surface flaw analysis should give reasonable results. Tentatively, the results of such a superposition are judged to be a conservative method of handling secondary stresses. This matter should bear some further study.

Consistent with the proportionality of $J_{applied}$ to strain, Reuter (see Appendix I of NUREG-0744), in performing a sensitivity analysis of the effect of variation of the stress-strain curves on stress brackets, also noted this proportionality to strain.

Indeed, for high stress levels (σ/σ_o equal to or greater than yield) he has shown that rewriting the stress bracket in terms of strain has some merit. That observation is consistent with the above suggestion of using superimposed strain to treat superimposed secondary stress circumstances.

Table 1 Stress Correction Factors for J for Plane Stress (Through Flaws) and Plane Strain (Surface Flaws) With Ramberg-Osgood Hardening*

$\frac{\sigma}{\sigma_o}$	{Plane Stress}[1]	{Plane Strain}[2]
0	0	0
0.2	0.134	0.127
0.4	0.546	0.516
0.5	0.898	0.819
0.6	1.38	1.20
0.7	2.05	1.65
0.8	3.39	2.35
0.9	7.35	3.78
1.0	16.1	6.80
1.05	24.6	9.54
1.10	37.9	13.6
1.15	58.3	19.9
1.20	89.1	29.3

where:

$$J = \frac{\sigma_o^2 a}{E} \cdot \{\ \} \cdot [\text{geometric correction}]$$

[1] for through-wall flaws

[2] for surface flaws

* { }, the stress correction factors, are to be used in the equation: $J = \frac{\sigma_o^2 a}{E} \cdot \{\ \} \cdot [\ ]$ where [ ] is the appropriate geometric correction factor. Source: Reference 17.
For use with the stress-strain law:

$$\frac{\phi}{\varepsilon_o} = \frac{\sigma}{\sigma_o} + \bar{\bar{\alpha}} \left(\frac{\sigma}{\sigma_o}\right)^n;$$

for typical A-533B steel at 93°C using

σ_o = 60 ksi, $\bar{\bar{\alpha}}$ = 1.115, and n = 9.7
(see NUREG/CP 0010, Shih, 1979).

APPLICATION OF J VERSUS T DIAGRAM TO NUCLEAR PRESSURE VESSEL CONDITIONS AND MATERIALS

As explained in the text with Figure 4, crack instability occurs when the $J\text{-}T_{applied}$ curve intersects the $J\text{-}T_{material}$ curve. In discussion of both the surface flaw and through flaw from the LEFM range into the fully plastic range, it was noted by equations (24), (30), (31), (32), (44), and (50), that $J\text{-}T_{applied}$ is a nearly straight line through the origin of a J versus T diagram. Summarizing all those equations, the slope is

$$\frac{J_{applied}}{T_{applied}} = \frac{\sigma_o^2 a}{E} \text{ [0.5 to 1]} \tag{53}$$

On the other hand, the region of the J versus T diagram for which the material property data are absolutely assured to be accurate by "J-controlled growth" criteria, equation (18), is

$$\frac{J}{T_{material}} = \frac{\sigma_o^2 b}{E\omega} \tag{54}$$

where $\omega \geq 5 >> 1$

In practice, the postulated flaw sizes, a, for analytical purposes are likely to be the order of 1/4 to 1 times the vessel wall thickness for surface and through flaw sensitivity studies, whereas the remaining uncracked ligaments, b, in experimental specimens are likely to be a much smaller fraction of the vessel wall thickness. Thus, to compare equations (53) and (54), it is noted that

$$a \text{ [0.5 to 1]} >> \frac{b}{\omega} \tag{55}$$

or the loading line for $J_{applied}$ versus $T_{applied}$ will not intersect the materials curve in the region where $\omega \geq 5$. However, both the $J\text{-}T_{material}$ analysis, and $J\text{-}T_{applied}$ analyses are assured to be correct up to the experimental J levels where $\omega > 5$. Therefore, at that level there is still an assured safety margin factor on T; in fact by the inequality (55), that is

$$\text{margin} = \frac{T_{material}}{T_{applied}} = \frac{a\ [0.5 \text{ to } 1]\omega}{b} >> 1 \qquad (56)$$

which is a safety margin against instability considering equation (9).

Alternatively, it can be argued that since there is a fair margin against instability at the J level where $\omega \to 5$ in the test data, loading would necessarily have to increase further, raising the apparent J, in order for instability to occur. Using the linear (cummulative) extrapolation of the data as suggested in Figure 3, loading would at least progress beyond the point where the extrapolated data intersect the line representing equation (54) with b replaced by a. At that point, the analysis of the postulated vessel flaw is at a J-level where $\omega \geq 5$ so the analysis is still accurate. The load or pressure corresponding to J at that point can be found from the $J_{applied}$ equations. Some further unknown margin exists at still greater loads since instability has not yet ensued even though at high loads neither "J-controlled growth" nor the analysis method are absolutely assured.

A. Application to End of Life by Irradiation Damage to Actual Vessels

Considering the above discussion, the former (more conservative) criteria, rather than the alternative, will be adopted here as a limiting (safe) J-level for purposes of safety assessments. Both the available data on irradiation-damaged material and prospects of data from surveillance and other programs are limited to test specimen sizes of uncracked remaining ligaments, b, of slightly over 1 in. Inserting that size into equation (54) along with other typical irradiation-damaged material properties (for example, $\sigma_o > 85$ ksi, $E = 30 \times 10^3$ ksi) with $\omega = 5$ gives

$$\frac{J_{material}}{T_{material}} = \frac{\sigma_o{}^2 b}{E\omega} = \frac{(85)^2(1)}{30(5)} \cong 50 \ \frac{\text{in.-lbs}}{\text{in.}^2} \qquad (57)$$

Figure 13 is a J versus T diagram showing some of the available irradiated J-R curve data, as well as some low toughness unirradiated data. The curves shown were reported by Loss (see Part II, Appendix E of NUREG-0744) and the experimental details and the method of development can be found in the publication. It is sufficient to note here that in the opinion of this author they are properly obtained data meeting the conditions for "J-controlled growth" over the full range for which the curves are plotted. Indeed, Loss and his associates should be commended for this work.

A J/T = 50 line was plotted on Figure 13 intersecting the material data curves. Each curve has associated with it a number, which is the Charpy impact upper shelf energy (in ft-lbs) from tests of the same material and condition. Thus in the neighborhood of the Code-significant Charpy energy of 50 (that is, the range 35 to 78 ft-lb), it was noted that the J-levels at the intersections varied significantly. Also it was noted that these intersections with J/T = 50 were at J-levels considerably above the critical, J_{Ic}, values for these materials (sometimes as much as 3 times). Hence, J_{Ic} is far too conservative and not directly connected to crack instability for reasonable judgments of actual reactor safety for upper shelf conditions.

On the other hand, linear extrapolation of the material data curves from the J/T = 50 line to loading J/T curves for vessel postulations (usually J/T > 500), indicated a modest increase in J for instability above the J/T = 50 values. Consequently, the J/T = 50 intersection values, denoted J_{50} in further discussion here, appear to be reasonable (slightly conservative) for use in reactor vessel analysis. That is to say that these J_{50} values, established from J-R curve tests of actual vessel material including weld metal, are proposed and recommended as reasonable limiting values for vessel analysis for the current state of the art.

B. The Possibility of a Charpy Correlation With J_{50} Values

The previous discussion, recommending J_{50} values measured directly from a plane strain J-Integral R-curve test, did so for very relevant reasons. The test directly measures crack extension, Δa, behavior for increases in applied

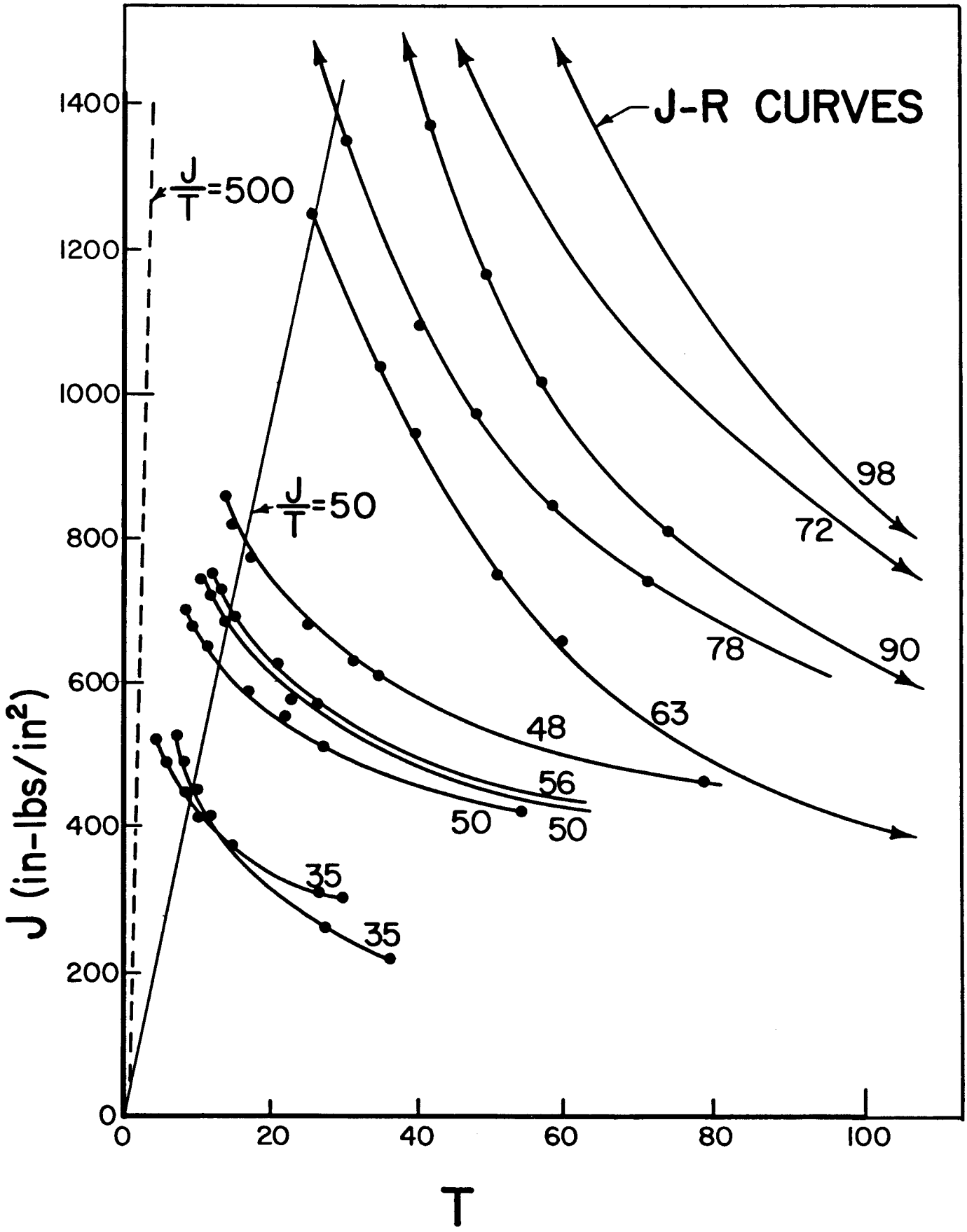

Figure 13 Typical data from Loss on irradiated nuclear vessel materials

J under rigorous J-controlled conditions. The results are directly applicable for estimating the instability of crack extension under local crack tip conditions of plane strain with J-controlled growth for postulated vessel cracks. Short of extensive testing of full scale vessels with cracks, it is the most direct and rigorous approach available.

Correlations or data extrapolations, though tempting, do not have an important role except in cases where no other avenue of approach exists, and even then only with a vast amount of statistical data available to illustrate exceptions. One potential case is that of existing reactors with doubtful material chemistries, including welds, whose surveillance capsules do not contain material samples from which proper J-R curves may be obtained. Some capsules have only Charpy bars and no other way to establish J-R curve properties.

For such an extreme case, the question is: can the Charpy test in some way be correlated to the relevant property for analytical judgments, J_{50}, no more, no less? As a consequence, Loss's data were plotted on Figure 14 to explore this possibility. For both irradiated and unirradiated base metal and weld metal, a scatter band of data resulted. The scatter band was fairly broad, but its lower boundary seemed well enough defined to provide hope that such a correlation may be possible for use where J-R curves are impossible to obtain.

It is noted that the data are from a single source and are not a very numerous (statistically significant) sample. So as hopeful as one may view this attempt at correlation, it remains to be firmly established.

Indeed if it is established as a correlation, it remains from statistical considerations to determine an adequate margin between the lower boundary of the data down to acceptable J_{50} values for use in analysis to assure safe utilization. This judgment is left for others after an adequate data base is available.

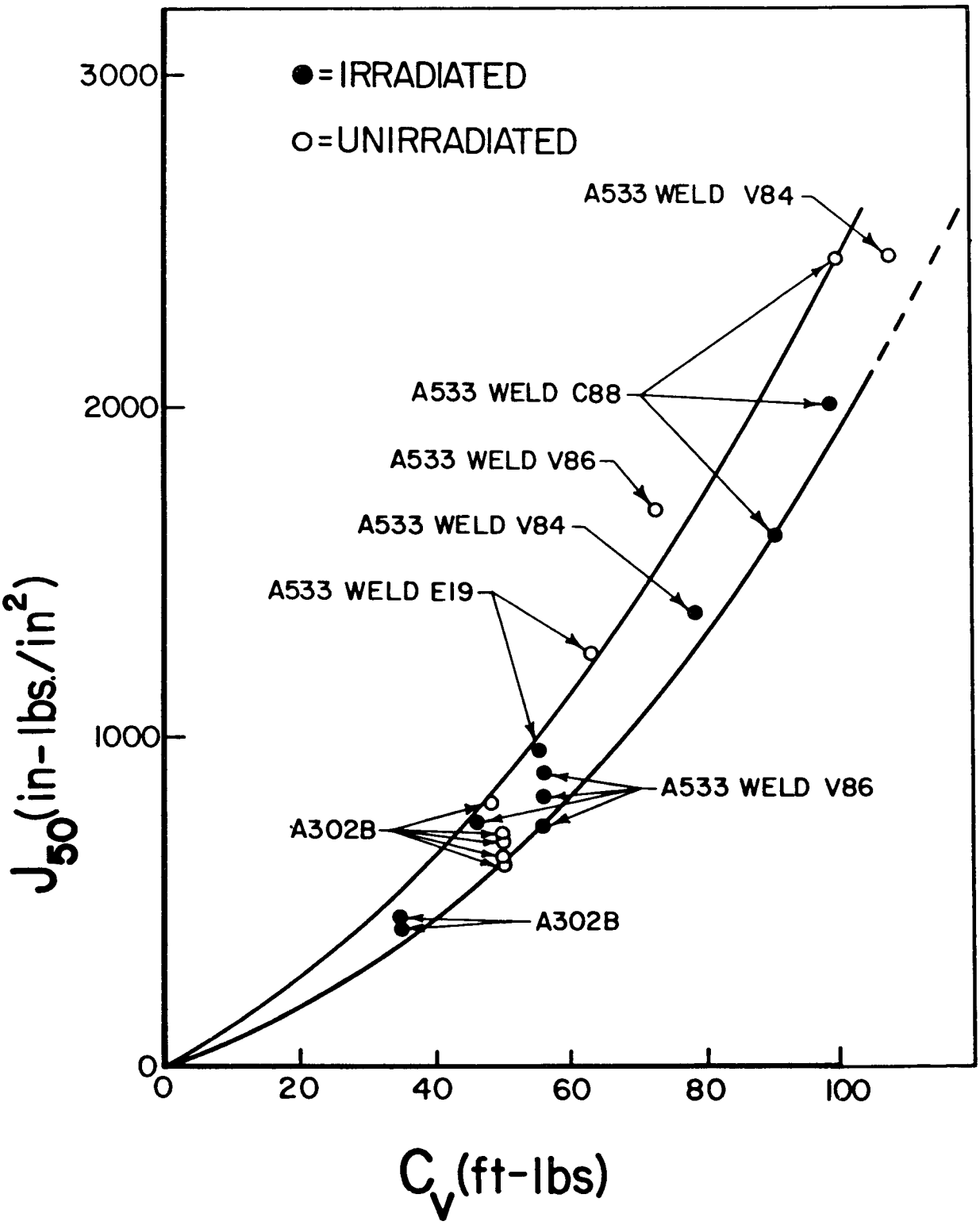

Figure 14 An attempted correlation of J_{50} values with Charpy upper shelf values from data by Loss

C. The Adequacy of the Current Data Base

The NRC has recognized for more than 5 years that J-R curves on irradiation-damaged material were going to be needed by NRC to make adequate safety judgments. NRC has also recognized the need for establishing adequate hot cell test procedures to assure J-R curves of suitable quality. However, progress in establishing an adequate data base has been slow. Although a J-R curve measurement procedure, the single specimen compliance method, was developed,[20] it has not been evaluated by round-robin testing. Standardization of this or any other J-R curve test method by the ASTM is even further away. It is significant that fracture toughness specimens in nuclear RPV surveillance programs involve several designs (for example, the IX WOL specimen, round CT, and so forth). Thus far, there have been no reports on the value of J-R curves derived from them, even though some existing older reactors are approaching the 50 ft-lb Charpy Code limit.

Consequently, it is noted that analysis presented herein, if judged relevant and timely, may suffer from an inadequate supporting data base. The J and T analysis formulas herein admittedly are at best good approximations, but at this time their precision is consistent with the best available methods for obtaining supporting data.

SUMMARY DISCUSSION AND CONCLUSION

The analysis methods developed in this report have attempted to combine several objectives. The methods suggested are first logical extensions of LEFM Code methods for flaws analysis in nuclear pressure vessels making use of established elastic-plastic fracture mechanics methodology so as to be quantitatively applicable to above transition temperature conditions. This has been done by making use of "tearing instability" concepts under "J-controlled growth" conditions to formulate crack instability criteria which are not overly conservative. The method is integrated with the use of J-R curves, which are the only available and widely accepted direct quantitative fracture properties characterization for above transition temperature conditions.

Staying within the J-controlled growth region for material properties tests, specifically for bend or compact specimen J-R curves, is shown to suggest limiting the loading on postulated vessel cracks to an applied J-level, J_{50}, where the test data intersect J/T = 50. This assures conservatively avoiding crack instability by the tearing mode. At near or below the transition temperature, the cleavage mode bears other considerations. On the other hand well above the transition temperature, which is usually consistent with nuclear vessel normal operating conditions, cleavage is avoided. As a further expedient for situations such as some surveillance programs where only Charpy specimens are available, it is shown that upper shelf Charpy energies seem to correlate with J_{50} values. This correlation and other data requirements suggest developing a broader data base.

The analysis and resulting equations developed here for applied values of J, T, and J/T are appropriate approximations permitting the separation of stress level effects and geometrical effects into independent factors. This has led to clearly delineating the regions of interest on J versus T diagrams for the location of potential crack instability points for postulated vessel cracks at or above about J/T = 500. Thereafter, once a safe value is selected, such as limiting J to a value J_{50} (for $J/T \leq 50$), the approximations have served their purpose. Nevertheless, they are clearly and conservatively developed herein and are suggested as sufficiently accurate for broad usage with the advantages of simplicity and familiarity to fracture mechanics practitioners.

REFERENCES

Documents marked with an asterisk may be ordered from the NRC/GPO Sales Program, Washington, DC 20555 and/or the National Technical Information Service, Springfield, VA 22161.

1. ASME Section XI Task Group on Flaw Evaluation, "Flaw Evaluation Procedures," T. V. Marston, ed., EPRI Special Report NP-719-SR, August 1978.

2. P. C. Paris, H. Tada, A. Zahoor, and H. Ernst, "A Treatment of the Subject of Tearing Instability," USNRC Report NUREG-0311, August 1977. (See also ASTM, STP 668, 1979.)*

3. J. W. Hutchinson and P. C. Paris, "Stability Analysis of J-Controlled Crack Growth," ASTM, STP 668, 1979.

4. "Proceedings of the CSNI Meeting on Plastic Tearing Instability," compiled by P. C. Paris , USNRC Report NUREG/CR-0100, January 1980.*

5. C. F. Shih, "An Engineering Approach for Examining Growth and Stability in Flawed Structures," a contribution in Reference 4.*

6. J. W. Hutchinson, "Singular Behavior at End of Tensile Cracks in Hardening Material," Journ. of Mech. and Phys. of Sol., Vol. 16, No. 1, January 1968.

7. J. R. Rice and G. F. Rosengren, "Plane Strain Deformation Near a Crack Tip in Power-Law Hardening Material," Journ. of Mech. and Phys. of Sol., Vol. 16, No. 1, January 1968.

8. J. R. Rice, "A Path Independent Integral and the Approximate Analysis of Strain Concentration by Notches and Cracks," Trans. of ASME, Journ. of Appl. Mech., Vol. 35, pp 379-386, 1968.

9. P. C. Paris, "Fracture Mechanics in the Elastic-Plastic Regime," ASTM, STP 631, 1977.

10. E. S. Folias, Int. Journ. of Fract. Mech., Vol. 1, p. 104, 1965.

11. F. Erdogan and J. J. Kibler, Int. Journ. of Fract. Mech., Vol. 5, p. 229, 1969.

12. S. Krenk, "Influence of Transverse Shear on Plasticity Around an Axial Crack in a Cylindrical Shell," Trans., 4th Int. Conf. on Structural Mech. in Reactor Technology, San Francisco, paper G5/3, 1977.

13. D. P. Rooke and D. J. Cartwright, "Compendium of Stress Intensity Factors," Her Majesty's Stationary Office, London, 1976.

14. H. Tada, P. Paris, and G. R. Irwin, The Stress Analysis of Cracks Handbook, Del Research Corporation, 226 Woodbourne Drive, St. Louis, MO 63105, 1973.

15. J. W. Hutchinson, A. Needleman, and C. F. Shih, "Fully Plastic Crack Problems in Bending and Tension," Fracture Mechanics, N. Perrone and others, ed., Univ. of Virginia Press, 1978.

16. A. Zahoor, contribution in "Further Results on the Subject of Tearing Instability -II" (prepared by H. Tada and P. C. Paris), USNRC Report NUREG/CR-1220, January 1980.*

17. H. Tada and P. C. Paris, "Tearing Instability Analysis Handbook," USNRC Report NUREG/CR-1221, January 1980.*

18. C. F. Shih and J. W. Hutchinson, "Fully Plastic Solutions and Large Scale Yielding Estimates for Plane Stress Crack Problems," Trans. of ASME, Journ. of Engin. Mat. and Tech., Vol. 98, No. 4, October 1976.

19. R. S. Burrington, Handbook of Mathematical Tables and Formulas, Handbook Publishers Inc., Sandusky, Ohio, 3rd ed., 1949.

20. G. A. Clarke, W. R. Andrews, D. W. Schmidt, and P. C. Paris, "Single Specimen Tests for J_{Ic} Determination", ASTM, STP 590, 1976.

NOTATION

a	Crack length (for through thickness cracks) or crack depth (for surface cracks).
a_{eff}	Effective crack size with a plastic zone correction added.
a_o	Initial crack size prior to growth.
Δa	Crack length change.
b	Uncracked ligament size.
c	Half the surface length of a surface crack.
E	Modulus of elasticity.
$f(a/c)$	A surface flaw geometry correction.
f^*	A coefficient in a hardening stress bracket.
$F(a/c)$	A coefficient in a hardening stress bracket.
$g(a/t)$	A coefficient in a hardening stress bracket.
$G(a/t)$	A coefficient in a hardening stress bracket.
G^*	A coefficient in a hardening stress bracket.
J	Rice's J-Integral, total energy (elastic and plastic)
J_{Ic}	Critical value of J-integral
J_{appl}	The intensity of the crack tip emergency field, J, applied.
J_{mat}	The material resistance value of J for an observed crack length change, Δa.
K	The intensity of an elastic crack tip stress field.
K_{Ic}	Fracture toughness
K_{Id}	Dynamic fracture
n	A hardening exponent (for describing material properties).
P	Applied load.
r	Radial distance from a crack tip.
r_y	A plastic zone size.

R	Radius of a pressure vessel.
s	Arc length on a contour around a crack tip.
t	Wall thickness of a pressure vessel.
T	Tearing modulus.
T_{app}	Applied tearing modulus.
T_{mat}	The material resistance to tearing modulus or an observed crack length change, Δa.
T_i	Applied traction (stress).
u_i	Displacement corresponding to an applied traction.
U	Elastic system energy stored (corresponding to deformation plasticity theory).
W	Plate or test specimen width.
x,y	Rectangular coordinates, coplanar with and measured perpendicular to a crack surface, respectively.
Y	A geometrical correction for crack tip field intensity in shells (a function of $\lambda = a/\sqrt{Rt}$).
$\bar{\alpha}$, $\bar{\bar{\alpha}}$	Coefficients in hardening laws for stress-strain curves.
β	Stress state (plane stress versus plane strain) coefficient in a plastic zone correction.
σ	A coefficient adjusted for stress state in relating δ to J.
Γ	A contour around a crack tip.
δ	Crack opening stretch (displacement).
δ_p	Load point displacement.
Δ	Applied displacement (loading).
ε	Strain.
ε_o	Flow Strain.
ε_{ij}	Components of strain.
E_{ij}, $\bar{\Sigma}_{ij}$	Functions of θ and n in power hardening fields of strain and stress.

θ	Angular coordinate measure from the extension of a crack plane.
λ	A shell parameter, $a/\sqrt{Rt}$.
σ	Applied (tension) stress.
σ_{ij}	Components of stress.
σ_o	Flow stress (in tension).
σ_{eff}	Net ligament nominal (effective) stress.
ϕ_o	The complete elliptic integral of the second kind (see Reference 19).
ψ^*	A coefficient in a hardening stress bracket.
ω	Hutchinson's J-controlled growth validity assurance parameter.
	As, for example, y'; derivative with respect to the argument.
{ }	Stress brackets or factors in equations for J and T applied.
[ ]	Geometry brackets or factors in equations for J and T applied.